Investigating the Influence of the Electrochemical Environment on the Flotation of a Mixed Sulphide Mineral System of Bornite and Chalcocite

Department of Chemical Engineering
University of Cape Town

Prepared by:
Tanaka Tafirenyika – TFRTAN001

Key words: Flotation, Grinding Media, Sulphide Ores

Acknowledgments

Completing a masters by research has always been known to be a daunting task, let alone during a global pandemic that changed the way we work, live, and interact with each other. The perceivably insurmountable pressure of the task that was before me sometimes got the best me, but somehow, I have the privilege of claiming the completion of this daunting task, under unprecedented conditions. If there is one thing that this journey has taught me – life is a team sport, and this thesis is dedicated to the team that has continuously banded together to get me across this crucial part of my life journey.

- To my supervisors Associate Professor Kirsten Corin and Professor Cyril O'Connor, your support went above and beyond your technical expertise. Your confidence, understanding and patience, even when I did not deserve it, truly made my research journey pleasant and one I will remember fondly. I strongly believe there is no better combination of supervisors that exist. I have absorbed so much knowledge from you, words cannot express the gratitude I have for being fortunate enough to work with you
- To the CMR staff – Heather, Shireen, Kenneth, Monde, Gary, Refilwe and Nqobile, you are indeed the backbone of the research centre, your willingness to hold my hand during my moments of confusion and travel with me wherever the research took us is what made this work possible.
- To my friends, Kumbi, Mutsa, Kassandra, Naledi, Ayanda, Joy, Zola, Fadzi, and the Spencers, you keep me sane, entertained, and hopeful amongst many other things. You are the quintessential proof of the saying the blood of the covenant is thicker than the water of the womb. My life would be dismal without all of you
- To my parents Asuya and Shephard, you have always gone above and beyond to make my life what it is. Not only did you excessively provide, consistently support, and unconditionally love me, you made yourselves my friends. I hope to always be the blessing that you have been to me
- Lastly, to God who has proven time and time again to genuinely move in mysterious ways, I fully trust You now.

Funding Acknowledgement

This project received funding through the South Africa/China Joint Research Centre hosted at Mintek and sponsored by the South African Department of Science and Innovation.

Plagiarism Declaration

I know the meaning of plagiarism and declare that all the work in the document, save for that which is properly acknowledged, is my own. This thesis/dissertation has been submitted to the Turnitin module (or equivalent similarity and originality checking software) and I confirm that my supervisor has seen my report and any concerns revealed by such have been resolved with my supervisor.

Tafirenyika, Tanaka

Signed by candidate

Synopsis

There is a growing demand for copper driven by its applications in renewable energy and electric vehicles. Sulphide ores are an important source of copper. These ores contain, on average, 2% copper and require extensive processing to extract this as pure copper. Flotation is a critical front-end process used to remove gangue minerals and concentrate the copper minerals. However, flotation is an electrochemically intense process with multiple redox reactions taking place simultaneously. The interdependency of these processes makes it extremely difficult to isolate the effect of one parameter, and hence it is difficult to predict flotation behaviour.

The electrochemical activity of sulphide minerals contributes to the overall activity in the flotation pulp. This ability to conduct electrons is called their rest potential, and different sulphide minerals have different natural rest potentials and therefore different extents of activity. The ability to conduct electrons gives rise to galvanic interactions between different minerals, minerals and media or a mineral-media-mineral complexes in solution. This dictates how collectors interact with the mineral surface, and ultimately the flotation response. Other variables in the electrochemical environment such as the dissolved oxygen, (DO), pH, redox potential (Eh) and water composition are also essential in controlling flotation outcomes.

The aim of this investigation is to determine the influence of the electrochemical environment on the flotation of two copper sulphide minerals: bornite and chalcocite. The focus areas include; collector-mineral interaction, surface charge and flotation recovery of the bornite and chalcocite under varying pH conditions.

For this investigation, the interaction of collector with bornite and chalcocite are considered in 2 water compositions: synthetic plant water (SPW1) and deionized water (DIW) at 5 different pH levels, increasing from 3 to 11. Starvation dosages of sodium isobutyl xanthate (SIBX) are used both in the batch flotation and collector adsorption tests conducted. Zeta potential tests are carried out to determine the surface charge of the minerals under the varying conditions. Further to the pure mineral studies, batch flotation tests are carried out using a synthetic ore under natural pH, Eh and DO conditions, with grinding done in a Magotteaux Mill® to monitor pulp chemical conditions during milling.

From pure mineral flotation studies, it was observed that high mineral recovery is possible in both acidic and alkaline conditions via different hydrophobicity inducing mechanisms. In acidic conditions, low pH, two possible processes are occurring, the first being the inhibition of the formation of oxy-hydroxy species that adsorb onto the mineral surface and block sites for collector adsorption. The second is the decomposition of xanthate resulting in the formation of carbon disulphide that is known to be hydrophobic and is speculated to form a film around the mineral surface and render it hydrophobic enhancing flotation. In alkaline conditions, the well-established mechanisms of xanthate ion adsorption and dixanthogen formation take place on the mineral surface and enhances the flotation. Thus, the surface charge of the minerals as the conditions changed from acidic to alkaline resulted in a change in the surface-active species from the pure mineral to the oxide. However, for bornite, owing to the mineral structure containing iron, when oxidation occurs, iron hydroxide species form which precipitate at the mineral surface and inhibit collector adsorption, reducing the floatability of the mineral. The surface charge of the minerals' changes with changing pH due to a change in the surface-active species from the pure mineral to the oxide and hydroxide.

Flotation of chalcocite and bornite in a mixed mineral system resulted in higher copper recovery compared to the weighted sum recoveries of the individual minerals. This suggests a possible synergistic effect when floating chalcocite and bornite together. Electrochemically active impurities present in the mineral samples made it difficult to decouple the exact nature of the interaction between the two minerals, but nonetheless provides insightful observations as industrial operations have to process equally complex mineral systems.

Glossary

BET	Brunauer–Emmett–Teller theory
Cu	Copper
DIW	Deionised water
DO	Dissolved Oxygen
DOW 200	DOW 200 frother
Eh	Redox potential
ETDA	Ethylenediaminetetraacetic acid
Fe	Iron
FTIR	Fourier-transform infrared spectroscopy
g	grams
g/mol	Grams per mole
g/ton	Grams per ton
IEP	Iso electric point
IS	Ionic strength
l/min	Litres per minute
mg/L	Milligrams per litre
mol	mole
mV	millivolts
ORP	Oxygen reduction potential
ppm	Parts per million
rpm	Revolutions per minute
SIBX	Sodium isobutyl xanthate
SPW1	Synthetic plant water
TDS	Total dissolved solids
UV/VIS Spectroscopy	ultraviolet-visible spectroscopy
XPS	X-ray photoelectron spectroscopy
XRD	X-ray diffraction
µl	Micro litres
µm	Micrometre

Table of Contents

Table of Figures

List of Tables

1 Introduction

1.1 Background

Flotation of sulphide minerals is an electrochemically intense process with numerous variables contributing to the final electrochemical environment. The interdependency of these processes further complicates the decoupling of these variables to understand and predict the driving force for flotation and resulting electrochemical environment. Despite the complexity, this approach of investigating flotation processes and mechanisms has provided insight into how minerals and flotation reagents, such as collectors, interact with each other (Woods, 2003).

In solution, sulphide minerals are known to be conducting and are electrochemically active, with the extent of electrochemical activity dependent on the mineral type (Payant, et al., 2012). When two or more sulphide minerals are in solution together, a galvanic cell is set up those results in the free flow of electrons in the solution. The measured potential of this cell equilibrates between the value of the highest and lowest potential mineral in the system (Payant, et al., 2012). This exposes the lower rest potential minerals to a higher charge density environment, which should result in great surface oxidation and enhanced collector adsorption.

The pulp potential plays a critical role in determining the floatability of sulphide minerals, as the hydrophobicity is heavily dependent on the redox reactions that take place on the mineral surface (Wills & Finch, 2016). In addition to the electron flow from the galvanic cell, the Dissolved Oxygen (DO), pH and water composition play fundamental roles in determining the final hydrophobicity as oxygen is required for all the competing electrochemical reactions while pH and water composition determine the species present in the medium.

The chemical and electrochemical conditions in the grinding environment have been used to enhance flotation, as well as selectively float minerals in a mixture containing more than one mineral. This is because the type of grinding media used affects the flotation response (Greet, et al., 2004; Bruckard, et al., 2011; Peng, et al., 2003; Huang, et al., 2006). It has been found that using forged steel media introduces iron oxidation species into the system through wear and tear of the media, and corrosion

due to the wet conditions. However, correlating laboratory scale studies to industrial realities has often been difficult due to differences in the ease of manipulation of laboratory and industrial conditions. To better simulate industrial conditions in laboratory scale studies, the Magotteaux Mill®, a highly instrumented mill capable of monitoring and controlling the pulp chemistry during grinding, was developed (Greet, et al., 2004).

1.2 Subject and Motivation

Flotation is an electrochemically intense process, with the preceding grinding process influencing the electrochemical behaviour of the system. Furthermore, the ability of sulphide minerals to participate in redox reactions further complicates the possible reactions taking place on the mineral surface. Understanding the active species are active under known conditions may allow for the prediction of selective flotation of one mineral over another

1.3 Objectives

The aims of this investigation are to:

- Investigate the interaction of collector with bornite and chalcocite under specific pulp chemical conditions.
- Investigate the surface charge of bornite and chalcocite under specific pulp chemical conditions.
- Compare the flotation response of individual minerals; bornite and chalcocite, to their flotation response when they are both present in a mixed mineral system.

1.4 Scope and Limitations

The scope of the work was limited to 2 sulphide minerals, namely bornite and chalcocite. The work was carried out with only pure mineral samples whose composition is given in 4.2.1. Water quality was limited to 2 compositions, Deionized water (DIW) and UCT's Synthetic Plant Water (SPW1) (Wiese, et al., 2005). The pH was the prevailing parameter used to change the electrochemical environment, which was carefully adjusted using hydrochloric acid (HCl) and sodium hydroxide (NaOH).

2 Literature Review

This chapter discusses in detail the theory and literature preceding the investigation.

2.1 Milling

Comminution is a size reduction process done to enhance the mineral liberation by using a combination of impact breakage, abrasion and attrition (Liming, 2015). The two main comminution processes are crushing and grinding, where crushing is the initial size reduction process from extraction that produces coarse particles that undergo further size reduction through grinding in mills. Comminution is an energy intensive process owing to the amount of force required to break down the rock. Grinding is the most energy intensive comminution process as the size reduction achieved in grinding is much greater than that of crushing (Workman & Eloranta, 2003). Crushing generally achieves a reduction ratio of 3 to 7 depending on the type of crusher, while grinding on average has a reduction ratio of 100 (Balasubramanian, 2017;Liming, 2015). Due to the high reduction ratio, grinding alters the grain size, grain surface and shape, ultimately changing the state of the material. Grinding is done in different types of mills, with tumbling mills being one of the more commonly used types (Liming, 2015).

2.1.1 Tumbling Mills

Tumbling mills are classified as any mill consisting of a drum that rotates on a horizontal axis, which pulverizes material mixed with a grinding media (Liming, 2015). Tumbling mills can be characterized using operational and output parameters such as wet or dry operating, media type and size as well as particle size reduction. Tumbling mills can further be classified into subcategories, semi-autogenous (SAG) or autogenous (AG) grinding mills, rod mills, tube mills, pebble mills and ball mills.

Ball mill is used to refer to any mill that uses spherical balls as the grinding media. Forged steel balls have been commonly used as the media of choice owing to their effectiveness and low cost. However, grinding media made from electrochemically inert material such as ceramic or stainless steel have been seen to reduce the interference of ionic species that leach into the pulp through wear and tear during wet grinding. Ball mills are particularly popular because of their versatility; they can be

used in primary operations to process material from the crushers, or in a secondary circuit obtaining its feed from a rod mill or SAG mills (Liming, 2015).

2.1.2 Magotteaux Mill®

When conducting laboratory scale studies, to model on site behaviour, the aim is to establish the same Eh as industrial plant conditions at the beginning of processing (Woods, 2003). However, scale up factors from the lab, along with other mechanical influences in the plant, such as aeration from cyclone classification, result in different Eh profiles between lab-based studies and those observed on the plant. This subsequently results in different flotation behaviour which cannot be compared. (Woods, 2003). The same conundrum presented itself when Magotteaux wanted to justify the use of high chrome media in industrial plants by proving its adjustment of the pulp potential provides sufficient improved metallurgical performance to justify the cost (Greet, et al., 2004).

The development of the Magotteaux Mill® shown in Figure 2-1 was necessary as it allows the simulation of tumbling mills in the laboratory that have the same pulp chemistry characteristics as those on industrial plants, This is done by the measuring, monitoring and control of pH, Eh, dissolved oxygen (DO) and temperature through gas and reagent addition (Greet, et al., 2004). This then enables an analogous flotation response that is easily transferable in scale up.

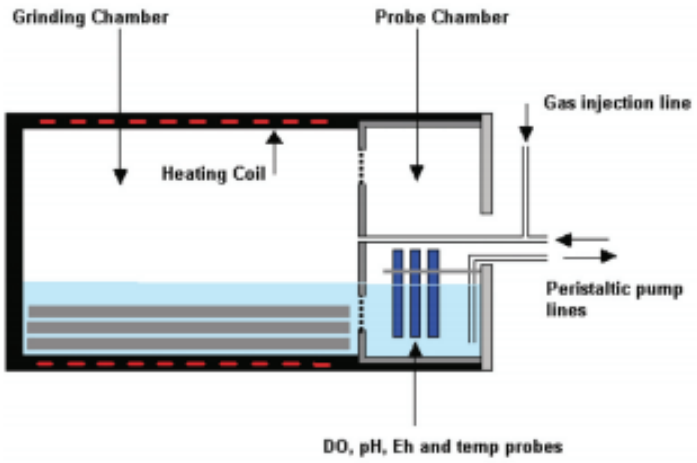

Figure 2-1: Magotteaux Mill® Schematic from (Greet, 2009)

The only advantage that had been associated with high chrome media was the reduction in media corrosion and wear, which was not enough economic justification

to offset the increase in media cost. On average, the increase in media cost, as chrome content increased, went up by 4 times, with media consumption only reducing from 0.02 kg/kWh to 0.01 kg/kWh (Kawatra, 2006). The rate of media consumption depends on media hardness, which for ceramic media affects the mill performance as some minerals can be harder than the media which subjects the media to experiencing comminution. Steel and chrome media hardness does not affect mill performance, as they are generally more compact and harder than the ores, only media consumption through abrasion and attrition is impacted (Kawatra, 2006).

2.2 Sulphide Minerals

Sulphide minerals are a major source of nonferrous metals used in a variety of industrial applications such as construction, aviation, electronics, etc. (Hu, et al., 2009). Pyrite is the most abundant sulphide mineral, consisting of only Iron and sulfur (FeS_2). However, the majority of sulphide minerals are extracted for their nonferrous components, particularly copper, which is present in chalcopyrite, chalcocite, bornite and covellite. Among these, chalcopyrite (Cu_2S) is the most abundant and has been the most extensively processed ore for copper extraction due to its economic value and association with PGM ores, which has resulted in a significant amount of sulphide mineral studies focusing or at least incorporating chalcopyrite. The extensive body of literature available on chalcopyrite has shown that it readily floats under various conditions, which does not make it an ideal mineral for a fundamental study.

2.2.1 Bornite

Bornite (Cu_5FeS_4) is a mixed copper and iron mineral with a Mohrs hardness of 3 and specific gravity of 5.1 (Anthony, et al., 1990). When freshly exposed, it has a reddish-brown metallic colour. The metallic shine soon loses its lustre and develops a tarnish which has earned it the name peacock chalcopyrite, owing to the rainbow-like array of colours as seen in Figure 2-2 (Daintith, 2008). It is mostly mined in Chile, Mexico and the United States. Its crystal structure is orthorhombic. It is typically the secondary mineral of chalcopyrite and chalcocite deposits in copper-molybdenum and copper-gold ores (Bulatovic, 2007). The floatability of bornite is dependent on the particle size, with fine bornite particles under 20 µm being difficult to float (Bulatovic, 2007)

Figure 2-2 Bornite with traces of Chalcopyrite (golden yellow section) on the outer layer (Anon., 2020)

2.2.2 Chalcocite

Chalcocite (Cu_2S) is an important copper mineral with 79.8% copper content. It has been one of the most profitable copper minerals as it can produce concentrates with 37% to 40% copper as compared to chalcopyrite which produces 20% to 30% copper content in the concentrate (Da Silva, 2019). Chalcocite has a metallic lustre, dark grey to black in colour, Figure 2-3. It has a monoclinic crystal structure (Anthony, et al., 1990). Chalcocite, though scarce, can still be found as a primary mineral with chalcopyrite, bornite and covellite as secondary minerals in copper-molybdenum ores. Chalcocite floats well with xanthate collectors with dithiophosphates or thiocarbamates as secondary collectors and can be depressed by sulphur containing reagents such as sodium sulphide and sodium hydrosulphide (Bulatovic, 2007).

Figure 2-3 Chalcocite with deposits of chalcopyrite on top (MSR Blog, 2020)

2.3 Froth Flotation Principles

Flotation is a physio-chemical process used in the mineral processing industry to separate gangue minerals from valuable target minerals (Kawatra, 2011). The hydrophobic and hydrophilic properties of different compounds arise from differences in surface energy and potential of the particles. This difference is what allows compounds to be separated when placed in an electrolytic solution such as plant

water. In a flotation cell Figure 2-4 particles are in one of four states; suspended in the pulp phase, fully immersed and attached to a bubble, attached to the air-water interface in the froth phase, or entrained/entrapped in-between bubbles/particles (King, 2012). The pulp phase is the slurry mixture where the valuable mineral forms bubble/particle aggregates (Finch, 1995). Particles remain suspended in the pulp zone by the continuous circulation of the agitator (King, 2012). The valuable mineral then separates from the gangue when it enters the froth zone through the pulp and froth interface.

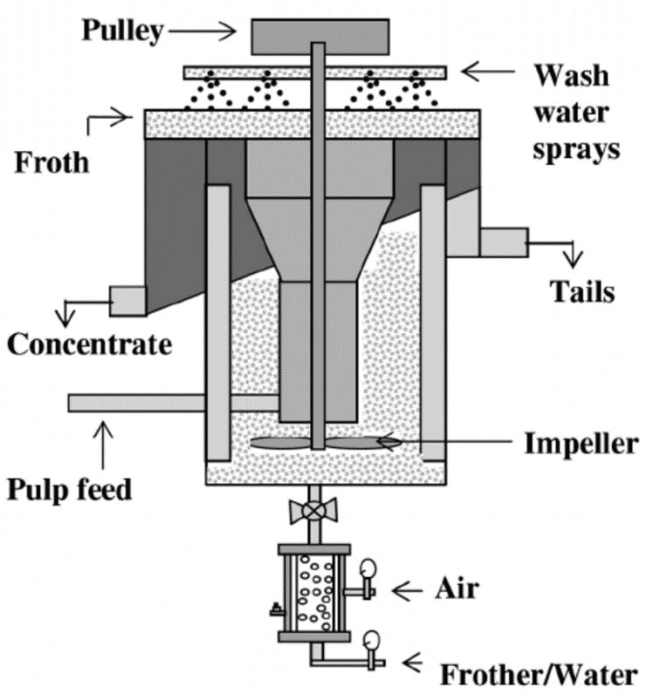

Figure 2-4 Flotation cell adapted from (Parga, et al., 2009)

There are three mechanisms through which particles can be transported from the pulp to the froth phase: true flotation, entrainment, and entrapment (Wills & Napier-Munn, 2006). True flotation refers to the selective attachment of minerals to air bubbles, entrainment is the non-selective recovery of fine particles swept in the upward flow of water and physical entrapment is the capture of minerals between particles in the froth attached to air bubbles (Bulatovic, 2007). Entrainment is a key transportation mechanism used to determine the efficiency of separation between the target valuable minerals from the unwanted gangue (Kawatra, 2011).

At constant bubble concentration, the recovery of floatable minerals is described using a first order mechanism with respect to particle concentration using Equation 2-1 (Garcia-Zuñiga, 1935).

$$R(t) = R_{\infty}[1 - e^{-kt}] \qquad \text{Equation 2-1}$$

$$R_{\infty} = maximum\ recovery\ at\ infinite\ time$$

$$R(t) = overall flotation\ recovery$$

$$k = first\ order\ rate\ constant\ (min^{-1})$$

For a pure particle, the rate constant, k, is a function of the size and hydrophobicity of particles (Xiangning, et al., 2017). In general, k is also a function of the particle liberation for a certain collector dosage and pulp conditioning. R(t) is used as a measure of the flotation performance and is a ratio of the mass collected in the concentrate to the mass in the feed by true flotation (Kawatra, 2011).

2.3.1 Bubble-Particle attachment

True flotation, which happens via the bubble-particle attachment process, is the dominant mechanism responsible for the recovery of valuable minerals in the concentrate. This makes it the most vital process whose control significantly affects the performance of a flotation circuit. Bubble particle attachment is governed by the interfacial energies between the solid, liquid and gas phases present. This surface energy can be determined using the Young/Dupre relation shown in Equation 2-2.

$$\gamma_{lv} cos\theta = (\gamma_{sv} - \gamma_{sl}) \qquad \text{Equation 2-2}$$

$$\gamma_{lv} - liquid\ and\ vapour\ interface\ surface\ energy$$

$$\gamma_{sv} - solid\ and\ vapour\ interface\ surface\ energy$$

$$\gamma_{sl} - solid\ and\ liquid\ interface\ surface\ energy$$

$$\theta - contact\ angle$$

From the equation, it can be seen that a crucial function of the interfacial energy is the contact angle formed at the junction between the solid, liquid and gaseous phases as seen in Figure 2-5 (Kawatra, 2011). Increasing the contact angle increases the strength of the bubble-particle attachment. Three distinct angle classifications are θ=0^0, 90^0 and 180^0. At 0^0 the particle is fully immersed in the fluid and cannot penetrate the bubble and will remain in the pulp zone. At 90^0 the particle is partly immersed in

both the bubble and the fluid while at 180^0 it is fully immersed in the bubble and will float to the froth phase (Israelachvili & Ninham, 1976). Generally, when the contact angle is more than 90^0, the surface is considered hydrophobic and conversely less than 90^0 is considered hydrophilic. However, practically this is not the case with most sulphide minerals exposed to collector as the collector alkyl chain length controls the maximum receding contact angle (Grano, et al., 2007). Liberated sulphide minerals floated using isobutyl xanthate (R=4) typically have a contact angle of 78^0 (chalcopyrite has been shown in numerous studies to have a limiting angle of 78^0 at high adsorption densities of an R=4 alkyl group collector) and changing the collector to a longer alkyl group chain length of R=5 increases the characteristic contact angle to 85^0 (Grano, et al., 2007).

2.3.2 Hydrophobicity

Hydrophobicity is a physical property typical of non-polar compounds. It refers to the tendency to be repelled from a mass of water and is quantified using contact angle measurements (Kumbar, et al., 2014). Hydrophobic particles tend to aggregate when in contact with water, which essentially minimises their surface contact for water. This results in distinct separation between water and hydrophobic substances. The differences between hydrophobic and hydrophilic interfaces can be identified by characterizing the contact angles. If water is to be removed from a hydrophobic surface, there will be no residual droplets on the surface whereas with hydrophilic surfaces, there will be some residual droplets that remain behind as seen Figure 2-5. This is because with hydrophobic surfaces, the interaction between surfaces is greater than that with the water molecules, and conversely the interaction of water with a hydrophilic surface is greater than the interactions between the surfaces (Chaplin, 2003).

The process of inducing or enhancing hydrophobicity is specific to the mineral classification. Silicates for example, are known to be exclusively influenced by hydrogen bonding through the significant cohesive energy of water and therefore are generally hydrophilic. Sulphide minerals on the other hand behave differently as some minerals show natural hydrophobic properties and some hydrophilic (Kawatra, 2011).

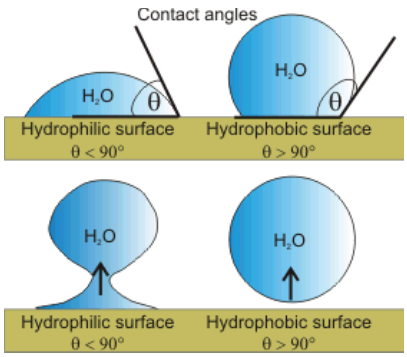

Figure 2-5 Hydrophobic and hydrophilic interfaces taken from (Chaplin, 2003)

2.4 Interfacial Electrochemistry

When a solid surface is cleaved in a liquid environment, the surface will become charged either upon breakage or by adsorption of ions thereafter. The presence of free electrons, alongside with charged surfaces are jointly crucial in establishing interfacial charges. The numerous ions present in the liquid medium aggregate into distinct layers as seen in Figure 2-6 depicting the Gouy-Chapman Model, with the 3 most common being the stern layer, the slipping plane and the diffuse layer (Kohli & Mittal, 2015). The Stern layer is a monolayer of ions that are strongly attracted to the surface, causing them to have low mobility into the bulk and generally fixed positions. The slipping plane is the second layer of particles that are strongly attracted to the Stern plane but have greater mobility than the Stern plane. The diffuse layer is the bulk system where ions have high mobility and are shielded from the surface resulting in weak attraction.

When there is an equal amount of positively and negatively charged ions, there is a net zero charge of the interface. The conditions at which this occurs is known as the isoelectric point (IEP) which enables the existence of electrical potential differences (Bulatovic, 2007). The potential difference between the solution and the particle surface gives rise to the formation of the electrical double-layer potential. This potential difference is created by an uneven distribution of the counter-ions attracted to the surface of the particle and the co-ions contrastingly repelled by it (Holmberg, 2002; Chhabra & Basavaraj, 2019).

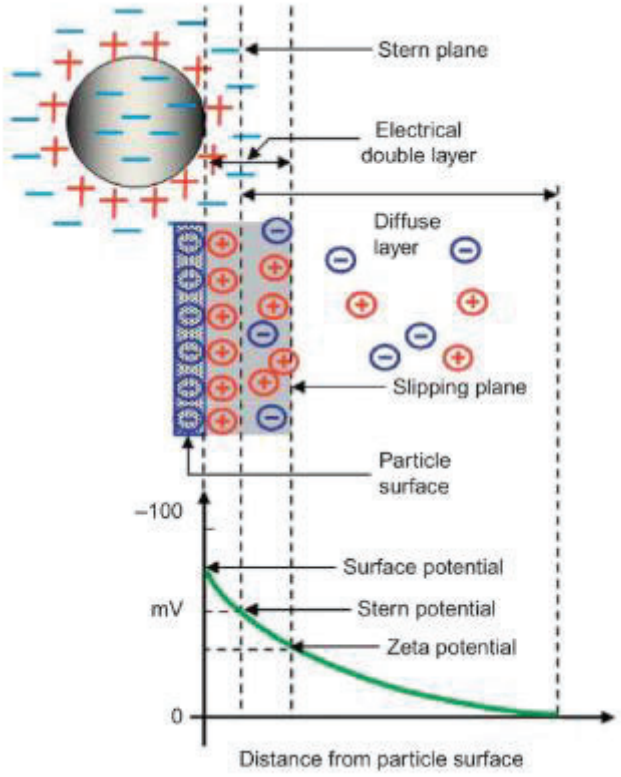

Figure 2-6 Representation of the different electrochemical layers taken from (Kohli & Mittal, 2015)

2.4.1 Electrical Double Layer

The combination of the Stern layer and the slipping plane is known as the electrical double layer (EDL) as seen in Figure 2-6. The exact distribution of the counterions surrounding the charged surface is significant as it governs the potential decay into the bulk from the charged surface as seen in Figure 2-6. Thermal motion, electrostatic attraction, and other interactions and forces influence the distribution of the counterions (Chhabra & Basavaraj, 2019). Three main models have been used to describe this distribution: Helmholtz, Gouy-Chapman and Stern-Graham models (Holmberg, 2002).

2.4.1.1 Helmholtz Model

The Helmholtz model shown in Figure 2-7 treats the charged surface as a parallel-plate condenser and assumes that all the counterions are lined up parallel to the surface. This results in a very swift decay of the potential to zero within a minuscule distance from the surface. This model does not consider the action of thermal motion which causes a random and diffuse distribution around the charged surface.

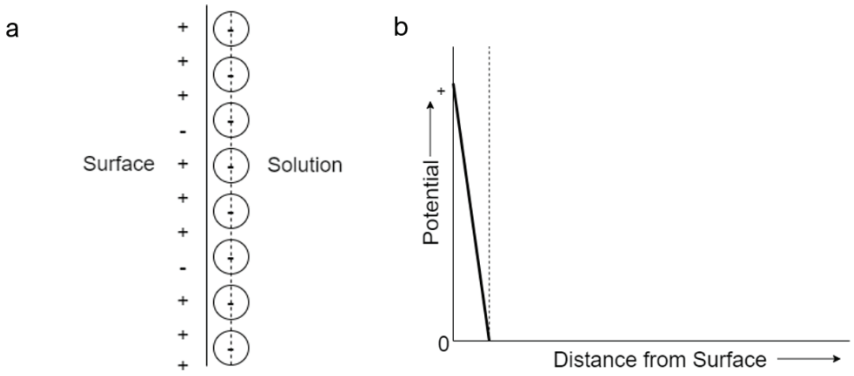

Figure 2-7 Illustration of the Helmholtz model; (a) counterion distribution and (b) electrical potential variation as a function of distance from the surface

2.4.1.2 Gouy-Chapman Model

In contrast to the Helmholtz model, the Gouy-Chapman model shown in Figure 2-8 considers the action of thermal motion, resulting in a scattered pattern of ions around the surface. This results in an initial rapid rate of decrease near the surface due to the screening effect, and as the distance from the surface increases, the rate slowly decreases. This model is only appropriate for low charge density, planar surfaces and distances far away from the surface and is inaccurate for the alternate conditions.

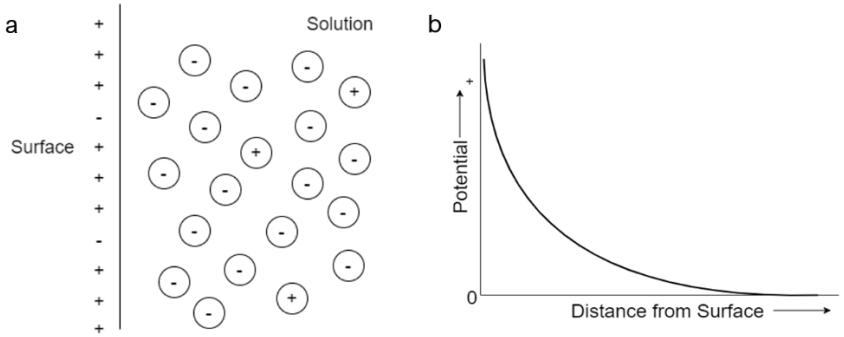

Figure 2-8 Illustration of the Gouy-Chapman model; (a) counterion distribution and (b) electrical potential variation as a function of distance from the surface

2.4.1.3 Stern-Graham Model

The Stern-Graham model shown in Figure 2-9 breaks down the layers into two components; a fixed layer of firmly adsorbed counterions on the surface (known as the Stern layer) and a diffuse layer as described in the Gouy-Chapman model. The potential decay consequently is divided into two sections, the first being a rapid and linear decay in the stern layer, followed by gentler and gradually decreasing decay in the diffuse layer (Holmberg, 2002).

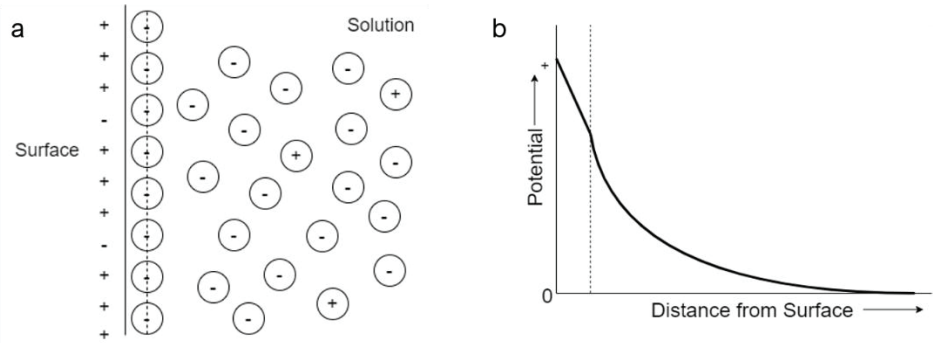

Figure 2-9 Illustration of the Stern-Graham model; (a) counterion distribution and (b) electrical potential variation as a function of distance from the surface

2.4.2 Zeta Potential

The zeta potential can be described as the electrokinetic potential and is the potential that exists between the slipping plane and the surface of the particle (Kohli & Mittal, 2015). This surface potential exists at the plane of shear (which is after the Stern plane) between the particle and the surrounding medium as they both move with respect to each other (Holmberg, 2002). When an electric field is applied, the charged surface will move in one direction, and the counter-ions in the slipping plane would migrate in the opposite direction, and conversely if the charged surface and the counter-ions move relative to each other, an electric field is created (Holmberg, 2002). Essentially, the zeta potential is a method to help quantify the surface charge of the particle. The zeta potential is heavily dependent on the pH as it controls the ionic species present in the medium which in turn causes a variation of the surface charge density with pH. The pH at which the zeta potential is 0 is known as the isoelectric point (IEP). When the pH is higher than the IEP, the surfaces are negatively charged and conversely when it is lower than the IEP, the surface is positively charged (Poole, 2020).

2.4.3 Thermodynamic Stability

The adsorption of collector and formation of ionic species on the mineral surface is a multi-faceted complex process that is kinetically and thermodynamically controlled (Zanin, et al., 2019). Collector and mineral systems have optimum pH ranges they can operate in. Pourbaix diagrams are chemical space maps that demarcate regions of thermodynamic stability using the pH and the Eh. These regions are useful in determining what chemical reactions are possible. There are 3 defined regions of stability in Pourbaix diagrams: immunity, passivity, and corrosion (Beverskog &

Puigdomenech, 1995). In the immune region, the element is stable and will not undergo electrochemical reactions. In the passive region, the element has a coating layer, that could either be an oxide or hydroxide, that acts as a diffusion barrier for any reactive species and significantly reduces the rate of reaction. The corrosive region is where the thermodynamically stable species is a reaction product which leaves the element susceptible to further reactivity and will therefore corrode (Beverskog & Puigdomenech, 1995). Sulphide mineral flotation mainly takes place in alkaline regions where the collectors are stable, as seen in Figure 2-10 which superimposes the flotation regions of sulphide minerals on the Pourbaix diagrams of butyl xanthate and ethyl dithiophosphate (Zanin, et al., 2019).

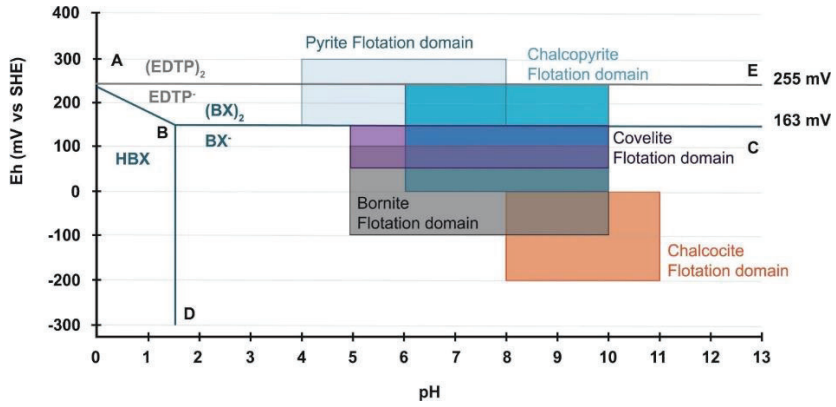

Figure 2-10 Eh-pH flotation regions for sulphide minerals superimposed on Pourbaix diagrams of butyl xanthate and ethyl dithiophosphate taken from (Zanin, et al., 2019)

The Nernst equation (Equation 2-3) has been used to show the dependant relationship of the redox potential on pH. If this is applied to water, the resulting Pourbaix diagram with the three distinct regions produces a water-oxygen line described by Equation 2-4 that demarcates where water decomposes to produce oxygen (above the line) and where water is stable (below the line) (Greet, et al., 2006). This can further be simplified for oxygenated aqueous solutions without well-defined redox couples to produce Equation 2-5 (Johnson, 1988). For chemical reactions that take place in aqueous solutions, this implies that; if the change in Eh and pH result in a line parallel to the water-oxygen line, water equilibria is maintained. This means that a change in pH is proportional to the change in Eh using Equation 2-5. If the Eh and pH changes result in a line perpendicular to the water – oxygen line, then oxidative reactions are taking place (Greet, et al., 2006).

Nernst Equation Equation 2-3

$$E = E^0 + \frac{0.059}{n} log_{10}\left(\frac{a_{reactants}}{a_{products}}\right)$$

Water – Oxygen line equation Equation 2-4

$$E_{O_2} = 1.23 + 0.015\ log_{10} p_{O_2} - 0.059pH$$

Simplified Water – Oxygen line for aqueous solutions Equation 2-5

$$E_{O_2} = 0.9 - 0.059pH$$

2.5 Flotation Reagents

Flotation reagents are an essential component of the flotation process as they enable, induce or extenuate certain properties to make the mineral recovery process economically viable. The natural difference in wettability of mineral surfaces is not enough to achieve desirable separation, which leads to the use of reagents to enhance the surface chemistry by increasing the hydrophobic and hydrophilic nature of target and gangue minerals respectively (Bradshaw, et al., 2005). During process development, the reagents and control strategy to be used are carefully considered as they will not only dictate grades and recoveries, but also form a key part of the consumable operating expenses of a commercial plant (Bulatovic, 2007). Flotation reagents are classified according to their functionality; frothers, regulators and collectors.

2.5.1 Collectors

Collectors are used to enhance floatability by adsorbing onto the mineral surface and rendering it hydrophobic. Collectors are distinguished as being ionic and non-ionic, with Figure 2-11 showing the major subcategories of ionic collectors. Sulphide mineral collectors are classified as sulfhydryl hydroxyl collectors comprised of xanthates, dithiophosphates and carbamates. The most commonly used collectors are xanthates due to their reasonable water solubility, stability in alkaline conditions as well as their low manufacturing cost and efficiency in adsorbing to target minerals (Wills & Finch, 2016; Lovell, 1982). Xanthates are anionic collectors for sulphide minerals and are produced from aliphatic alcohols, carbon disulphide and alkali hydroxides. However, xanthates readily decompose to carbon sulphide (CS_2) which is toxic particularly for aquatic life when discharged into freshwater systems (Wills & Finch, 2016).

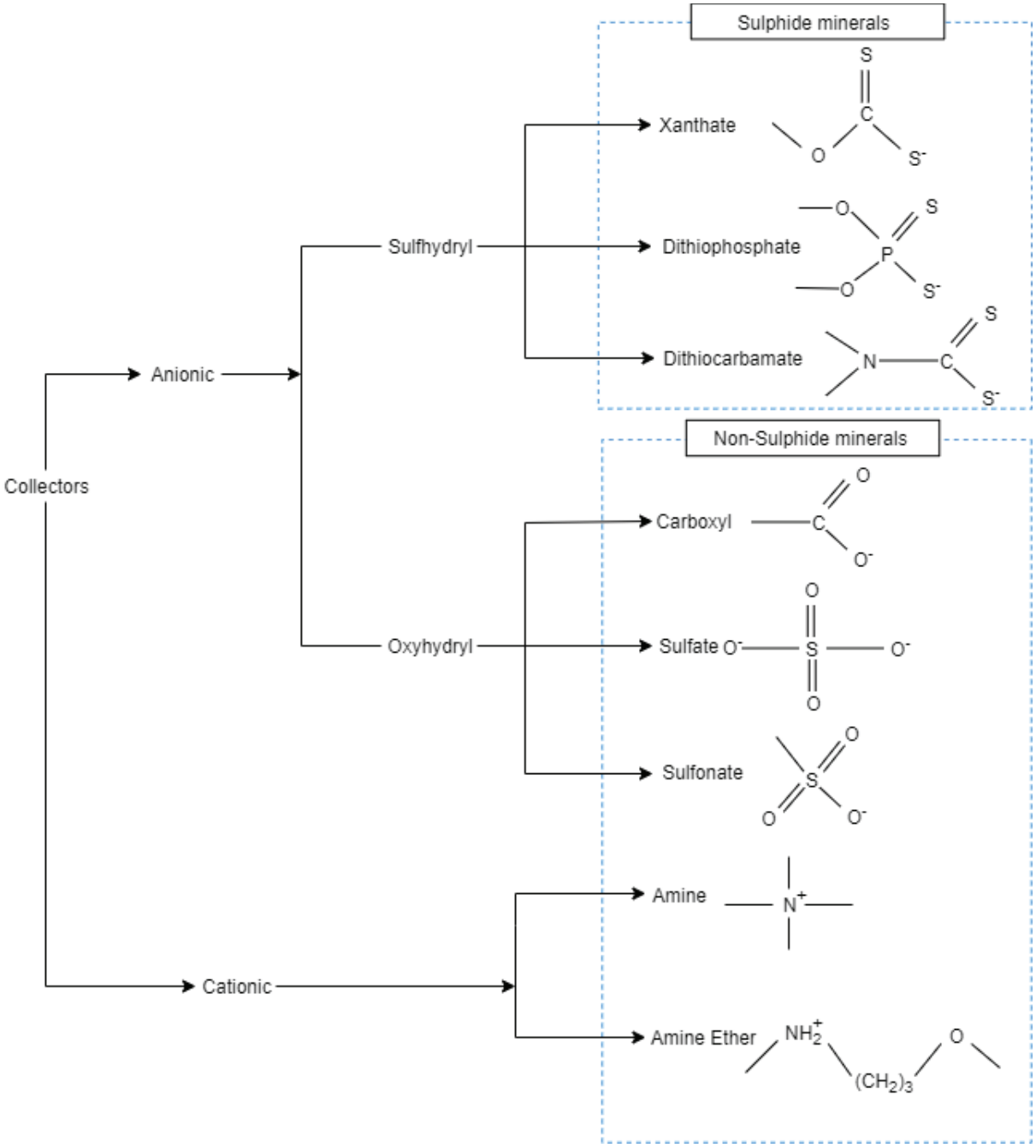

Figure 2-11 Collector Classification extracted from (Wills & Finch, 2016)

An understated but important factor that contributes to the efficacy of the collector is the point of addition. Collector addition has traditionally been done in the float cell and is allowed some conditioning time before concentrate recovery. However, dosing the collector during the milling process has proven to be beneficial as the collector can adsorb onto freshly cleaved mineral surfaces that have not yet oxidised (Greet, et al., 2010).

Collector adsorption rate is dependent on the availability of DO within the system, as it is necessary to complete the collector complexation process (Owusu, et al., 2013). Collector complexation is a process where metal xanthates or dixanthogens are formed as they are responsible for inducing hydrophobicity and oxygen becomes the final electron acceptor in the process (Bulatovic, 2007). Depending on the specific mineral type and extent of sulphide oxidation, the surface can become naturally hydrophobic resulting in its natural flotation without the need to add collector for enhancement.

There are three main mechanisms in which collectors and minerals interact; adsorption of the collector, oxidation of the thiol collector to form its dithiolate and chemisorption as seen in Table 2-1 (Hu, et al., 2009). Chemisorption is generally the thermodynamically favourable process and offers the most optimal use of collector through the formation of a monolayer on the mineral surface (Woods, 2003). A potential dependence of chemisorption exists which obeys the Frumkin adsorption isotherm (Equation 2-6) which takes into account the interaction of species and shows that the presence of a species on an adsorption site reduces the probability of adsorption on neighbouring sites and is a phenomenological equation derived from macroscopic observations (Woods, 2003).

$$K_{eq} = K_{eq_0} e^{\beta \theta_{eq}} \qquad \text{Equation 2-6}$$

$$K_{eq} = Adsorption\ equilibrium\ constant$$

$$\theta_{eq} = Site\ coverage\ at\ equilibrium$$

$$\beta = coverage\ parameters$$

Table 2-1 Collector Adsorption mechanisms from (Hu, et al., 2009)

$$\text{Thiocollector adsorption} \qquad \text{Equation 2-7}$$

$$X^- \rightarrow X_{ads} + e^-$$

$$\text{Oxidation to dithiolate} \qquad \text{Equation 2-8}$$

$$2X^- \rightarrow X_2 + 2e^-$$

$$\text{Chemisorption} \qquad \text{Equation 2-9}$$

$$MeS + 2X^- \rightarrow MeX_2 + S^0 + 2e^-$$

$$MeS + 2X^- + 4H_2O \rightarrow MeX_2 + 8H^+ + 8e^- + SO_4^{2-}$$
$$2MeS + 4X^- + 3H_2O \rightarrow 2MeX_2 + 6H^+ + 8e^- + S_2O_3^{2-}$$

2.5.2 Frothers

Frothers are heteropolar compounds that act as stabilizers to keep them dispersed in the pulp, as well as form a stable froth layer that will not burst as the minerals are being recovered (Darling, 2011). They do this by lowering the surface tension of water and increasing the film strength of bubbles which facilitates better bubble-particle attachment (Bulatovic, 2007). Some frothers' effectiveness is dependent on the pH of the pulp, which results in two major classifications of frothers: acidic and neutral. Acidic frothers effectiveness decreases as the pH increases from acidic to alkaline conditions. Most acidic frothers are either phenols or alkyl sulfonates (Bulatovic, 2007). The more commonly used frothers are the neutral ones whose performance is independent of the pulp pH and mostly cyclic alcohols, aliphatic alcohols, alkoxy paraffins and glycols (Bulatovic, 2007; Darling, 2011)

2.5.3 Regulators

Regulators (also referred to as modifiers) is a classification used to group reagents whose purpose is to modify the action of the collector and improve selectivity, thus in their presence collectors adsorb only onto the target minerals. Regulators that interact with the mineral surface to facilitate collector adsorption are known as activators. Conversely, depressants are used to induce hydrophilicity of specific minerals to inhibit collector adsorption onto them and thus significantly reduce their recovery in the concentrate (Bulatovic, 2007).

2.5.4 Factors affecting flotation performance

The flotation process is complex, with many variables that can affect the performance and response of the circuit. Klimpel (1984) grouped the variables into three distinct categories as shown in Figure 2-13:chemistry, equipment, and operation. The scope of this study is largely focused on the chemistry of the flotation circuit with some mineralogical aspects.

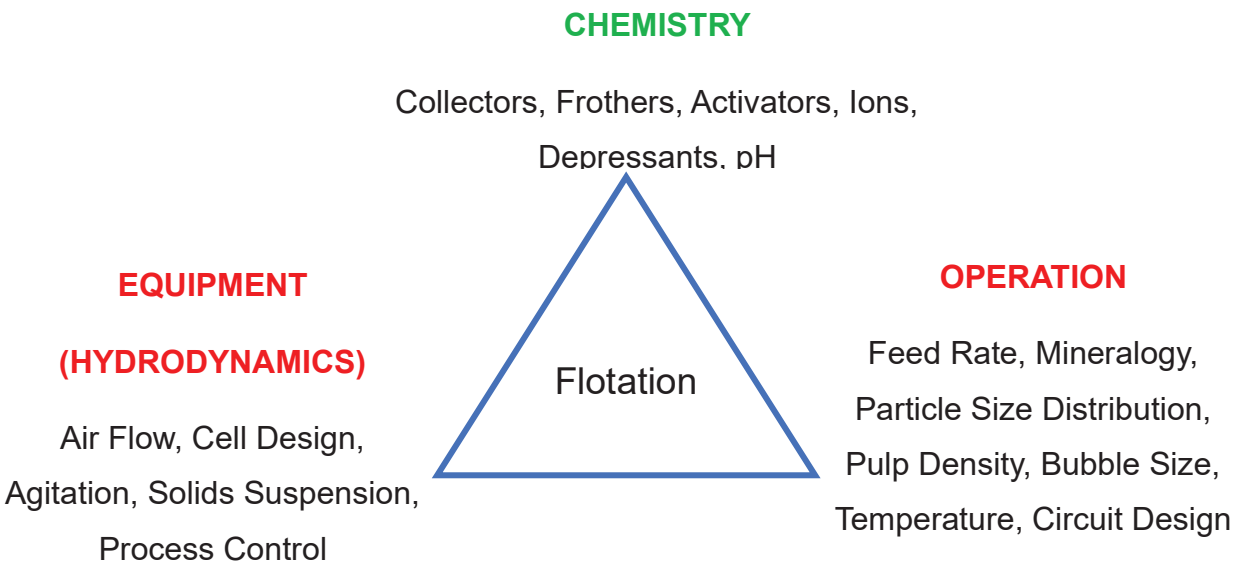

Figure 2-12: Flotation Parameters from (Klimpel, 1984)

2.6 Pulp Potential

The electrochemical approach of understanding flotation chemistry has provided reasonable justification for understanding the mechanisms by which collectors and mineral surfaces interact with one another (Woods, 2003). The fundamental reactions that govern the electrochemical activity are the anodic oxidation of mineral surfaces facilitated by interacting with the collector, and the simultaneous cathodic oxygen reduction process that allows the electron transfer to take place (Woods, 2003). The resulting potential when two or more electrochemical processes are taking place on the same electrode, in this instance being the mineral surface, is what is referred to as the pulp potential in a slurry (Wills & Finch, 2016).

The pulp potential plays a crucial role in the floatability of sulphide minerals. The hydrophobicity of the target minerals is heavily dependent on the redox reactions that take place on the mineral surfaces as these dictate the extent to which the collectors can adsorb onto the mineral surface (Hintikka & Leppinen, 1995). It is thus an important factor to monitor and control as it plays a pivotal role in the recovery of the target minerals. There are several factors that change the electrochemical environment, and thus affect the pulp potential. Two factors that are prevalent in the milling environment are the DO and the pH.

2.6.1 Dissolved Oxygen (DO)

Oxygen is an essential component required in the electrochemical system as it is key to complete redox reactions. There are several electrochemical interactions within the grinding environment which accelerate the rate of oxygen depletion (Bruckard, et al., 2011). Some of the processes and species that consume oxygen are; collector reactions, media corrosion (mild steel and forged steel media) and the sulphide minerals oxidation (Fuerstenau, et al., 2007). The competition for oxygen results in diminished oxygen levels in the system which has been observed to adversely impact the recovery (Bruckard, et al., 2011). Practically, DO makes it difficult to control the Eh on a plant as it will shift the potential to higher values through the relation shown in Equation 2-10.

$$Eh = 1.23 + 0.015 log P_{O_2} - 0.059 pH \qquad \text{Equation 2-10}$$

2.6.2 pH

pH control can be used to selectively float specific ores in a mineral mixture. This is due to the ore itself either exhibiting alkaline or acidic properties, which in turn dictates under which pH conditions a particular ore will float (Bulatovic, 2007). For instance, pyrite does not float in alkaline conditions despite the caustic nature of alkaline solutions helping in cleaning the surface to enhance collector adsorption (Bulatovic, 2007). Flotation is typically done under alkali conditions as the majority of collectors are stable under such conditions, and fortuitously corrosion of piping and equipment is minimized (Wills & Finch, 2016). The pH dependence of pulp potential is largely due to the enhancement or depression of the electrochemical reactions controlled by the presence or lack thereof, of ions for electron exchange. Hydroxyl and hydrogen ions interfere with and modify the electrical double layer and zeta potential around the mineral surface. This affects the hydrophobicity of the mineral which in turn impacts its floatability (Bulatovic, 2007).

For a given concentration of collector, there is a pH value where a given mineral will float or be depressed if it is below or above the value respectively. This critical value is dependent on; the mineral, collector type, collector concentration and temperature . shows how the critical pH changes with xanthate collector concentration for pyrite, galena and chalcopyrite. The lines on the graph outline the boundary at which minerals

become sufficiently hydrophobic to float . From Figure 2-13, it is evident that increasing pH at constant collector concentration allows for selective flotation of chalcopyrite from galena and pyrite as galena is not hydrophobic enough to float (region B), and for selective flotation of galena from pyrite, but no selectivity between galena and chalcopyrite as both are hydrophobic enough to float (region C). All minerals will float in region D and all minerals are not hydrophobic enough to float in region A

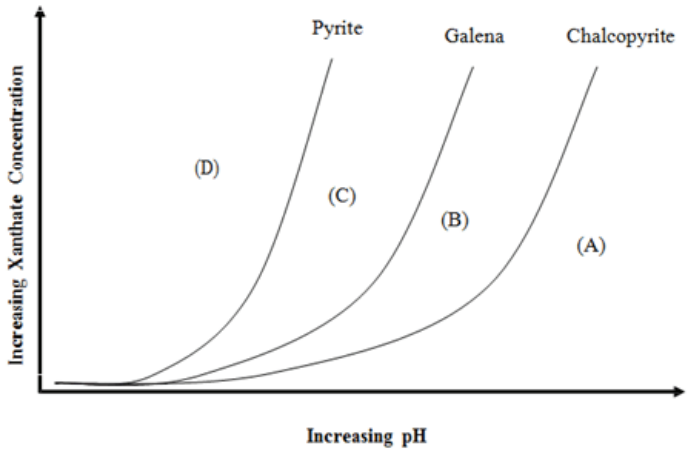

Figure 2-13: critical pH change with increasing collector concentration for pyrite, galena and chalcopyrite

Optimised pH regulation has operational advantages as lime (used to achieve alkalinity) is used in 6 different processes on a mine; post crushing, pre rougher flotation, pre concentrate regrind, pre cleaner flotation, in tailings disposal and post concentrate thickening (Zanin, et al., 2019). For sulphide mineral flotation, on average, the cost of lime may be double the cost of collector per ton of ore processed (Fee & Klimpel, 1986). This does vary significantly across operations but does present a huge opportunity for cost reduction and improved profitability for mining operations.

2.6.3 Industrial Relevance of Grinding Chemistry

Greet et al., (2006) conducted a study to observe the pulp chemistry of several plants to investigate the trends that influence the variability in industrial operations. An Eh-pH diagram of the pulp from different sections of a plant approximately 10 days apart was given. Despite the mineralogy of the ores being significantly different across the 10 day period, it was noted that they both maintained water equilibrium during flotation, but had different Eh-pH changes in the grinding circuit. This suggests that most of the significant reactions occur during grinding (Greet, et al., 2006). The investigation was

done using slurry from circuit streams for copper/gold and lead/zinc operations to observe how pulp potential parameters change across the circuit, and it was seen that the DO and Eh followed similar trends in terms of points of increase and decrease within the circuit as shown in Figure 2-14 and Figure 2-15 (Greet, et al., 2006). The changes were attributed to media corrosion during milling and aeration of the pulp, which suggests a strong correlation between Eh and DO.

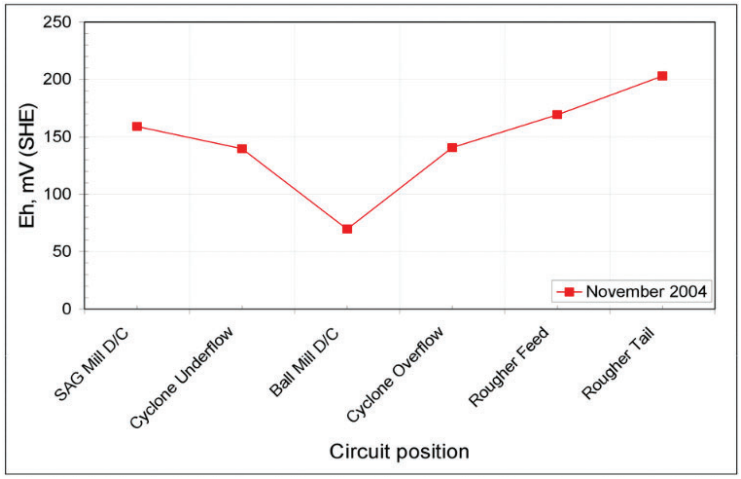

Figure 2-14 Pulp potential profile as a function of the circuit position taken from (Greet, et al., 2006)

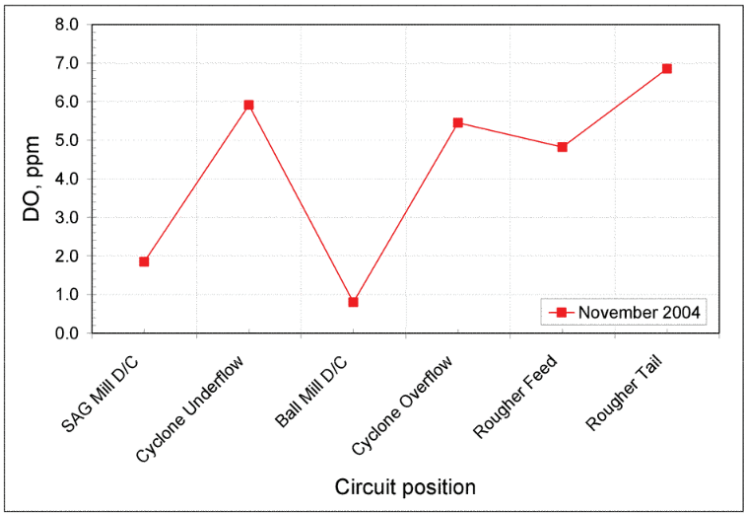

Figure 2-15 DO profile as a function of circuit position taken from (Greet, et al., 2006)

The DO and Eh decreased from the underflow to the ball mill and this was attributed to the corrosion of the forged steel grinding media that leached into the pulp and consumed oxygen in electrochemical reactions. The increases from the ball mill are due to the use of air as a flotation gas which enriched the pulp with oxygen; the environment became increasingly oxidising and increased the potential. Although the

trends for both copper/gold and lead/zinc operations were similar, the magnitudes were vastly different with the ball mill discharge being 75 mV and -35 mV for copper/gold and lead/zinc respectively. The differences in magnitude were linked to 2 parameters: mineralogy and operating pH. The sulphide content in the copper/gold ore was 5%, significantly less than the lead/zinc ore which on average reported 20% sulphide content, thus more reactive. The copper/gold operation ran at a pH of 12 which retarded corrosion while the lead/zinc operation ran at a pH of 8.5 where corrosion happened readily.

Yuan, et al., (1996) studied the possibility of gases with different oxygen activity to adjust the pulp potential and consider the influence on copper-zinc selectivity. A factorial design was conducted with; 2 grinding media types, 4 pre-conditioning types (no pre-conditioning, 0% oxygen (pure nitrogen) gas, 5% oxygen gas and air which is assumed to have 21% oxygen) and 3 flotation gas types (the same gases used in pre-conditioning). There was a strong relationship between the pre-conditioning gas and flotation gas used after using mild steel for grinding on the flotation selectivity. The pre-conditioning gas influenced the electrochemical activity of the pulp as gases with a higher partial pressure of oxygen resulted in an increase in the rate of oxidation of ferrous ions, with 5% oxygen and air flotation producing the best copper-zinc selectivity. For stainless steel grinding media, which generally provided good copper recovery, the interactions were statistically insignificant. The ferric ions leached from the media were suspected to influence the galvanic interactions observed with the mild steel. The pulp potential had a significant influence on the flotation results, with low recoveries observed at low potential values and higher recoveries as the potential increased.

2.7 Galvanic Interactions

Sulphide minerals have been known to be electrochemical conductors, hence when placed in an electrolytic solution such as process water which contains ionic species such as K^+, Na^+, Ca^{2+}, Mg^{2+}, SO_4^{2-}, Cl^-, F^-, as well as residual flotation reagents, they become electrodes, which can be demonstrated by connecting them to a reference cell which will result in a potential being recorded (Payant, et al., 2012). This conductivity is seen when measured against a known reference electrode, and once the mineral is in equilibrium with the environment, a potential is recorded. This

recorded electrical activity, known as the rest-potential, is what defines a mineral's electrochemical behaviour (Kwong, et al., 2003). Different sulphide minerals have different rest potential values when in solution. Table 2-2 lists the rest potential of some common sulphide minerals.

Table 2-2 Rest potential values extracted from (Payant, et al., 2012) (Chmielewski & Kaleta, 2011)

Mineral	Formula	Rest Potential vs S.H.E (Volts)
Pyrite	FeS_2	0.66
Chalcopyrite	$CuFeS_2$	0.56
Chalcocite	Cu_2S	0.44
Bornite	Cu_5FeS_4	0.40
Pyrrhotite	$Fe_{(1-x)}S$	0.31
Galena	PbS	0.28

Galvanic cells are setup when two or more electrochemically active minerals are placed in a solution that allows the flow of electrons (Holmes & Crundwell, 1995). This interaction alters the rate of the electrochemical reactions taking place at the mineral surface (Holmes & Crundwell, 1995).

2.7.1 Galvanic Interaction of Mineral Mixtures

When two sulphide minerals are in contact with one another in an electrolyte solution, the mineral with a lower rest-potential undergoes oxidation and acts as an anode while the mineral with the higher rest-potential acts as a cathode as seen in Figure 2-16 (Payant, et al., 2012).

The galvanic interactions between two sulphide minerals favours flotation of the anodic mineral as an oxidized mineral surface improves collector adsorption. (Bruckard, et al., 2011) The potential of the mixture is neither a simple sum or difference of the two rest potentials, but rather a value between the two potentials depending on the minerals (Bundy, 2008). This potential is known as the mixed potential and arises due to the occurrence of multiple electrochemical reactions happening simultaneously as shown in Equation 2-11 to Equation 2-13. The minerals will polarize each other in solution until they reach an equilibrium potential value. The lower rest-potential mineral will thus now have an increased current density in the presence of the higher rest-

potential mineral compared to the density it experiences when it is by itself (Bundy, 2008).

$$ZnS \longleftrightarrow Zn^{2+} + S^0 + 2e^- \quad \text{Equation 2-11}$$

$$0.5\ O_2 + H_2O + 2e^- \longleftrightarrow 2OH^- \quad \text{Equation 2-12}$$

$$Fe^{3+} + e^- \longleftrightarrow Fe^{2+} \quad \text{Equation 2-13}$$

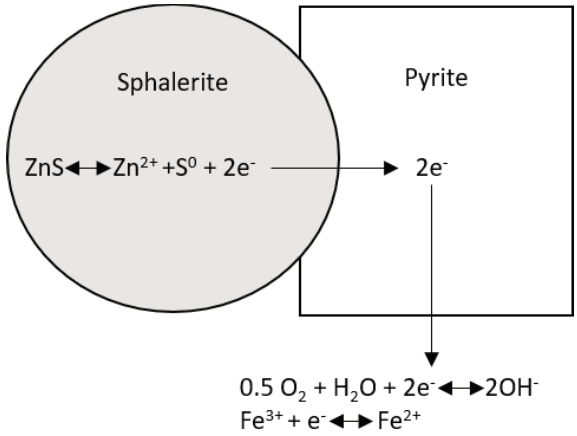

Figure 2-16: Mineral-Mineral galvanic interactions taken from (Payant, et al., 2012)

2.7.2 Galvanic Interactions of Grinding Media and Minerals

Like mineral mixtures, when grinding media comes in contact with sulphide minerals in an aqueous environment, a galvanic cell is set up as shown in Figure 2-18. Sulphide minerals generally have a higher rest potential to that of iron, which results in ferrous grinding media acting as the anode (Equation 2-14), and the sulphide mineral as the cathode as seen in Equation 2-15 (Rao, et al., 1976). The activity of grinding media is classified using the iron content, with the most active media containing the highest iron content, and noble media containing no iron, such as ceramic grinding media.

$$Fe \longleftrightarrow Fe^{2+} + 2e^- \quad \text{Equation 2-14}$$

$$0.5\ O_2 + H_2O + 2e^- \longleftrightarrow 2OH^- \quad \text{Equation 2-15}$$

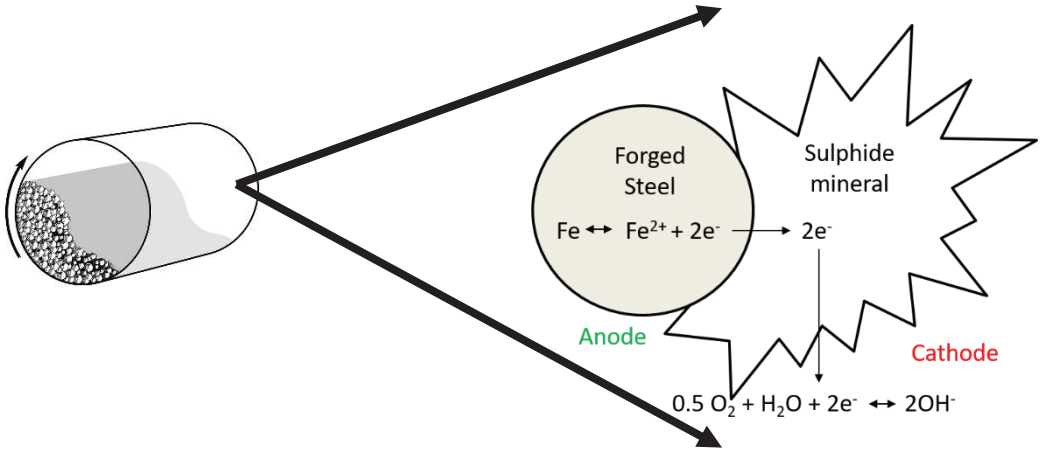

Figure 2-17 Media Mineral Galvanic Interactions

The resulting effect is decreased mineral floatability due to; an increase in oxygen consumption which produces a reducing environment that hinders collector oxidation and adsorption, as well as coating of the mineral surfaces with oxide layers which present hydrophilic tendencies and minimise self-induced flotation (Heyes & Trahar, 1979).

XPS analysis done by Huang & Grano (2005) revealed that more active material causes the formation of iron hydroxide species on the surface of the target minerals and that the presence of oxygen in the grinding system enhances the oxidation of the media and consequently increases the iron hydroxide species on the mineral surface. Yoa, et al., (2019) using XPS and a calcite ore, found that there were iron oxide species on the mineral surfaces of the calcite particles. Majority of the evidence suggests that iron oxide species are hydrophilic and inhibit flotation of minerals by reducing hydrophobicity and contaminating the surface where collector would have adsorbed (Yoa, et al., 2019; Wei & Sandenbergh, 2007; Greet, et al., 2004)

2.7.3 Galvanic Interactions of Grinding Media and Mineral Mixtures

In a system consisting of two or more minerals and grinding media, the mixed potential equilibrates somewhere between the highest and lowest rest potential in the system. The most noble mineral in the system is typically the cathode, and the ferrous media becomes the anode (Wills & Finch, 2016). The remaining mineral becomes an intermediary cathode and anode facilitating the movement of electrons. The mixed

potential will be higher than the natural rest potential of the grinding media resulting in it experiencing a higher charge density than normal leading to an increased rate of corrosion and leaching shown in Figure 2-18. The lower rest potential mineral surface will be more oxidised than the more noble minerals and will result in greater collector adsorption to that surface, and in turn will be preferentially floated (Pozzo, et al., 1990).

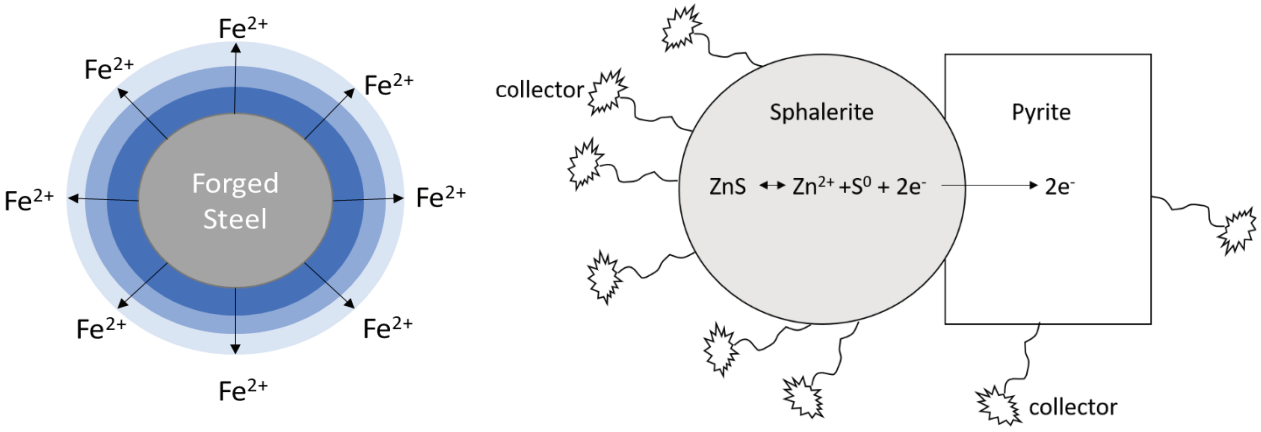

Figure 2-18 Increased charge density around grinding media and increased collector adsorption on lower rest potential mineral

3 Objectives, Key Questions and Hypotheses

Outlined in this chapter are the objectives and questions driving the research as well as the hypotheses to be investigated.

3.1 Objectives

The main objectives of this study are to determine:

1. The effect of pH on the flotation of and collector adsorption onto chalcocite and bornite
2. The effect of the water quality on the flotation and collector adsorption onto chalcocite and bornite
3. The electrochemical interactions taking place on the mineral surface of chalcocite and bornite
4. Copper recovery when chalcocite and bornite are floated together

3.2 Key Questions

1. What is the effect of pH on the adsorption and flotation of chalcocite and bornite?
2. What is the effect of pH on the surface charge of chalcocite and bornite?
3. How does the surface charge of chalcocite and bornite change in the presence of another mineral and ions?
4. Is there a synergistic effect on recovery by floating chalcocite and bornite together?

3.3 Hypotheses

1. At low pH, there will be inhibition of the formation of hydrophilic hydroxyl species on the mineral surface, resulting in more available surface area for collector adsorption and thus leading to an increase in the recovery by flotation.
2. As pH increases in a deionized process water solution, there is an increase in electron rich hydroxyl ions formed by reduction of oxygen, resulting in greater flow of electrons to the mineral surface, and this will consequently decrease the mineral surface charge, as measured by zeta potential

3. pH has a reduced impact on mineral surface charge in a system with increased ionic strength due to a higher likelihood of ions causing charge neutralisation in a complex water system
4. The mineral mixture of bornite and chalcocite will result in a galvanic cell that exposes the lower rest-potential mineral (bornite) to a highly oxidising environment and reduce the inert nature of the higher rest potential mineral (chalcocite), with electrons flowing from bornite to chalcocite, resulting in enhanced flotation of the bornite due a more oxidised surface that enhances collector adsorption

4 Experimental Design

The materials, methods, apparatus, and conditions used to test the hypotheses are detailed in this chapter.

4.1 Experimental Methodology

The study was carried out in two major phases; phase 1 consisting of grinding and batch flotation done at natural conditions with Synthetic Plant Water (SPW1) to obtain the Eh of the process and the corresponding mineral recovery. Phase two consisted of surface chemistry experiments to further understand the observations from the grinding and batch flotation tests. Surface chemistry tests were done at varying pH using 2 different water qualities outlined in Figure 4-1.

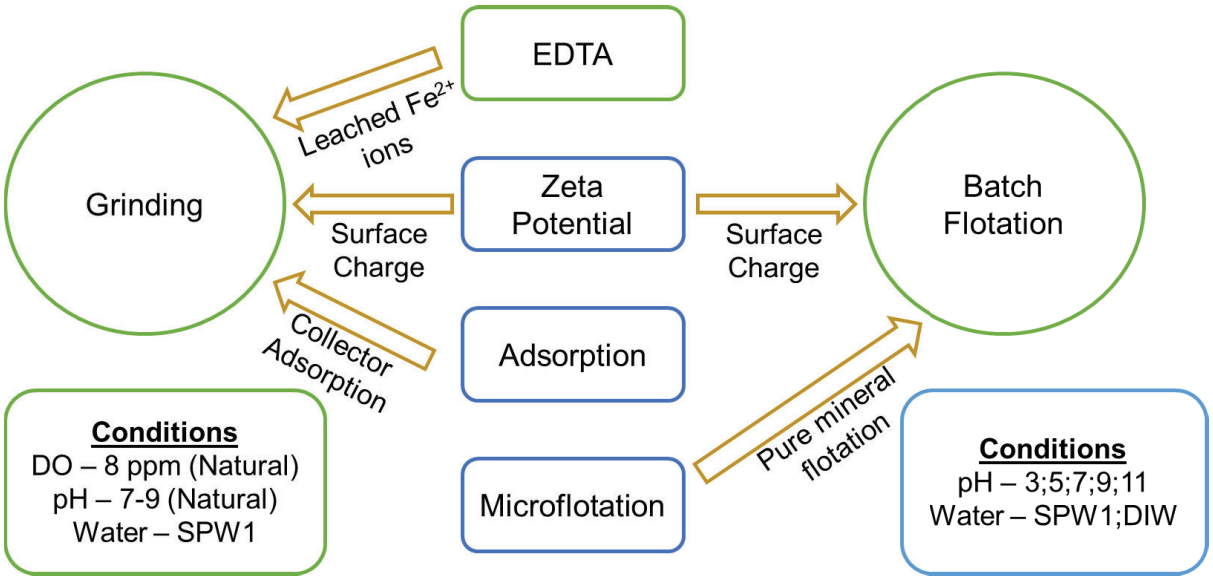

Figure 4-1 Research Methodology Overview

4.2 Materials

For this study, bornite and chalcocite were the sulphide minerals investigated. These minerals were selected owing to;

- the closeness in rest potentials of the minerals
- the presence and absence of Iron (Fe) in the minerals respectively
- the limited literature available on the flotation behaviour and properties of the minerals

Samples of bornite were sourced from Mineral World, Cape Town, South Africa, while samples of chalcocite were sourced from Central South University (CSU) in China.

4.2.1 Sample Mineralogy

The purity of the samples was assessed using X-Ray Diffraction (XRD). The mineral composition is shown in Table 4-1. Unfortunately, the sample purities were not optimal, particularly the large proportion of pyrite and marcasite in the chalcocite sample, thus any measurements of iron in chalcocite tests in this study are misleading.

Table 4-1 Sample Mineralogy

Mineral	Chalcocite	Bornite
chalcocite	62	-
bornite	-	42
chalcopyrite	<1	<1
pyrite	8	-
marcasite	24	-
magnetite	-	3
hematite	1	-
goethite	-	3
gibbsite	-	1
calcite	-	28
dolomite	-	3
quartz	4	16
mica	-	4
Total	**100**	**100**

4.2.2 Synthetic Ore Preparation

In industrial operations, a typical ore contains 0.25% to approximately 2% copper content with the average grade of 21st century copper ores being 0.6% (Barrera, 2020). To replicate this in laboratory conditions, a synthetic ore with 2.5% of copper mineral was created using industrial grade sand (quartz) and talc. The mineral was pulverized to a size fraction of -100 µm for batch flotation. Size fractions of -53 to +38 µm were used for adsorption and microflotation, while fractions of -32 µm Talc was included as

a gangue mineral due to its froth stabilizing properties which makes the results more reproducible and consequently reliable. The composition of the synthetic ore is shown in Table 4-2. The valuable mineral in the synthetic ore is not pure, and whose composition is shown in Section 4.2.1 for the chalcocite and bornite minerals respectively.

Table 4-2 Synthetic Ore Composition

Quartz	Copper Mineral	Talc
96.5%	2.5%	1%

4.2.3 Synthetic Plant Water

Synthetic plant water (SPW1) was used to mimic process water used in industrial operations with 1023 total dissolved solids (TDS) (Wiese, et al., 2005). Analytical grade salts with high purities, supplied by Merck, were used to create the concentrations shown in Table 4-3. It is important to note that current industrial operations can have significantly varied ion concentrations to that shown in Table 4-3 below, with sea water used in some instances.

Table 4-3 SPW1 Composition

Ion	Ca^{2+}	Mg^{2+}	Cl^-	SO_4^{2-}	NO_3^-	CO_3^{2-}	TDS	IS (mol/L)
Conc. (mg/L)	80	70	153	287	240	176	1023	0.0241

4.2.4 Pseudo Monolayer Collector Dosing

Sodium Isobutyl Xanthate (SIBX) was used as the collector in this investigation. The pseudo monolayers were used as approximations of how much collector is required to cover either half or the full of the surface area of the mineral for surface chemistry tests shown in Appendix 10.5. To calculate the required amount of collector, Brunner-Emmett-Teller (BET) surface analysis was conducted to calculate the mineral surface area. The head size of a molecule of collector was assumed to be 2.88 x 10^{-19} m^2 (Grano, et al., 1997). The calculation was carried out as shown below.

Table 4-4 collector dosage calculation for pseudo monolayer

Step	Calculation	Result

1	$mass\ of\ ore\ (g) \times\ BET\ surface\ area\ (\frac{m^2}{g})$	$surface\ area\ (m^2)$
2	$surface\ area\ (m^2) \div collector\ head\ size\ \frac{m^2}{molecule}$	$collector\ (molecules)$
3	$collector\ (molecules) \div Avogadro's\ number\ \frac{molecules}{mol}$	$monolayer\ moles\ (mol)$
4	$monolayer\ moles\ (mol) \times\ Molar\ mass\ \frac{g}{mol}$	$collector\ mass\ (g)$
5	$collector\ mass\ (g) \div concentration\ \frac{g}{ul}$	$collector\ volume\ (ul)$

4.3 Methods

This section outlines the experimental procedures carried out during the course of the investigations.

4.3.1 Zeta Potential

Zeta potential tests were conducted to determine the surface charge of the minerals at different pH values and in different water types to determine the effect of the presence and absence of ions in the solution on the surface charge of the minerals. The tests were done in using a Malvern ZetaSizer 4 shown in Figure 4-2 which uses electrophoretic mobility to calculate the zeta potential.

Figure 4-2 Malvern ZetaSizer 4

The tests were conducted at 5 pH values, 3, 5, 7, 9 and 11 with two water types, DIW and SPW1. The tests were conducted on pure bornite, pure chalcocite and a mixture of 50% bornite and 50% chalcocite. The experimental procedure was as follows and is shown in Figure 4-3;

1. Weigh 0.15 g of the sample and transfer to a beaker
2. Add 120 ml of water type that is filtered using 0.22 μm filter paper
3. Mix sample and water for 5 minutes on a magnetic stirrer
4. Ultrasonicate for 5 minutes to make sure sample is well dispersed
5. Return sample to magnetic stirrer and adjust pH with either HCl or NaOH until desired pH is attained
6. Allow 30 seconds for heavier particles to settle and transfer supernatant with lighter still particles into a vial for analysis using a Zeta Sizer

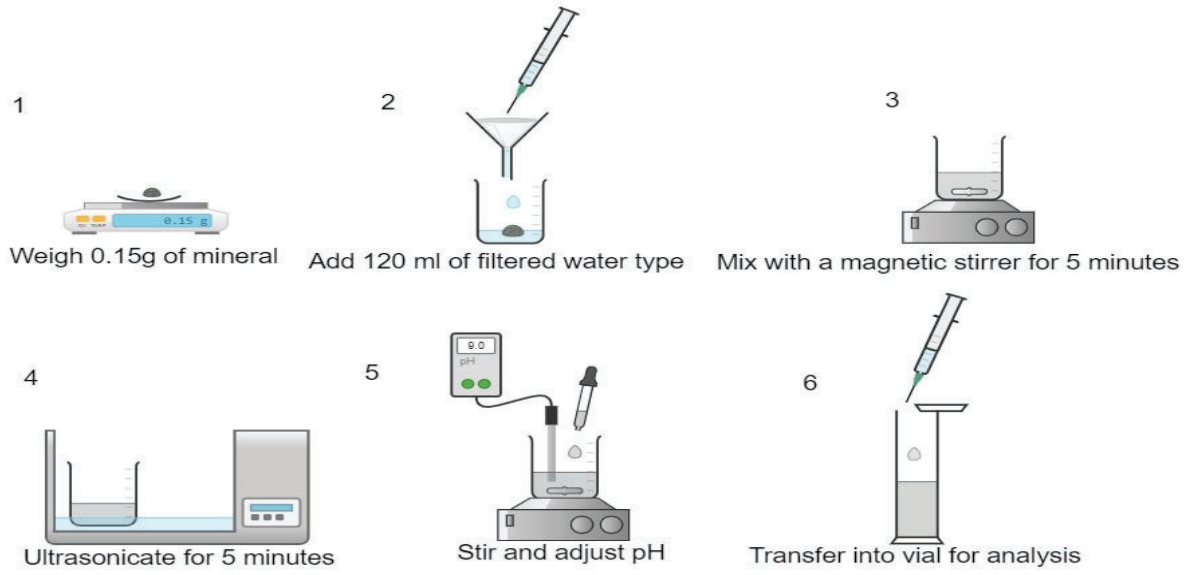

Figure 4-3 Zeta Potential Procedure Overview

4.3.2 Adsorption Studies

Collector adsorption tests were carried out on pure mineral samples to determine the residual collector in the solution, which indicates how much collector adsorbed onto the mineral surface per unit surface area. This was done using UV/Vis spectroscopy that measures absorbance according to the Beer-Lambert Law which relates the observed optical attenuation (absorbance) to the attenuation coefficient of the species, the optical path length and the concentration of the species as shown in Equation 4-1

$$A = \varepsilon \ell c \qquad \text{Equation 4-1}$$

$$A = Absorbance$$

$$c = concentration\ of\ attenuating\ species$$

From Equation 4-1, the molar attenuation is constant for a given substance, and the optical pathway used in the UV/Vis spectrometer is constant which leaves concentration as the only variable. The Beer-Lambert law is the linear $y = mx + c$ form with the absorbance being y, the molar attenuation and optical path length $\varepsilon\ell$ as the gradient m, the concentration being the variable x and c being the origin. Due to the extrapolatable relationship between absorbance and concentration, standard solutions of known SIBX concentration were made to measure their absorbance and produce a calibration curve for the different water types. Figure 4-4 show the calibration curves for SIBX in DIW and SPW1, respectively. The tests were run at a wavelength of 301 nm as SIBX has maximum absorbance at this wavelength. The tests were conducted in two water types, SPW1 and DIW; five pH values, 3, 5, 7, 9, 11; and 2 collector dosages, 0.5 monolayer and 1 monolayer.

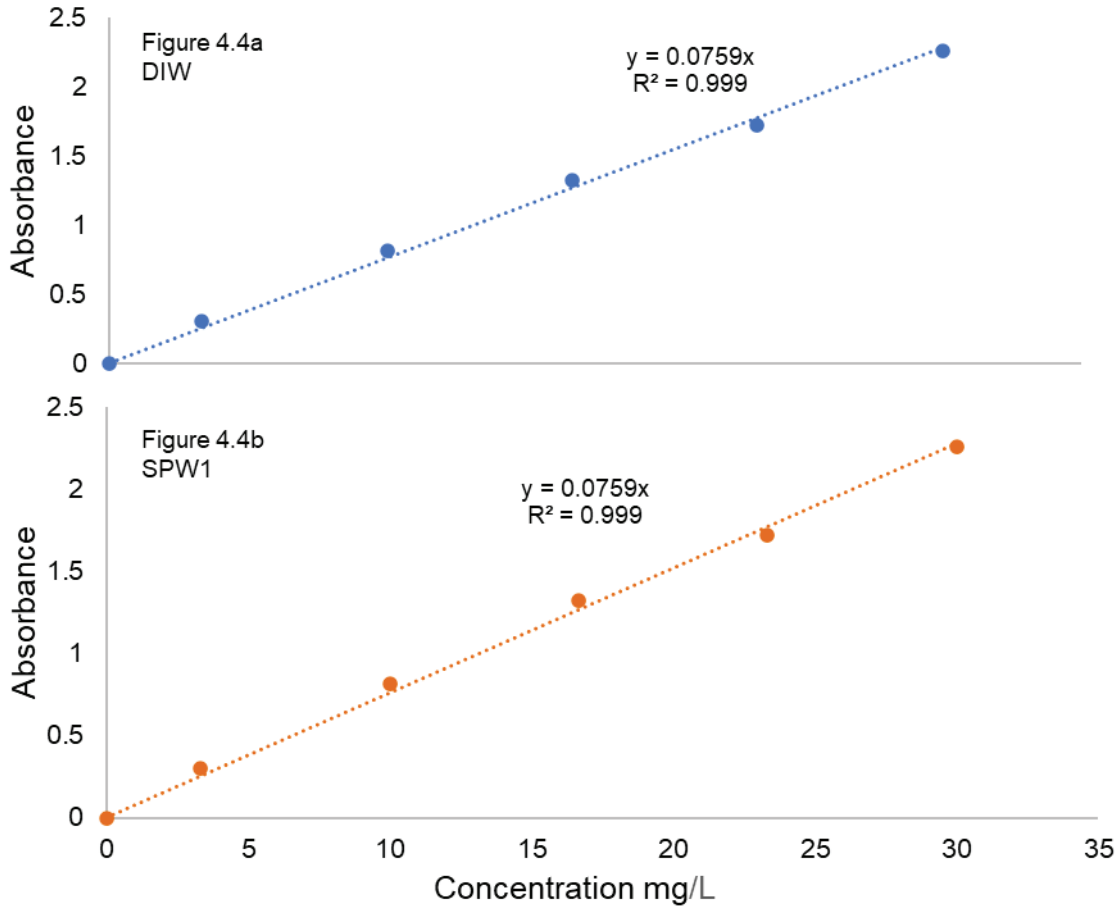

Figure 4-4 SIBX Calibration Curves for (a), DIW and (b) SPW1 respectively

For the experimental procedure, 2 grams of the mineral were added into 30mL of the water type in a conical flask. The slurry was put onto a magnetic stirrer and the pH adjusted to the desired value using solutions of 0.1M sodium hydroxide (NaOH), 1M NaOH, 0.1M hydrochloric acid (HCl), 1M HCl and 0.1M sodium tetraborate ($Na_2[B_4O_5(OH)].{}_8H_2O$) buffer solution. Once the pH value has been attained and stabilised, collector is dosed into the slurry. The top of the flask was covered in foil and the flask secured in an Ecobath shaker (Figure 4-5) at 25^0C and speed of 130 rpm for 3 minutes. After 3 minutes of mixing in the water bath, 10mL of the slurry was extracted using a syringe, and a filtered through a 0.45 µm filter. The filtrate was collected and transferred into a cuvette for analysis using a UV-Vis spectrophotometer (Figure 4-6).

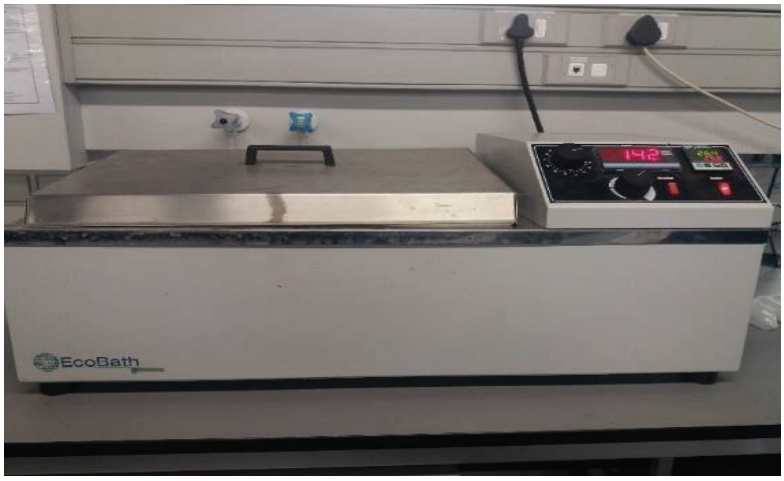

Figure 4-5 Ecobath shaker used for adsorption studies

Figure 4-6 UV/VIS Spectrophotometer used for adsorption

4.3.3 Microflotation

Microflotation was conducted on pure mineral samples at starvation doses of collector (0.5 pseudo monolayer) to determine the mineral flotation at various pH values in the microflotation cell shown in Figure 4-7. To achieve this, the water type being used was adjusted to the required pH by adding HCl or NaOH. Once the required pH was achieved, 3 g of the mineral were weighed out in a beaker and the adjusted pH water added to the mineral to create a slurry. The slurry's pH was adjusted to maintain the desired pH and dosed with collector. The slurry mixture was then transferred into the microflotation cell using a funnel and the beaker cleaned out using the adjusted water until all the slurry is transferred. The adjusted pH water was then added until the total volume of 250ml was reached, and the peristaltic pump was turned on to circulate the pulp at a speed of 65 rpm. The pulp was allowed to settle for 1 minute before adding water to fill the concentrate launder, being careful not to disturb the pulp. Air was introduced from the bottom of the cell at 7 mL/min. Air was introduced from the bottom of the cell at 7 mL/min. The concentrates were collected at 2, 6, 12, and 20 minutes of flotation. The tails were collected, and the cell cleared out to ensure there is no residual mineral. The concentrates and tails were filtered and dried at room temperature overnight and weighed.

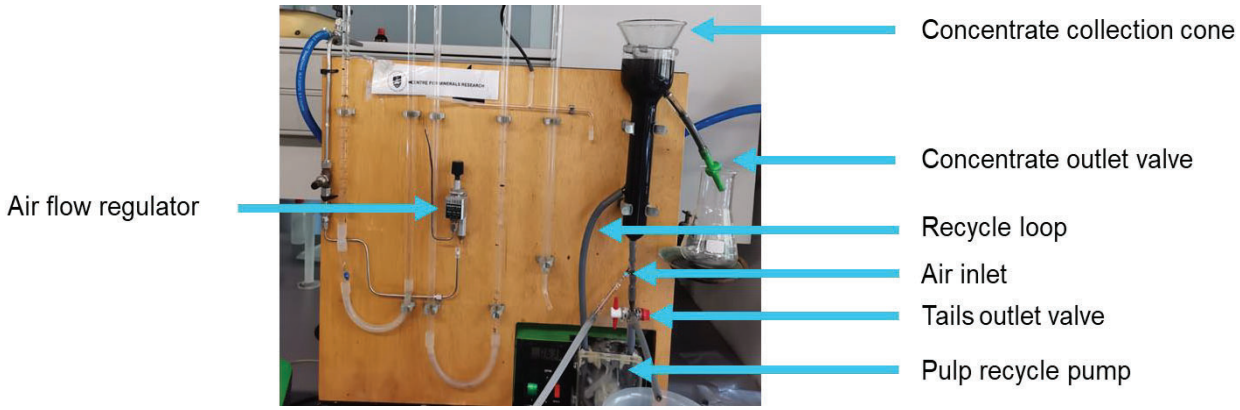

Figure 4-7 Microflotation Cell

4.3.4 Grinding

Grinding was conducted in the highly instrumented Magotteaux Mill® shown in Figure 4-8 which is capable of measuring and controlling the pH, Eh, DO and temperature. The pH, Eh and DO probes were calibrated daily using standard solutions of known values. The pH was calibrated with buffer solutions of pH 7 and 10, Eh with a solution

of 250 mV, and DO calibrated with both a 0 ppm DO solution as well as 8 ppm DO air calibrated. The grinding media used was 21% chrome which is relatively inert but was stored in a lime solution to prevent any possible oxidation.

Prior to grinding, 2 kg of the synthetic ore was made using quartz, talc and the mineral according to the composition outlined in Table 4-2. It was transferred into the mill with 1 L of SPW1 to make up 66% solids. 20 kg of grinding media was used. A 1 wt% solution of SIBX was made using 1 g of SIBX powder and 100 ml of distilled water. The mill was dosed with 20 ml of the collector solution (equivalent dosage of 100 g/ton). Dosing was done in the mill to maximise collector adsorption (Greet, et al., 2010) onto the mineral surface and minimise the formation of ferrous iron oxides on mineral surfaces that prevent adsorption and reduce floatability (Greet, et al., 2004). Conditioning in the mill was done at 10 rpm for 10 minutes followed by milling for 22 min and 18 seconds to achieve a grind of 60% passing 75 µm.

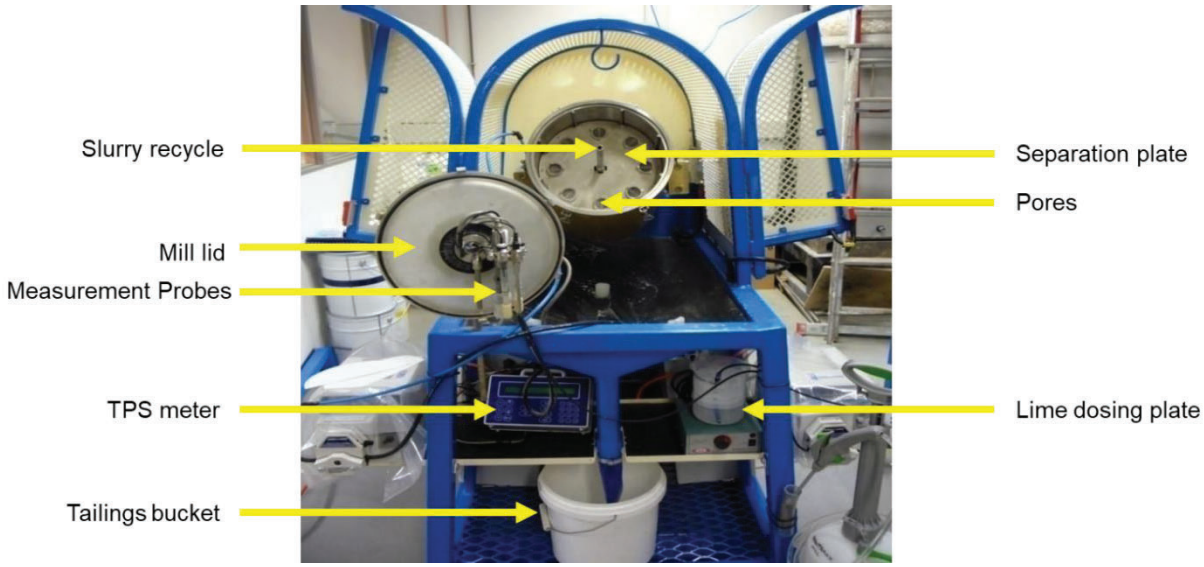

Figure 4-8 Magotteaux Mill®

4.3.5 Flotation

The flotation tests were carried out in a 4.5 litre Magotteaux flotation cell. This bottom driven cell was developed to allow froth to be removed from the whole cell surface and minimize error. The use of it in conjunction with the Magotteaux Mill allows the continuous monitoring of the pulp chemistry through probes that can be fitted in the rear of the cell and measure the pulp phase.

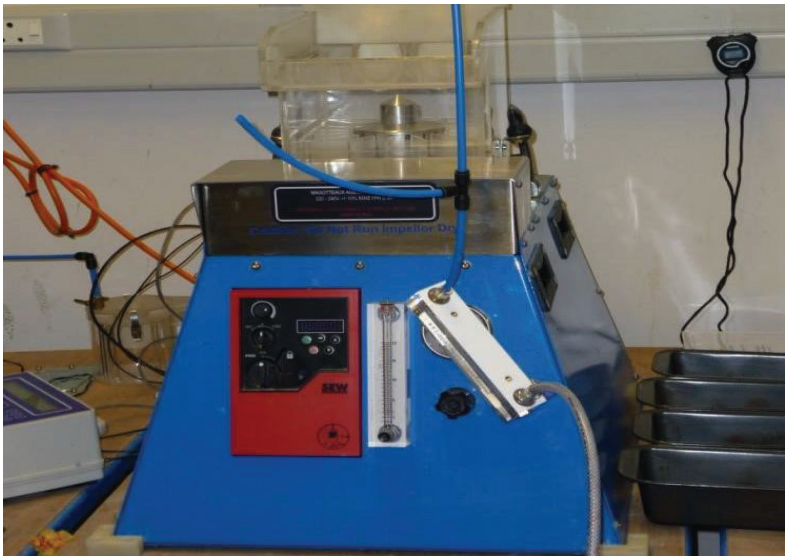

Figure 4-9 Magotteaux 4.5 litre flotation cell

After milling, the slurry was transferred into the float cell and the required cell volume was made up with SPW1. Once filled, the impeller was turned on to 1200 rpm and the slurry was stirred for 2 minutes. During these two samples of the feed were extracted, one for XRF analysis to determine feed composition and the other for EDTA extraction. After conditioning Dow 200 frother was added at a dosage of 50 g/ton and allowed to condition for 2 minutes. The air valve was opened and run at 13 L/min as the froth started to build up. 4 concentrates were collected after 2, 4, 6, and 8-minute intervals (Figure 4-10), totalling 20 minutes of flotation, with concentrate scrapped off every 15 seconds during each concentrate collection. The froth height was maintained at 2 cm by the consistent manual addition of SPW1.

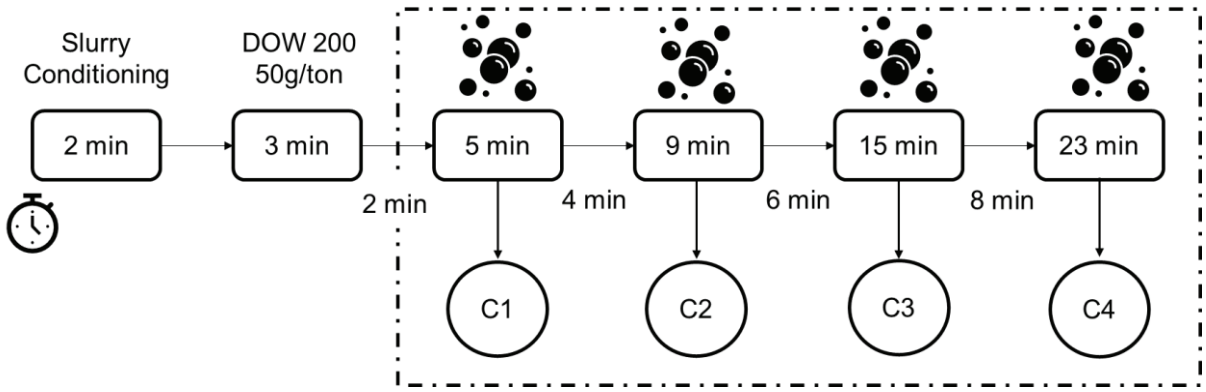

Figure 4-10 Batch flotation experimental sequence

5 Results

This chapter outlines the results obtained from the investigations carried out according to the research methodology outlined in the Experimental Design chapter.

5.1 Reproducibility

The tests were conducted in duplicate, and where variations beyond 10% occurred, a triplicate was done rule out any outliers. The precision of the data is shown using error bars calculated using sample set variance. Figure 5-1and Figure 5-2 illustrate how closely the duplicate runs were maintained to ensure reproducibility.

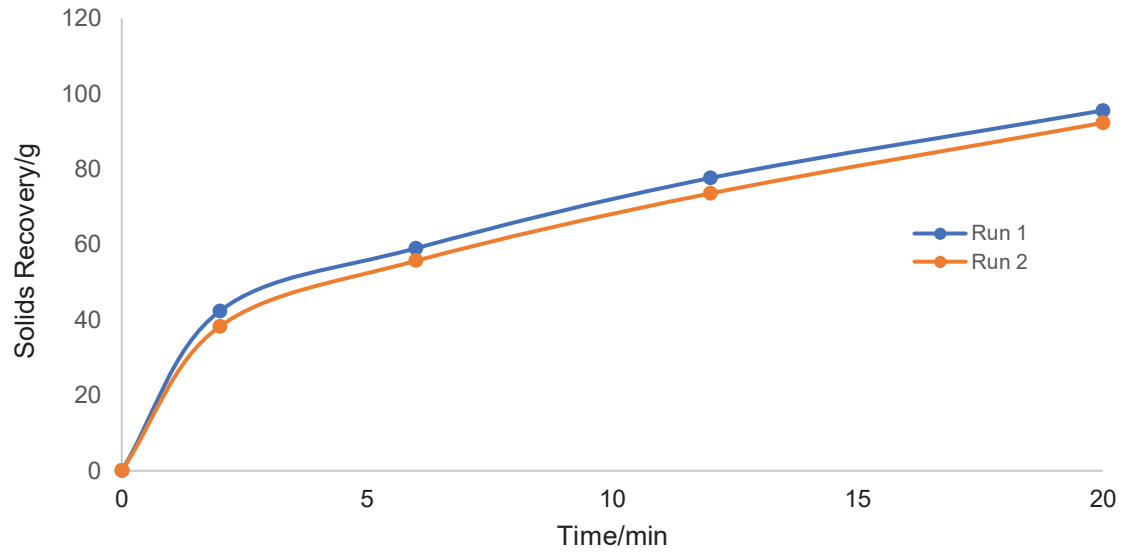

Figure 5-1 Duplicate runs showing solids recovery for chalcocite batch flotation

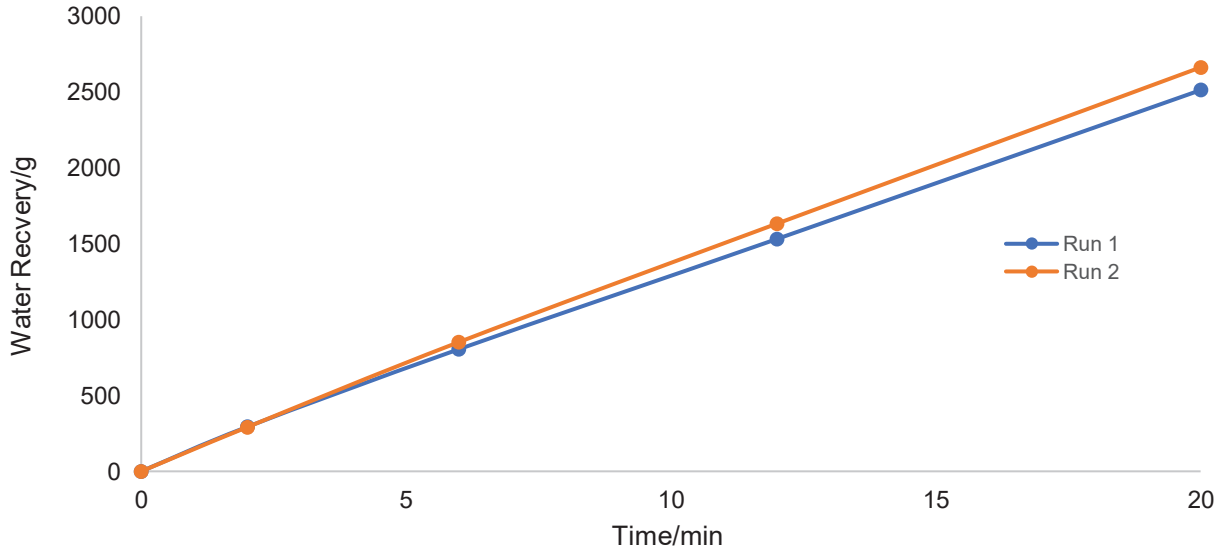

Figure 5-2 Duplicate runs showing water recovery for chalcocite batch flotations

5.2 Effect of pH on microflotation response of bornite and chalcocite

The flotation response of bornite and chalcocite under varying pH; 3-11, were tested using microflotation in order to determine the mineral recovery under changing electrochemical conditions. The microflotation tests were conducted using a collector dosage of 0.5 pseudo monolayer (see Pseudo Monolayer Collector Dosing).

5.2.1 Bornite

Microflotation of bornite using DIW, over the pH range 3-11, as seen in Figure 5-3 shows that bornite recovery between pH 5 and pH 11 is generally the same, with the recovery being lower at pH 3. Alkaline pH values show a similar trend to that under SPW1 where the solids recoveries at pH 7, 9 and 11. In contrast to SPW1, the highest recovery rate is at pH 5 and the lowest at pH 3 in DIW.

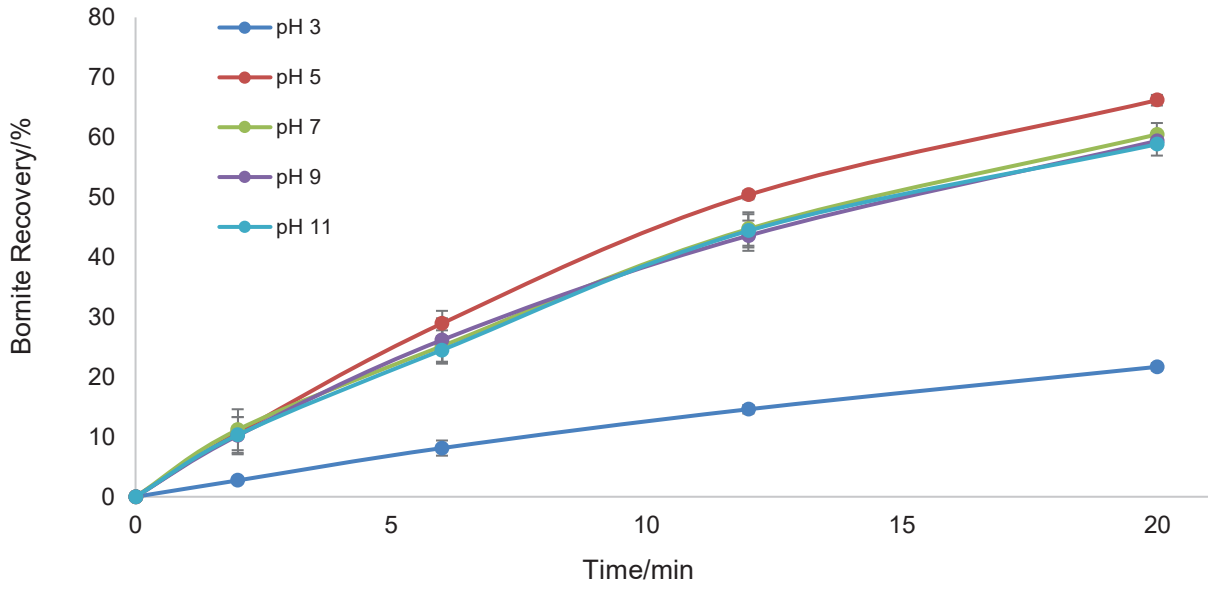

Figure 5-3 Pure Bornite recovery (%) by microflotation vs time (min) in DIW over the pH range 3-11. Error bars represent the standard deviation between duplicate test (where error bars cannot be seen, they are smaller than the data marker)

Figure 5-4 shows the microflotation response of bornite using SPW1. Bornite recovery for the first concentrate (first 2 minutes of flotation) is generally the same regardless of the pH. The recovery rate is similar and almost indistinguishable in neutral to alkaline conditions (pH 7, 9 and 11) whereas in acidic conditions, the recovery rate is lowest at pH 5 and highest at pH 3. The final solids recovery is higher in alkaline conditions and lowest at pH 5. The highest recovery is obtained at pH 3 which is an anomaly to the trend of lower recoveries in acidic conditions.

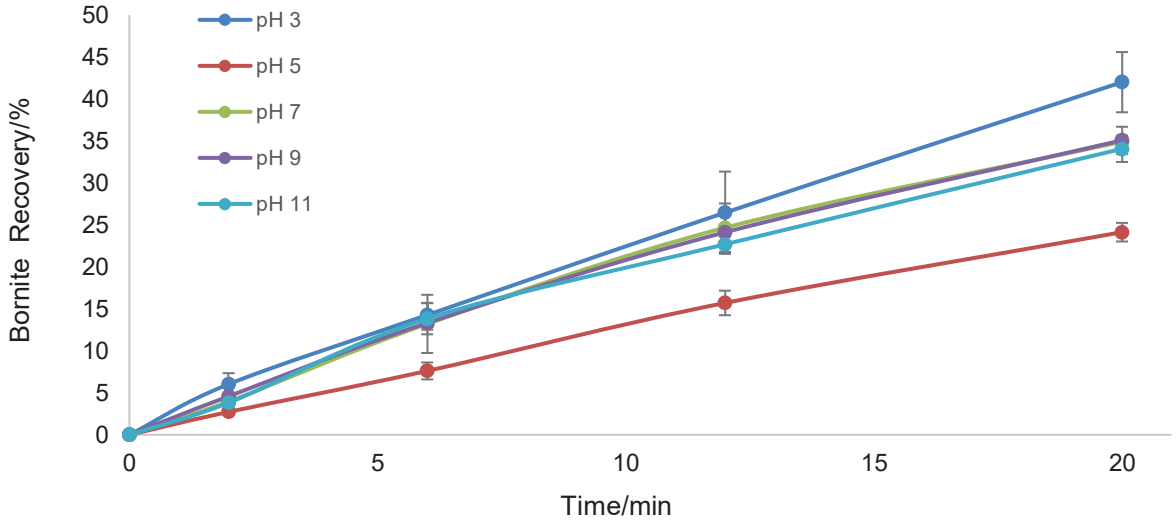

Figure 5-4 Pure Bornite recovery (%) by microflotation vs time (min) in SPW1 over the pH range 3-11. Error bars represent the standard deviation between duplicate test (where error bars cannot be seen, they are smaller than the data marker

5.2.2 Chalcocite

In DIW, after 2 minutes of flotation, a difference in recovery across the pH values begins to emerge and continues throughout the flotation period as seen in Figure 5-5. The lowest recovery is obtained at pH 5, similar to chalcocite in SPW1. The highest recoveries were obtained in the order pH 3 = pH 9> pH 11> pH 7> pH 5, with pH 9 slightly obtaining higher recoveries than pH 3 after 12 minutes of flotation.

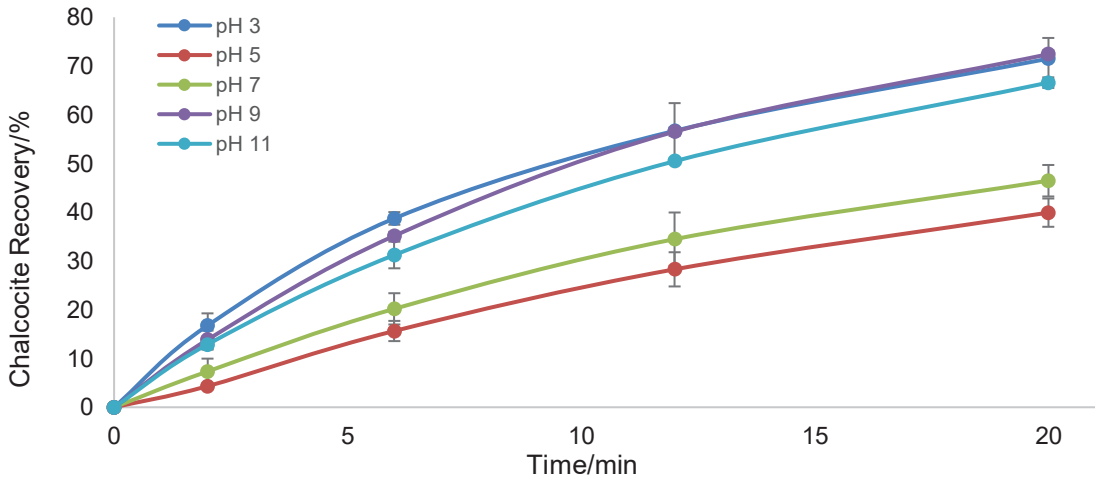

Figure 5-5 Pure Chalcocite recovery (%) by microflotation vs time (min) in DIW over the pH range 3-11. Error bars represent the standard deviation between duplicate test (where error bars cannot be seen, they are smaller than the data marker

Similar to bornite, chalcocite flotation in SPW1 for the first concentrate is generally the same regardless of pH except for pH 5 as seen in Figure 5-6. After the first

concentrate, there is variability of recoveries with changing pH as the highest recoveries were obtained in the order pH 3 = pH 7> pH 11> pH 9> pH 5. Between 2 and 12 minutes of flotation, pH 7 has a slightly higher rate of recovery compared to pH 3. After 12 minutes, pH 3 has a higher recovery rate after an acceleration in recovery visible between 2 and 12 minutes. In SPW1, there is a consistent final recovery difference between the different pH values, whereas in DIW, there appears to be 2 distinct regions of low and high recoveries

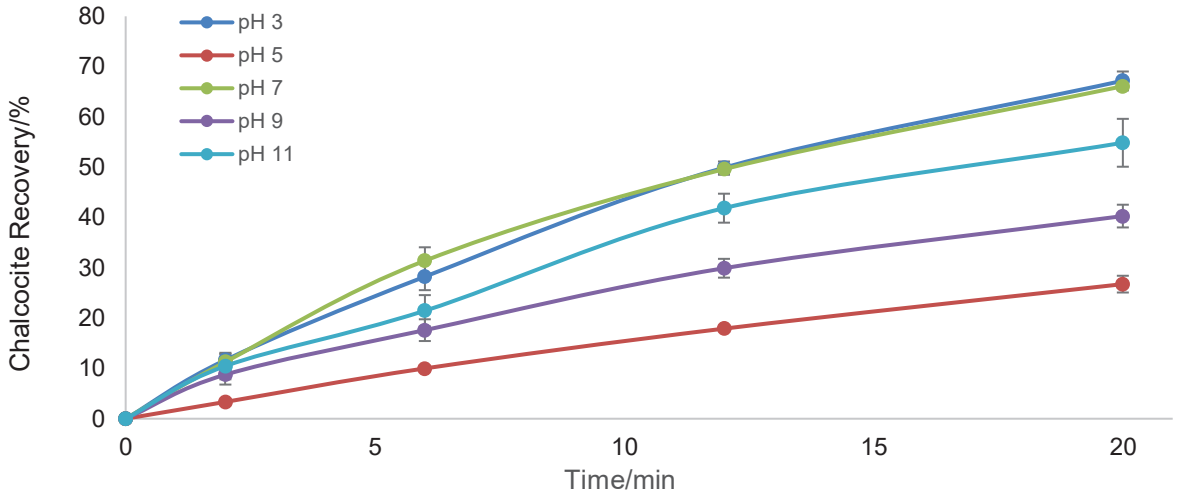

Figure 5-6 Pure Chalcocite recovery (%) by microflotation vs time (min) in SPW1 over the pH range 3-11. Error bars represent the standard deviation between duplicate test (where error bars cannot be seen, they are smaller than the data marker

5.3 Effect of pH on collector adsorption onto bornite, chalcocite and the mineral mixture

Collector adsorption onto the mineral surfaces was tested over the pH range 3-11 in SPW1 and DIW. The figures illustrate the residual xanthate that has not been adsorbed onto the mineral surface. Two collector dosages were used; 0.5 pseudo monolayer and 1 pseudo monolayer (see Pseudo Monolayer Collector Dosing).

5.3.1 Bornite

Figure 5-7 shows the concentration of SIBX remaining in the solution after conditioning in the slurry for bornite. The concentration of SIBX in solution decreases as the pH increase from 3 and reaches a minimum at 7 and begins to increase as the pH increases from 9 to 11. There is a higher residual concentration in DIW compared to SPW1 for the tests done with 1 monolayer of collector at all pH values except for pH 11. At pH 3, 5 and 7 there is a higher residual concentration in SPW1 than in DIW for

a dosage of 0.5 monolayer. For pH 9 and 11, there is significantly more residual collector in DIW than in SPW1.

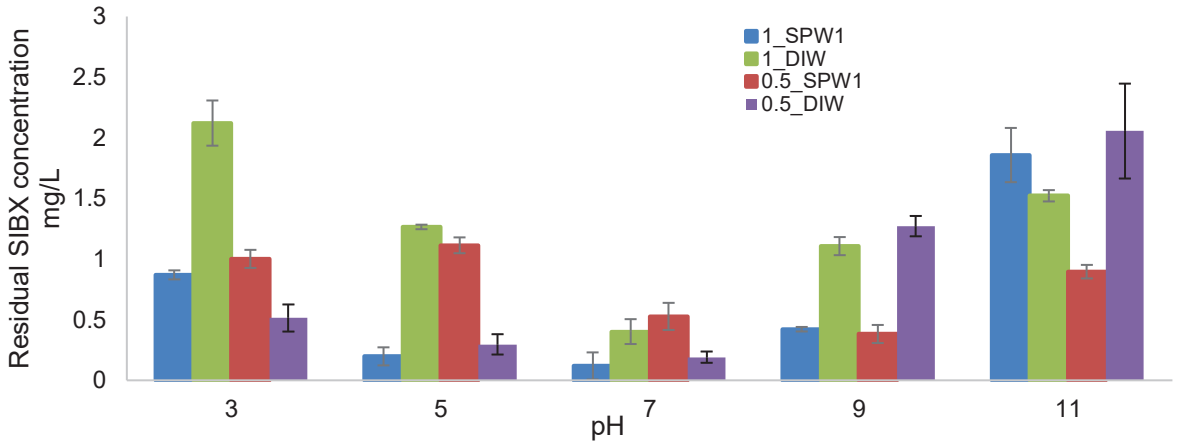

Figure 5-7 Residual SIBX in SPW1 and DIW over pH range 3-11 at 0.5 and 1 monolayer dosages for Bornite. Error bars represent the standard deviation between duplicate test (where error bars cannot be seen, they are smaller than the data marker

5.3.2 Chalcocite

Figure 5-8 shows the concentration of SIBX remaining in solution after conditioning with the slurry for chalcocite. Chalcocite generally had a high adsorption rate with minimal SIBX remaining across all pH values. Dosages of 1 monolayer had higher residual concentrations than that of their 0.5 monolayer dosages in each water type. pH 9 and 11 had significantly higher SIBX concentrations in the DIW water type with a 1 monolayer collector dosage.

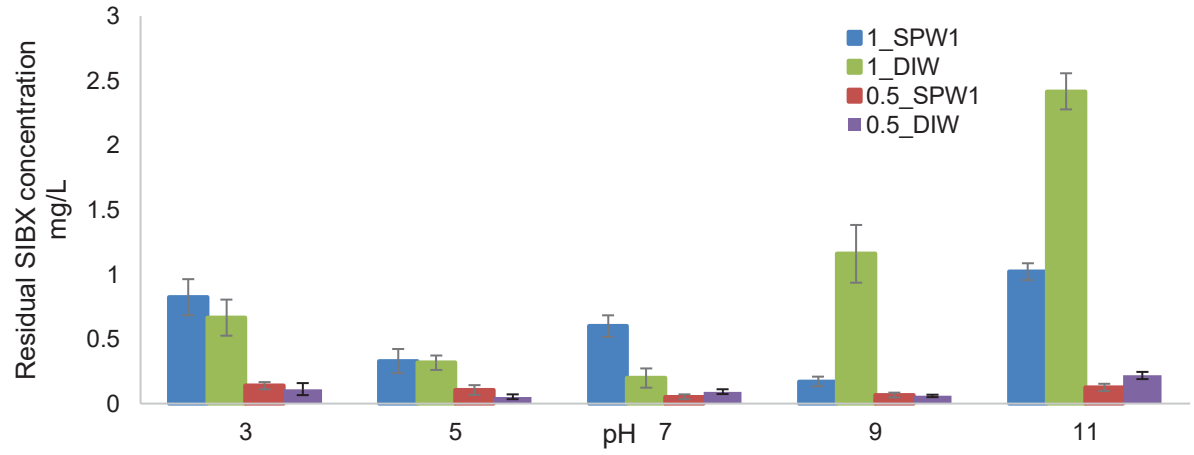

Figure 5-8 Residual SIBX in SPW1 and DIW over pH range 3-11 at 0.5 and 1 monolayer dosages for Chalcocite. Error bars represent the standard deviation between duplicate test (where error bars cannot be seen, they are smaller than the data marker

5.3.3 Chalcocite and bornite

Figure 5-9 shows the concentration of SIBX remaining in the solution after conditioning in the slurry with an equal mass mixture of chalcocite and bornite. The SIBX dosages were adjusted according to the surface area of the minerals present to have the same monolayer coverage for each mineral (see **Pseudo Monolayer Collector Dosing**). The mineral mixture generally shows low residual SIBX concentrations for pH 3 to pH 9, with all conditions having significantly higher residual concentrations at pH 11. There is a higher residual concentration in the DIW water type than SPW1 for a dosage of 1 monolayer at pH 9 , with the opposite trend appearing for pH 3 and 11 and insignificant variation for pH 5 and 7. At a dosage of 0.5 monolayer, there is a higher residual concentration in the SPW1 water type compared to DIW for pH 3, 5 and 7. At pH 9 and 11, there is a significantly higher concentration of collector in DIW compared to SPW1 for the 0.5 monolayer dosage.

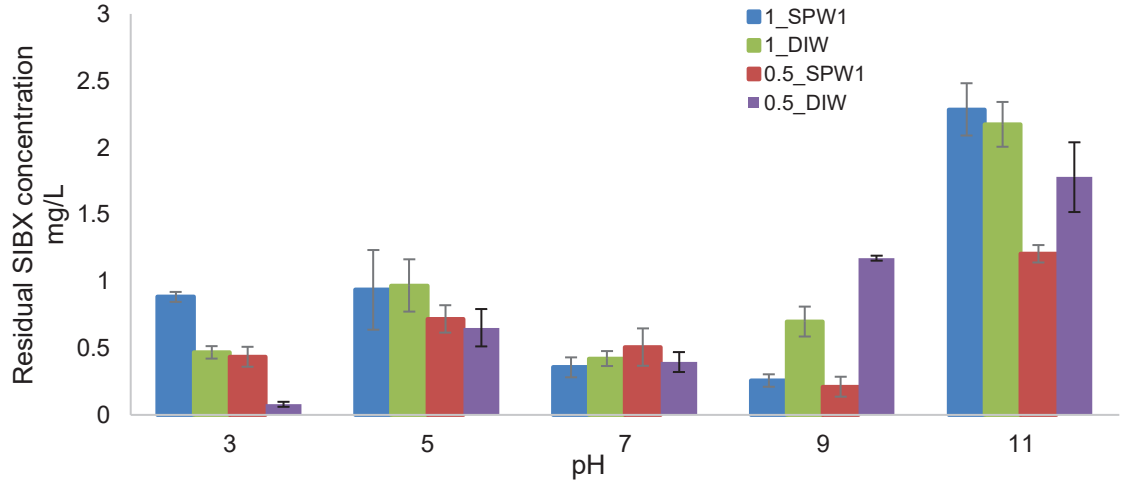

Figure 5-9 Residual SIBX in SPW1 and DIW over pH range 3-11 at 0.5 and 1 monolayer dosages for the mineral mixture. Error bars represent the standard deviation between duplicate test (where error bars cannot be seen, they are smaller than the data marker

5.4 Zeta Potential

Zeta potential tests were carried out over the pH range 3 – 11 to investigate the mineral surface charge. This was done to correlate with the flotation and collector adsorption under the same conditions and provide insight into the possible electrochemical interactions taking place at the surface that would result in the observed potential.

5.4.1 Water quality effect on surface charge

Figure 5-10 shows the zeta potential of bornite, chalcocite and the mineral mixture of chalcocite and bornite in SPW1. All minerals have the same trend of increasing potential from pH 3 and reaching a maximum at pH 5 after which a decrease is seen. Bornite exhibits two isoelectric points (IEP); one between pH 4 and 5 and the second between pH 5 and 6. The mineral mixture trend traces more closely to that of chalcocite, with a lower potential profile.

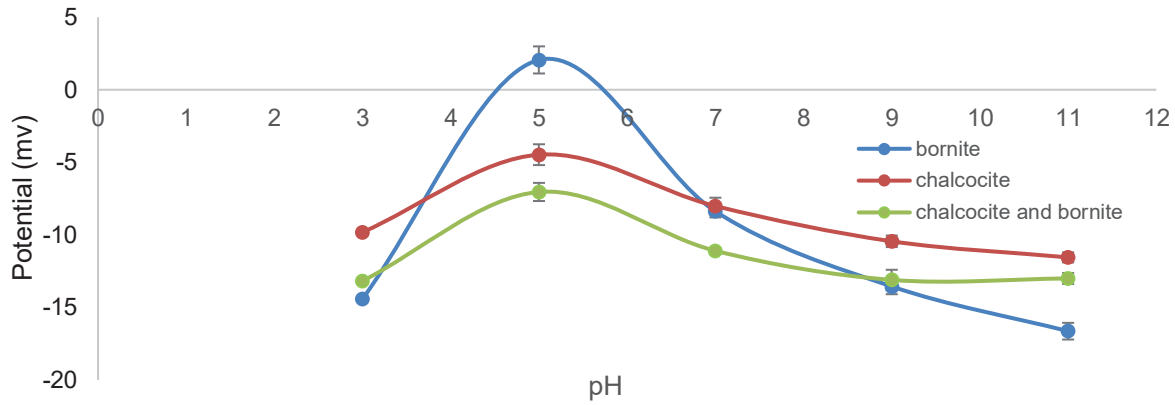

Figure 5-10 Zeta Potential of bornite, chalcocite and mixed mineral in SPW1 from pH 3 to 11. Error bars represent the standard deviation between duplicate test (where error bars cannot be seen, they are smaller than the data marker

Figure 5-11 shows the zeta potential profiles in DIW. The potential profiles have a similar trend to that in SPW1 of increasing potential from pH 3, reaching a maximum at pH 5 and then decreasing. In DIW, all minerals have two isoelectric points. Bornite has isoelectric points at pH 3.7 and pH 8; chalcocite at ~pH 3.5 and ~pH 6.5; and the chalcocite and bornite mixture at pH 4 and ~pH 8.5.

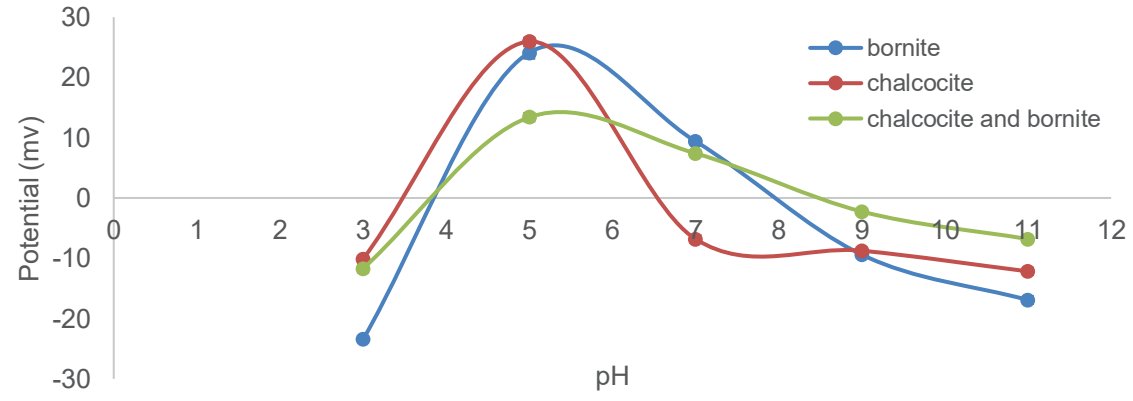

Figure 5-11 Zeta Potential of bornite, chalcocite and mixed mineral in DIW from pH 3 to 11. Error bars represent the standard deviation between duplicate test (where error bars cannot be seen, they are smaller than the data marker

5.4.2 Bornite

Figure 5-12 shows the zeta potential profile of bornite in SPW1 and DIW. In both SPW1 and DIW, the zeta potential increases from pH 3 and reaches a peak at pH 5. After pH 5, the potential continues to decrease, with a decelerating decrease rate from pH 9. In DIW, the first IEP is pH 3.68, with the second IEP at pH 8. The potential profile in DIW has a large range, with the most negative at pH 3, recording a potential of -23 mV and the most positive at pH 5 with a potential of 24 mV. In SPW1, the potential profile has a smaller range, with the most negative being -17 mV at pH 11 and the most positive at 2 mV at pH 5. The IEPs in SPW1 are much closer, with the first one at pH 4.5, and the second one at pH 5.75. The general effect that SPW1 exhibited was of flattening the potential to overall more negative values compared to DIW.

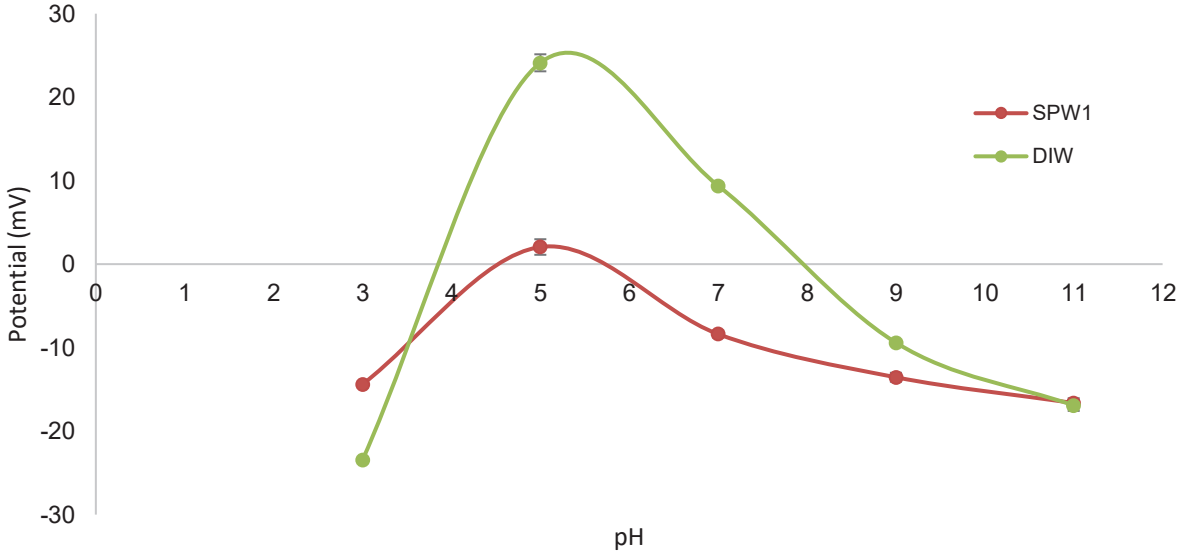

Figure 5-12 Zeta potential of bornite in SPW1 and DIW from pH 3 to 11. Error bars represent the standard deviation between duplicate test (where error bars cannot be seen, they are smaller than the data marker

5.4.3 Chalcocite

Figure 5-13 shows the zeta potential profiles of chalcocite in SPW1 and DIW. The trend in both water types is increasing from pH 3, reaching a maximum at pH 5 and decreasing subsequently. There are two IEPs in DIW: pH 3.50 and pH 6.55. The potentials in the two water types deviate significantly in value between pH 3 and 7 but have similar values at pH 3 and from pH 7 to 11. The difference is due to the different potentials at pH 5, with a higher potential in DIW at 25 mV compared to a peak of -4 mV at pH.

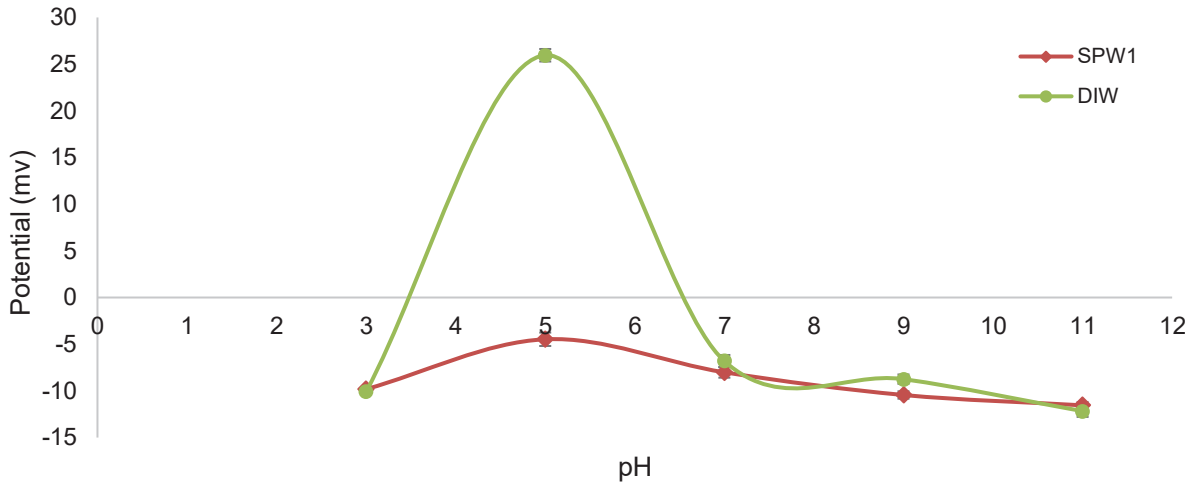

Figure 5-13 Zeta potential of chalcocite in SPW1 and DIW from pH 3 to 11. Error bars represent the standard deviation between duplicate test (where error bars cannot be seen, they are smaller than the data marker

5.4.4 Chalcocite and Bornite

Figure 5-14 illustrates the zeta potential profile of the mineral mixture of chalcocite and bornite in SPW1 and DIW. Similar to bornite and chalcocite's individual profiles, there is an increase from pH 3, reaching a maximum at pH 5 and a decrease thereafter. Similar to chalcocite, only the mineral mixture in DIW has IEPs; first one at pH 3.85 and the second at pH 8.50. The DIW profile generally has higher potentials at all pH values, exhibiting a negatively shifted profile from DIW to SPW1.

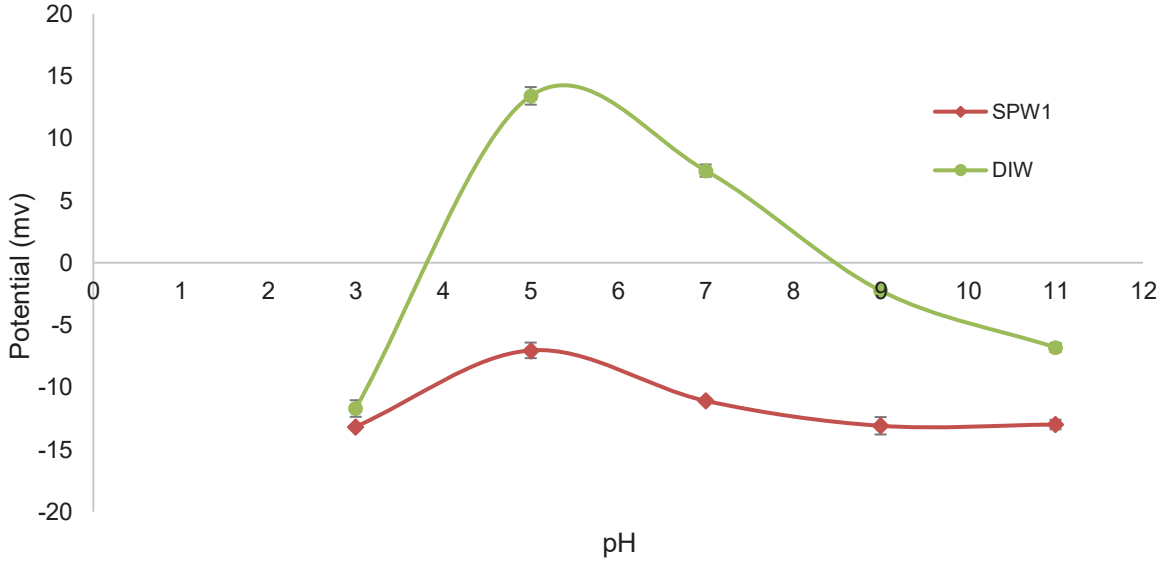

Figure 5-14 Zeta potential of chalcocite and bornite in DIW and SPW1 from pH 3 to 11. Error bars represent the standard deviation between duplicate test (where error bars cannot be seen, they are smaller than the data marker

5.5 Batch Flotation of synthetic ores

The flotation response of bornite, chalcocite and an equal mass mineral mixture of bornite and chalcocite, within synthetic ores containing 96.5% quartz, 1% talc as gangue and 2.5% mineral, were tested under natural conditions in SPW1 using relatively inert grinding media (21% chrome). Batch floats were done to observe how the electrochemical interactions between the chosen minerals impact flotation under natural conditions.

5.5.1 Solids and water recovery

Figure 5-15 and Figure 5-16 show the solids and water recoveries as a function of time, and the relationship between solids and water recovery in Figure 5-17. From the solids recovery as a function of time, it is evident from the first concentration that bornite has a higher recovery rate than chalcocite as indicated by the recovery after 2 minutes. The mineral mixture recovery rate traces closer to that of bornite. The final mineral recovery for all minerals is very close and almost indistinguishable. The water recovery as a function of time follows a linear pattern with very similar water recoveries between all three minerals.

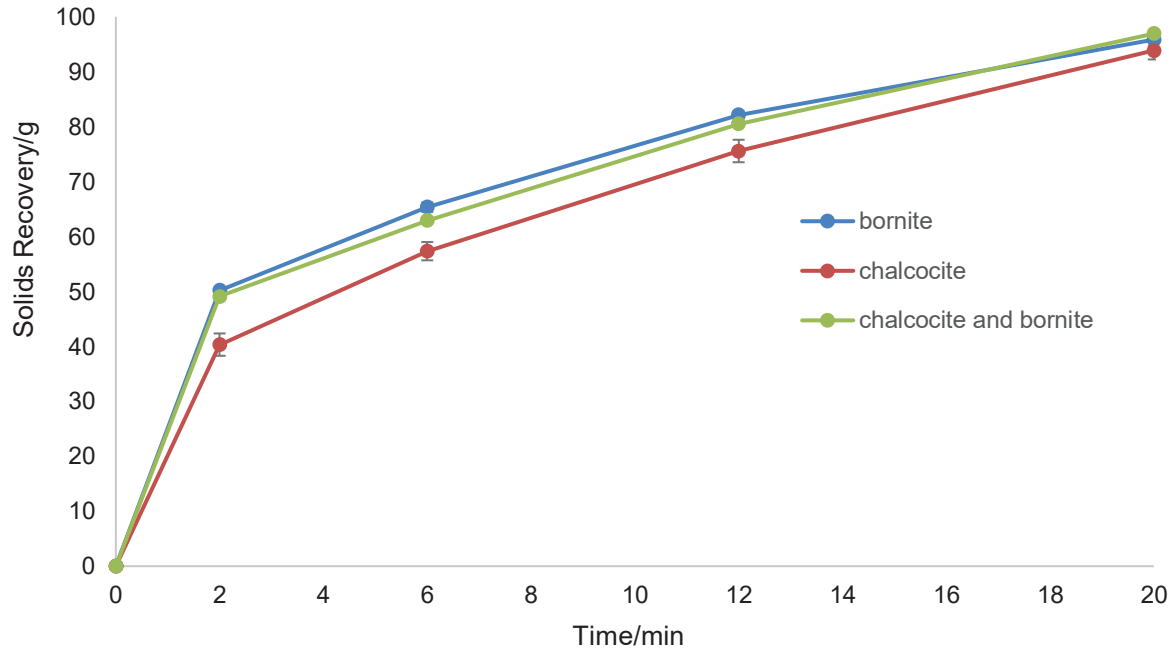

Figure 5-15 solids recovery vs time for the synthetic ores of bornite, chalcocite and the mineral mixture of bornite and chalcocite. Error bars represent the standard deviation between duplicate test (where error bars cannot be seen, they are smaller than the data marker

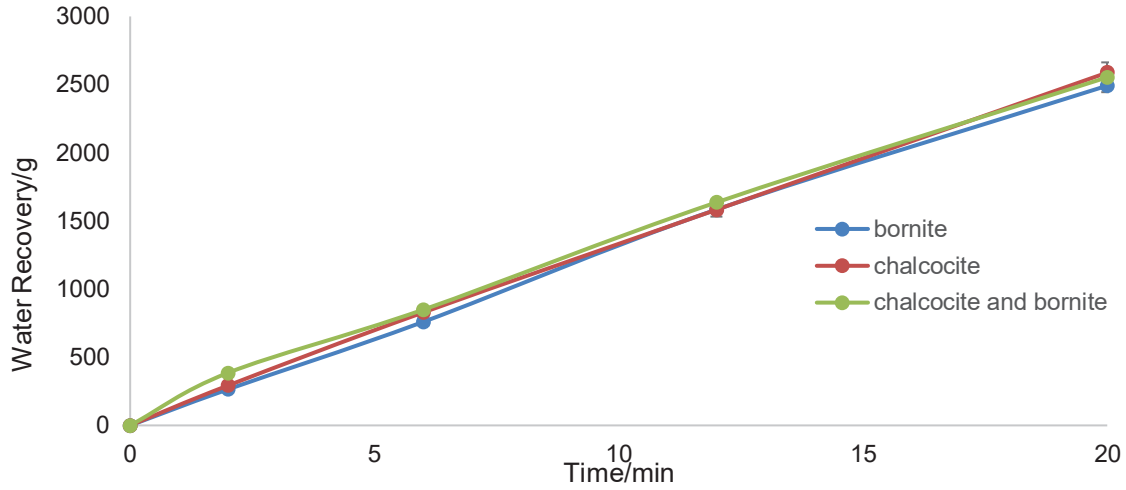

Figure 5-16 Water recovery vs time for the synthetic ores of bornite, chalcocite and the mineral mixture of bornite and chalcocite. Error bars represent the standard deviation between duplicate test (where error bars cannot be seen, they are smaller than the data marker

From Figure 5-17, it is evident that as water recovery increases, mass recovery increases as well, with the first concentrate showing the highest solids per unit water ratio for all three minerals. Bornite had the highest solids recovery per unit water recovered as shown in Table 5-1. The chalcocite and bornite mixture initially trace the same solids and water recovery as chalcocite for the first concentrate. Thereafter, the chalcocite and bornite water and solids recovery seems to be an average of the two individual mineral profiles.

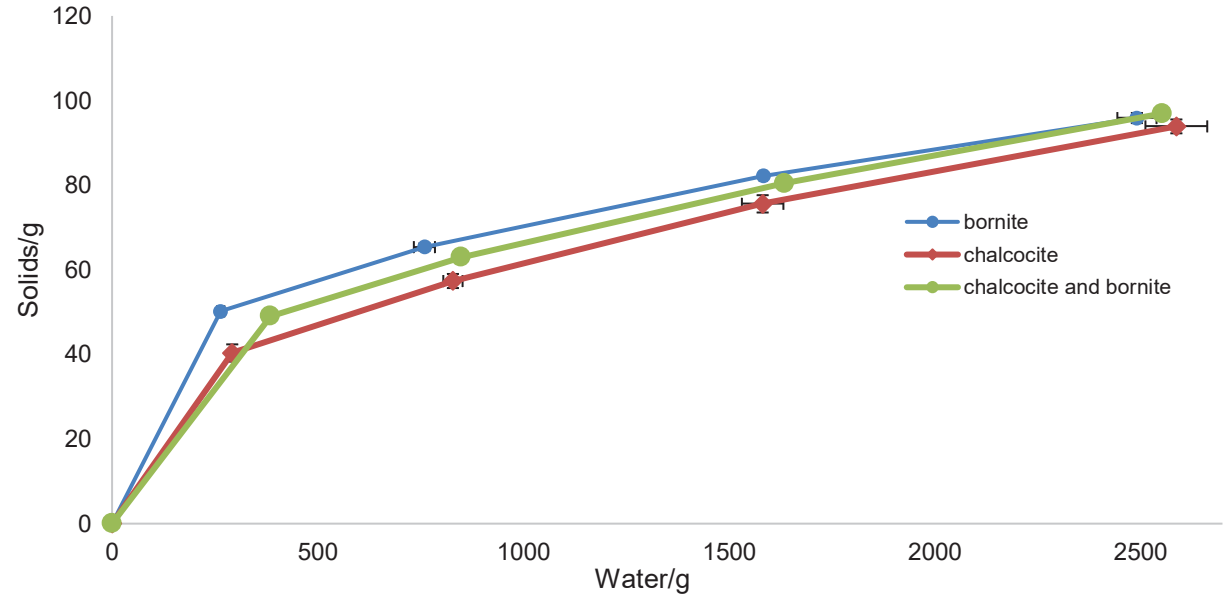

Figure 5-17 Solids recovery vs water recovery for synthetic ores flotation of bornite, chalcocite and the mineral mixture of bornite and chalcocite. Error bars represent the standard deviation between duplicate test (where error bars cannot be seen, they are smaller than the data marker

Table 5-1 Flotation solids per unit water ratio for the synthetic ores of bornite, chalcocite and the mineral mixture of bornite and chalcocite

Mineral	C1	C2	C3	C4
Bornite	0.190	0.086	0.052	0.038
Chalcocite	0.138	0.069	0.048	0.036
Chalcocite and Bornite	0.127	0.074	0.049	0.038

5.5.2 Copper Recovery

Copper recoveries were high, with more than 50% being recovered in the first concentrate. As seen in Figure 5-18- and Figure 5-19, first concentrate recoveries were 94%, 65% and 90% for bornite, chalcocite and the chalcocite and bornite mixture respectively. Chalcocite had lower copper percent recovery per unit water than bornite and the mineral mixture. Bornite initially has higher copper percent recovery per unit water in C1, but thereafter has the same ratio with the mineral mixture from C2 onwards as seen in Figure 5-19.

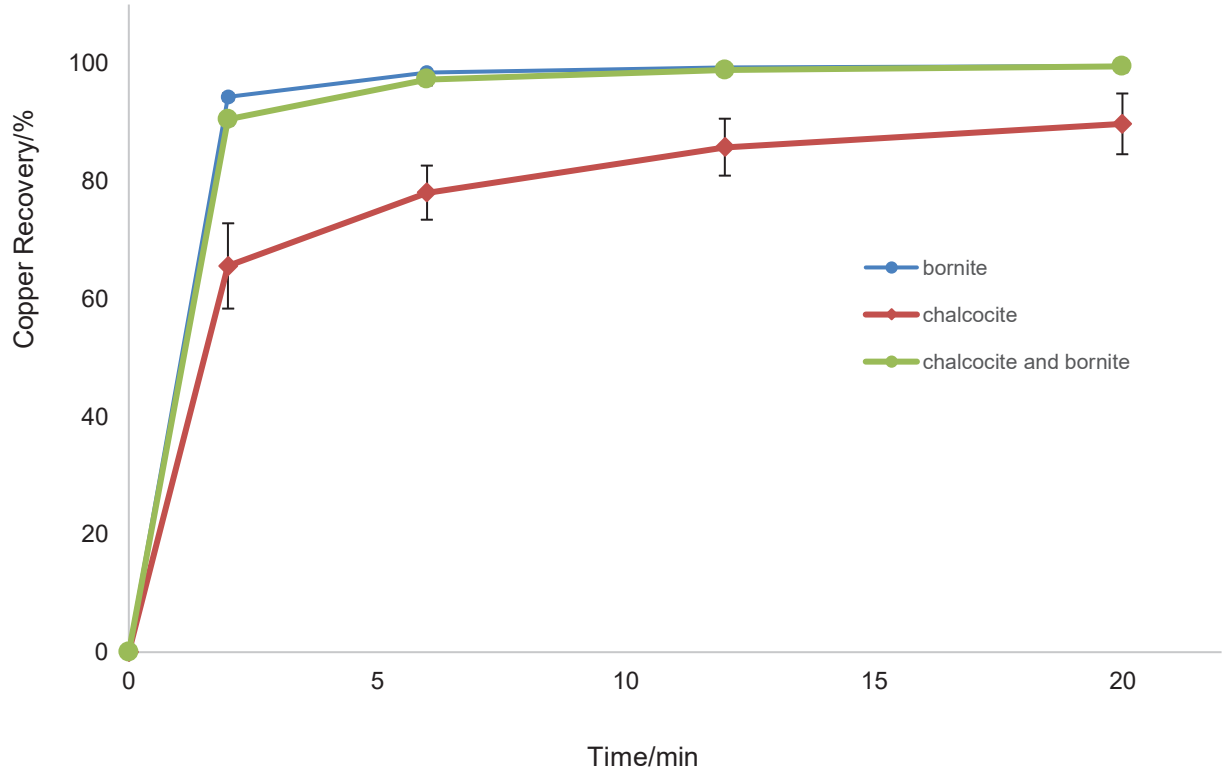

Figure 5-18 Copper recovery vs time for bornite, chalcocite and the mineral mixture of bornite and chalcocite. Error bars represent the standard deviation between duplicate test (where error bars cannot be seen, they are smaller than the data marker

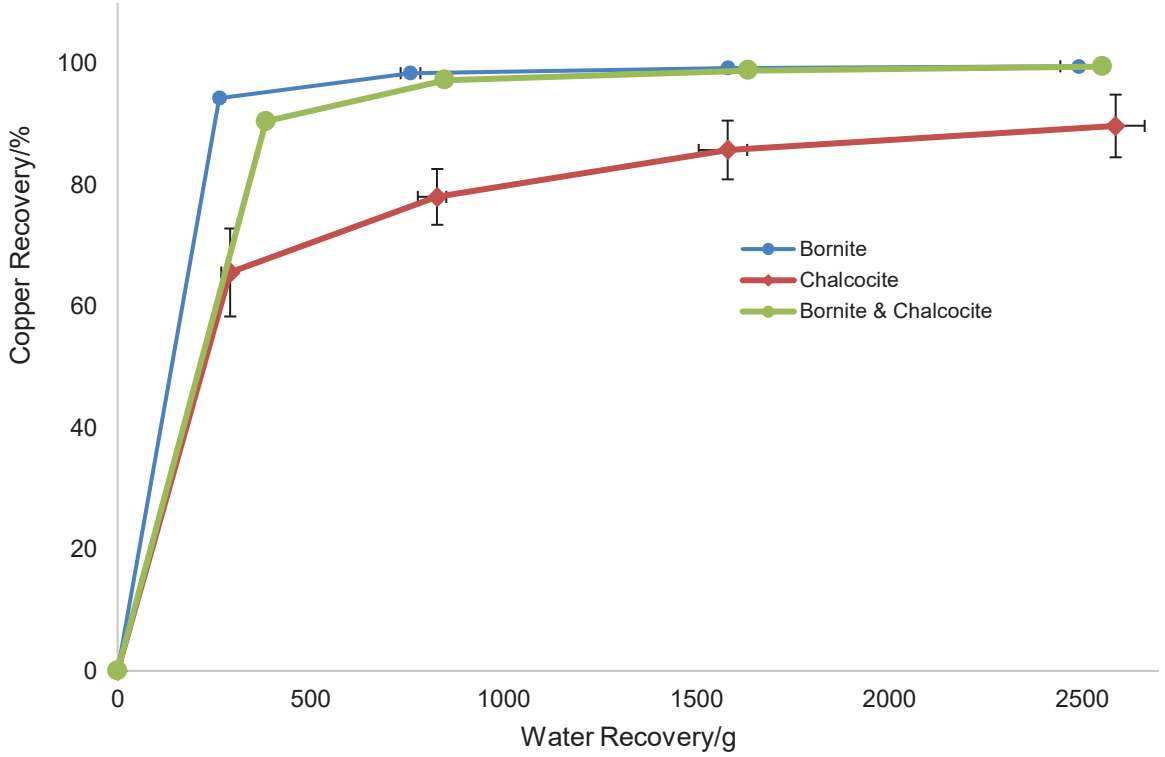

Figure 5-19 Copper recovery vs water recovery for bornite, chalcocite and the mineral mixture of bornite and chalcocite. Error bars represent the standard deviation between duplicate test (where error bars cannot be seen, they are smaller than the data marker

5.5.3 Copper Grade

For bornite and the chalcocite and bornite mineral mixture, due to the high copper recoveries of 90%+ in the first two concentrates, the grade significantly drops in the in the last concentrates as illustrated in Figure 5-20. The grades started off at 41% and 37% and ended off at 22% and 21% for bornite and the mineral mixture respectively. Chalcocite had a less drastic drop in grade as the initial copper recovery was lower starting off at 65% with a 27% grade. All three minerals have similar grade to recovery ratios initially, with bornite and the mineral mixture exhibiting similar ratios throughout, and chalcocite having a larger decrease in the ratio through to C4. The final recovery was 90% with a grade of 16%, which are both lower than the first concentrate recoveries and grades of 90%+ and 35%+ for bornite and chalcocite. Chalcocite's recovery of 90% was lower compared to bornite and the chalcocite and bornite mixture which both had final recoveries of 99% as seen in Figure 5-21.

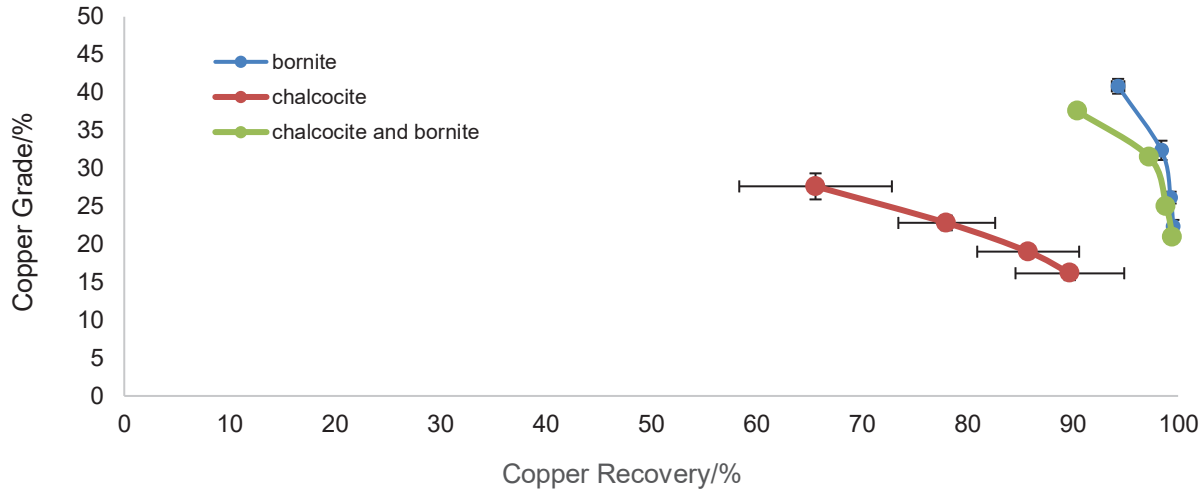

Figure 5-20 Copper grade vs recovery for bornite, chalcocite and the mineral mixture of bornite and chalcocite. Error bars represent the standard deviation between duplicate test (where error bars cannot be seen, they are smaller than the data marker

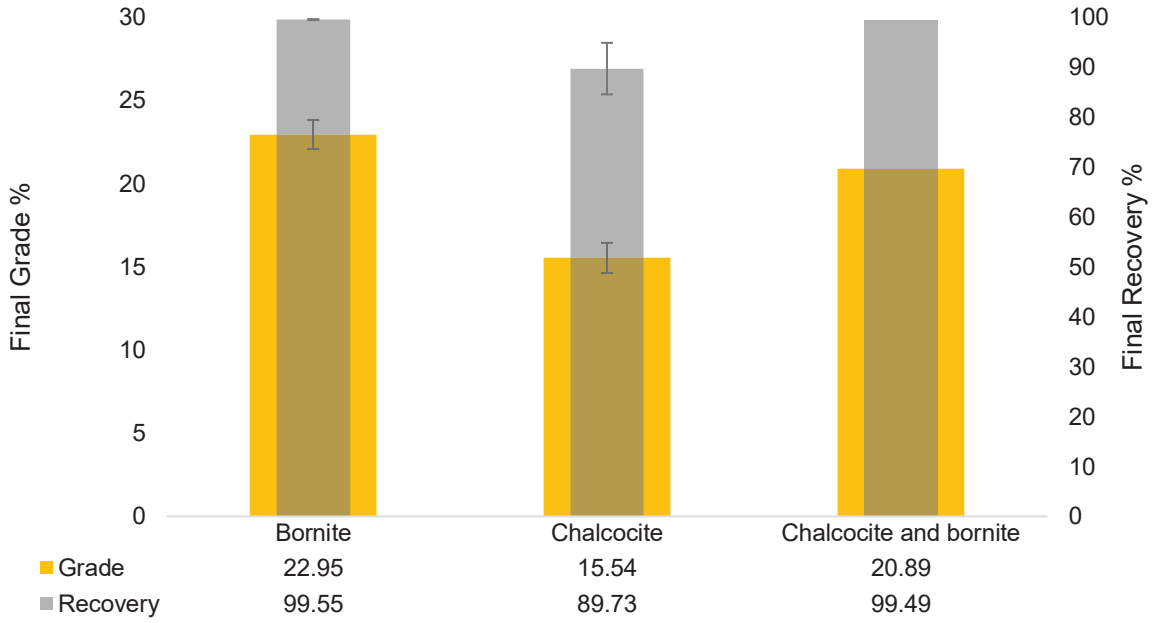

Figure 5-21 Final copper recoveries and grades for bornite, chalcocite and the mineral mixture of bornite and chalcocite. Error bars represent the standard deviation between duplicate test (where error bars cannot be seen, they are smaller than the data marker

5.5.4 Iron Recovery

Iron recoveries were similar and almost indistinguishable, with the chalcocite and bornite mixture exhibiting slightly higher iron recovery as seen Figure 5-22 and Figure 5-23. Bornite had the lowest iron recovery, with the bornite and chalcocite mixture tracing the iron recovery trend of chalcocite. The iron recovery observed in

chalcocite is largely due to the significant presence of marcasite and pyrite as impurities in the ore. Pyrite is known to readily float, and its flotation can be deduced from the decreasing copper to iron ratios seen in the concentrates compared to the feed as shown in Figure 5-24.

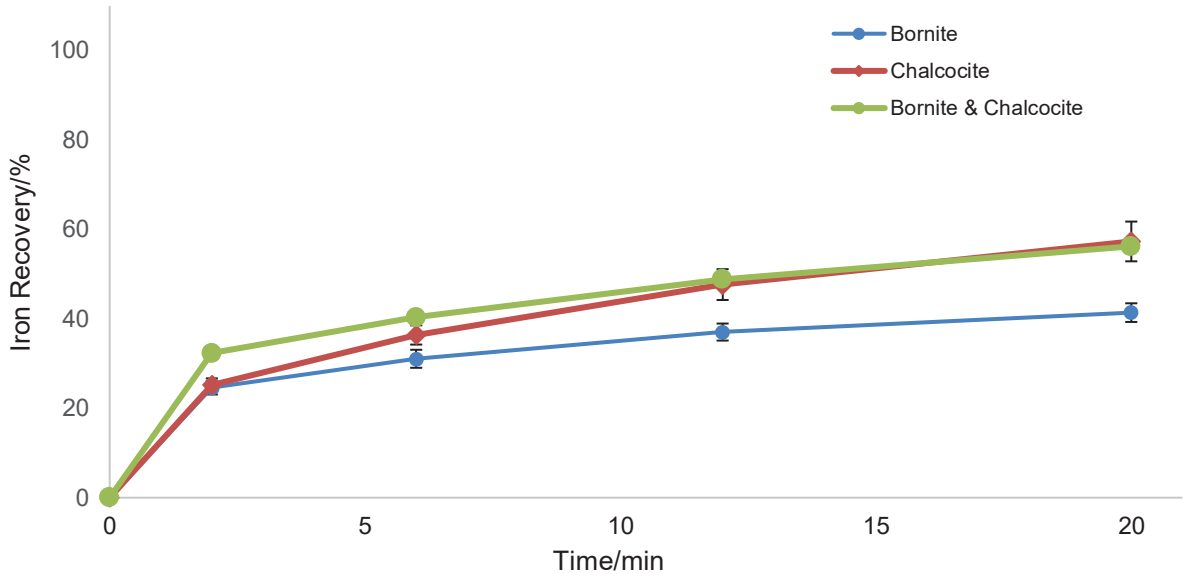

Figure 5-22 Iron recovery vs time for bornite, chalcocite and the mineral mixture of bornite and chalcocite. Error bars represent the standard deviation between duplicate test (where error bars cannot be seen, they are smaller than the data marker

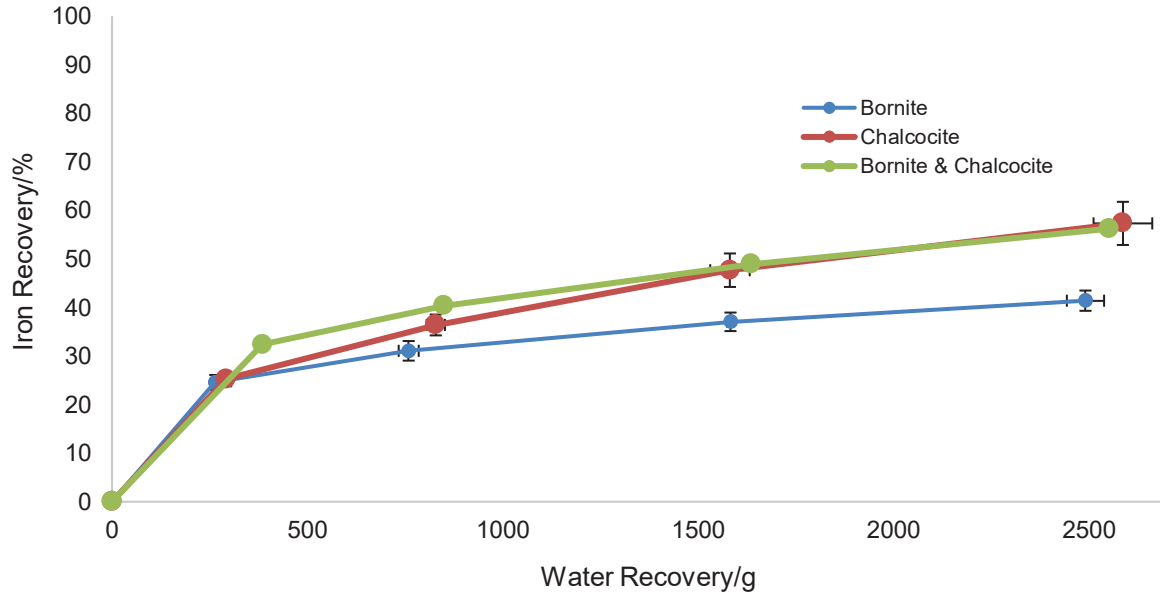

Figure 5-23 Iron recovery vs water recovery for bornite, chalcocite and the mineral mixture of bornite and chalcocite. Error bars represent the standard deviation between duplicate test (where error bars cannot be seen, they are smaller than the data marker

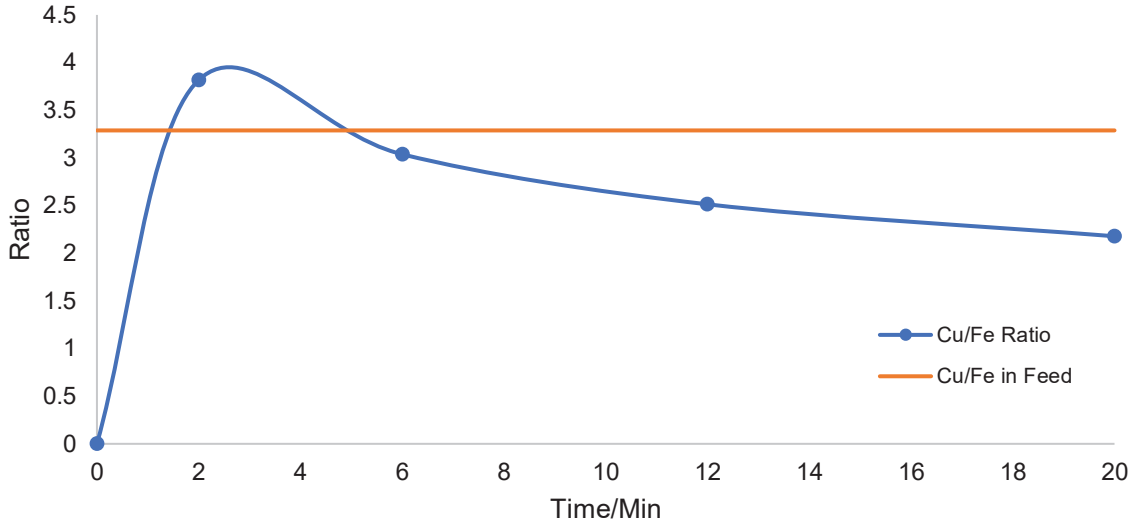

Figure 5-24 Copper to iron ratio for the chalcocite batch flotation test compared to the copper to iron ratio in the feed determined from the XRD

5.5.5 Iron Grade

The grade does not change drastically as the recovery increases, suggesting an almost consistent iron recovery throughout flotation seen in Figure 5-25. The initial bornite recovery of 26% had a grade of 9% and a final recovery of 41% with a decrease e to 8%. The significance of the impurities in chalcocite are seen in Figure 5-26 as chalcocite has the highest iron recovery with 57% recovered, closely followed by the mineral mixture with 56% and bornite recovering 41%.

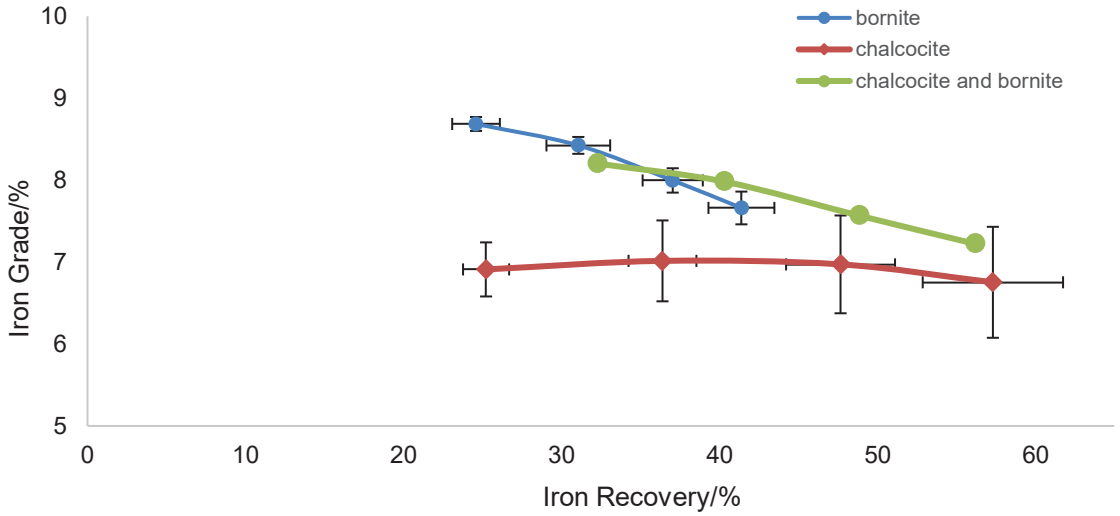

Figure 5-25 Iron grade vs recovery for bornite, chalcocite and the mineral mixture of bornite and chalcocite. Error bars represent the standard deviation between duplicate test (where error bars cannot be seen, they are smaller than the data marker

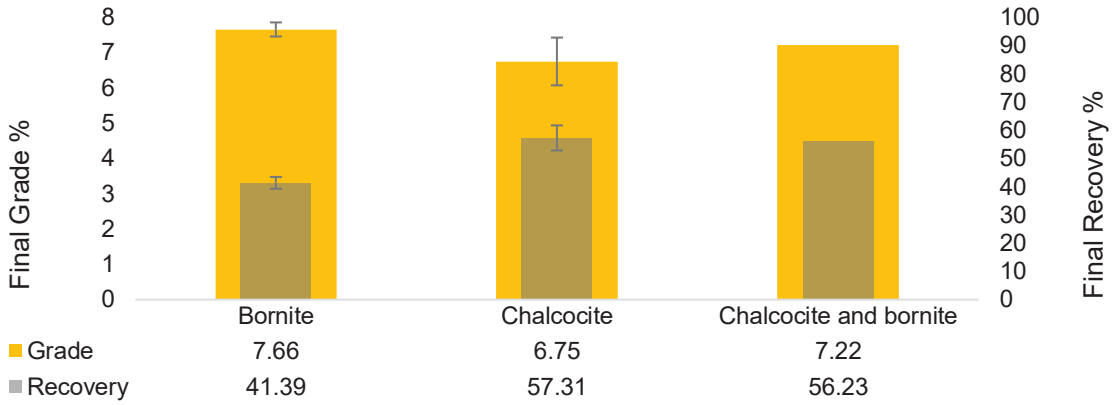

Figure 5-26 Final iron recoveries and grades for bornite, chalcocite and the mineral mixture of bornite and chalcocite. Error bars represent the standard deviation between duplicate test (where error bars cannot be seen, they are smaller than the data marker

5.5.6 ORP on grades and recovery

The oxygen reduction potential (ORP) of the slurry was measured during the grinding process to determine the pulp potential prior to flotation. The reduction potential varied greatly between the three minerals, with bornite recording a low potential of -5 mV, chalcocite significantly higher at 70 mV and the mixture seemingly equilibrating between the two at 20 mV. The increasing potentials with increasing iron recoveries and decreased copper recoveries as seen in Figure 5-27. bornite and chalcocite mixture have the same recovery but different potentials. Figure 5-28 shows the iron and copper grades at the different potentials. As the potential increases, the copper grade decreases from 23% for bornite to 15% for chalcocite. The iron grade does not change significantly with a decrease from 7.6% for bornite to 6.8% for chalcocite.

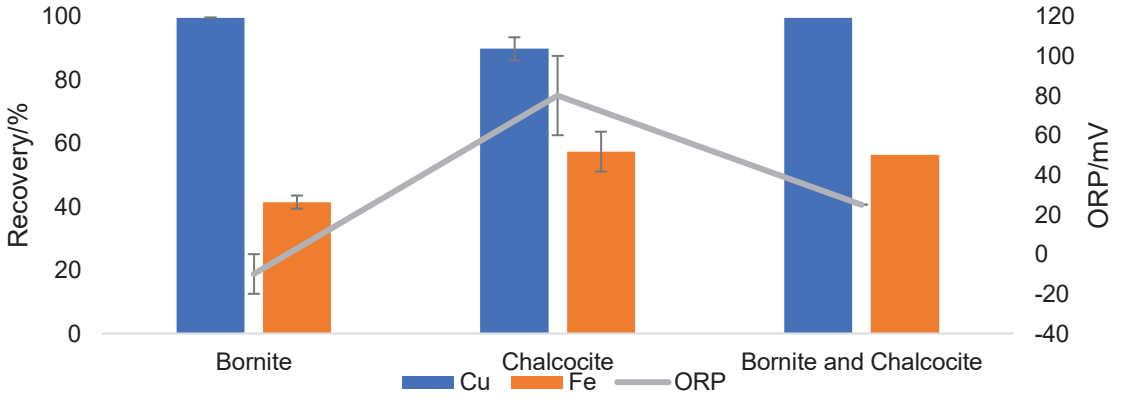

Figure 5-27 ORP conditions for Cu and Fe recoveries for bornite, chalcocite and the mineral mixture of bornite and chalcocite. Error bars represent the standard deviation between duplicate test (where error bars cannot be seen, they are smaller than the data marker

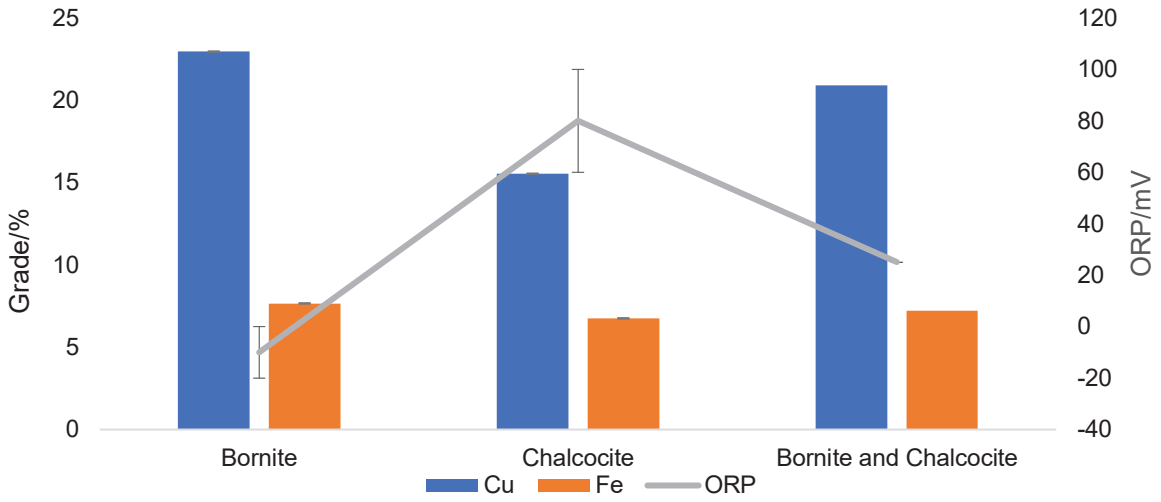

Figure 5-28 ORP for Cu and Fe grades for bornite, chalcocite and the mineral mixture of bornite and chalcocite. Error bars represent the standard deviation between duplicate test (where error bars cannot be seen, they are smaller than the data marker

6 Discussion

The purpose of this chapter is to discuss the results observed with a view to providing possible insights into the behaviour of the two minerals investigated. It is important to note that in understanding the mineral-collector interactions, there is a basis of known xanthate reactions that will be used to interpret the observations made. Xanthates are known to readily decompose whether in atmospheric conditions with oxygen, or in water. However, the decomposition follows various routes depending on the conditions. The xanthate species that will be present in the pulp will be dependent on the pH of the solution, the amount of dissolved oxygen, the metal ions in solution and the presence of any catalytic species that promote any of the decomposition processes. The decomposition reactions that are pertinent to flotation systems are shown in below.

Xanthate ion reactions taken from (Rao, 2004)

$$K^+ + ROCS_2 + H_2O \longrightarrow K^+ + OH^- + ROCS_2H \qquad \text{Equation 6-1}$$

Hydrolysis into xanthic acid

$$ROCS_2H \longrightarrow ROH + CS_2 \qquad \text{Equation 6-2}$$

Decomposition of xanthic acid

$$6ROCS_2^- + 3H_2O \longrightarrow 6ROH + CO_3^{2-} + 3CS_2 + 2CS_3^{2-} \qquad \text{Equation 6-3}$$

Hydrolytic decomposition

$$2CS_3^{2-} \longrightarrow 2CS_2 + 2S^{2-} \qquad \text{Equation 6-4}$$

Trithiocarbonate decomposition

$$2ROCS_2^- \longrightarrow (ROCS_2)_2 + 2e^- \qquad \text{Equation 6-5}$$

$$0.5\ O_2 + H_2O + 2e^- \longrightarrow 2OH^-$$

$$2ROCS_2^- + 0.5\ O_2 + H_2O \longrightarrow (ROCS_2)_2 + 2OH^-$$

Oxidation to dixanthogen

$$ROCS_2^- + H_2O \longrightarrow RO_2CS^- + S \qquad \text{Equation 6-6}$$

Oxidation to monothiocarbonate

$$ROCS_2^- + H_2O_2 \longrightarrow RO_2CS_2^- + H_2O \qquad \text{Equation 6-7}$$

Oxidation to perxanthate

Hydrolysis and decomposition of xanthic acid (Equation 6-1and Equation 6-2) are the primary reactions that take place under acidic conditions, with the extent of decomposition increasing as the pH decreases from pH 7. Hydrolytic composition (Equation 6-3 and Equation 6-4) happens under alkaline conditions where the reaction products are stable, and the presence of dissolved oxygen is critical for the oxidation reactions to take place (Equation 6-5, Equation 6-6 and Equation 6-7).

6.1 Effect of pH on microflotation recovery of bornite and chalcocite

Bornite and chalcocite were micro-floated with a collector dosage of 0.5 monolayer in SPW1 and DIW under varying pH from 3 to 11. Neutral and alkali conditions (pH 7 to 11) consistently showed relatively higher flotation recovery of between 58% and 60% for bornite and 45% to 72% for chalcocite in DIW compared to 34% to 42% recovery for bornite and 40% to 66% for chalcocite in SPW1. However, in acidic conditions, pH 3 recorded the highest recovery of 42% for bornite in SPW1, 71% for chalcocite in DIW and 67% for chalcocite in SPW1. pH 5 recorded the lowest recoveries in all tests except with bornite in DIW where pH 5 had the highest (66%) and pH 3 had the lowest (21%), which appears to be an anomaly. Bornite is known to float under anodic conditions as it undergoes dissolution (Zachwieja, et al., 1987). A crucial aspect that dictates the interaction between bornite and xanthate is the degree of oxidation on the bornite surface. The presence of iron in bornite results in a greater hydrophilic surface being formed due to the likely formation of iron hydroxide on the surface as seen in Equation 6-8, Equation 6-9 and Equation 6-10, resulting in more xanthates being required to neutralize the hydrophilic effects in alkaline conditions. This implies that acidic conditions possibly limit the formation of oxidation products on the surface of bornite resulting in better floatability. However, flotation for both minerals at pH 5 had the lowest recovery across both minerals and water type combinations, with the exception of bornite in DIW which appears to be an anomaly. From the xanthate reactions shown from Equation 6-1 to Equation 6-7, at pH<7, hydrolysis into xanthic acid should take place, followed by decomposition of xanthic acid to carbon disulphide. The extent of reaction and decomposition increase as the pH decreases to more acidic conditions. Therefore, it is likely that at pH 5, hydrolysis takes place, but the conditions are not strong enough for the decomposition reaction to take place, resulting in the xanthic acid being the final xanthate product. This leaves the system without a

hydrophobic inducing compound to enhance the flotation of chalcocite or bornite at pH 5. Higher recoveries were obtained at more acidic conditions due to the formation of the hydrophobic carbon disulphide that can form a film at the surface and induce hydrophobicity.

In SPW1, there was lower recovery across all pH values compared to DIW. The difference in the water types was the presence of cations and anions in SPW1 where there is none present in DIW. A previous study that looked at the speciation of SPW1 at various pH showed that from pH 2 to 12, there is a high concentration of sulphate species of Ca^{2+}, Mg^{2+} and Na^{+} (Manono, et al., 2019). The formation of these sulphate species takes place on the mineral surface, implying adsorption of cations onto the mineral surface and reducing the sites for collector adsorption, thereby reducing the floatability and recovery.

$$Fe \longleftrightarrow Fe^{2+} + 2e^{-} \qquad \text{Equation 6-8}$$

$$0.5\ O_2 + H_2O + 2e^{-} \longleftrightarrow 2OH^{-} \qquad \text{Equation 6-9}$$

$$Fe^{2+} + 2OH^{-} \longleftrightarrow Fe(OH)_2 \qquad \text{Equation 6-10}$$

The are 3 types of interactions xanthate can have with mineral surfaces viz. chemisorption of xanthate ions onto the surface to render it hydrophobic, reaction with the surface to form a metal xanthate or oxidation to form dixanthogen (Young, et al., 1990). For chalcocite, it has been speculated that the mechanism of interaction involves either chemisorbed xanthate or formation of the metal xanthate (Young, et al., 1990). Metal xanthate can be formed either from Cu^{2+} ions produced from dissolution under acidic conditions (Equation 6-11 and Equation 6-12), or from copper hydroxide in alkaline conditions (from corrosion) as seen in Equation 6-13. Another factor to consider is what form the xanthate species may have under various conditions. Under acidic conditions, xanthate has been known to decompose through hydrolysis with an intermediary xanthic acid species ($ROCS_2H$), which further decomposes into the alkyl alcohol and carbon disulphide as shown in Equation 6-2 (Rao, 2004). The hydrolysis of xanthate at low pH results in low xanthate ion concentration in the form detectable by UV-Vis spectroscopy at the 301 nm wavelength due to it not existing as a xanthate ion ($X^{-\cdot}$) The presence of the

hydrophobic carbon disulphide in the aqueous system, as well as the metal deficient sulphur from dissolution potentially results in a hydrophobic film surrounding the mineral surface and increasing the flotation recovery under acidic conditions. Potentials above -300 mV (less negative) have been shown to increase the surface coverage of xanthate on the surface of chalcocite and subsequently increase the flotation recovery as seen in Figure 6-1 (Woods, 2003). From the zeta potential tests, the potential at pH 3 is around -10 mV where the surface coverage is above 0.8 monolayer from Figure 6-1 which possibly explains the high recovery observed. The high recovery at low pH is possibly due to continuous metal dissolution on the mineral surface, leaving behind metal deficient sulphur (Equation 6-11) which increases the hydrophobicity of the remaining mineral and increasing the recovery.

$$MS \longleftrightarrow S + M^{2+} + 2e^{-} \qquad \text{Equation 6-11}$$

Metal dissolution to form metal deficient sulphur

$$Cu^{2+} + 2X^{-} \longleftrightarrow CuX_2 \qquad \text{Equation 6-12}$$

Copper Xanthate formation from dissolution

$$Cu(OH)_2 + 2X^{-} \longleftrightarrow CuX_2 + 2OH^{-} \qquad \text{Equation 6-13}$$

Copper Xanthate formation from corrosion

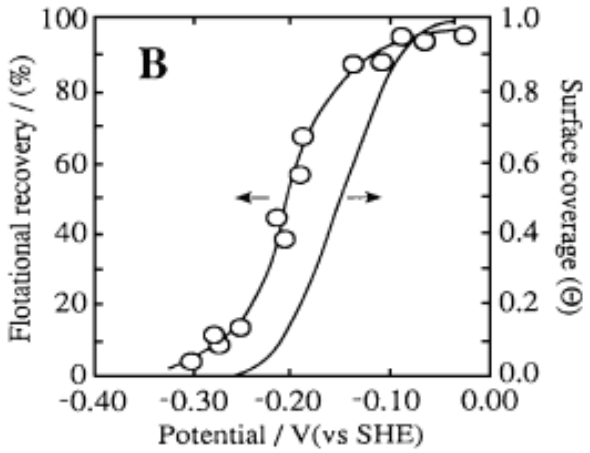

Figure 6-1 Potential dependence of flotation recovery and the adsorption isotherm for chalcocite and ethyl xanthate taken from (Woods, 2003)

6.2 Effect of pH on the surface charge of bornite and chalcocite

The zeta potential tests for both bornite and chalcocite showed 2 IEPs in the pH range 3 to 11 in DIW as seen in Figure 5-11 . Each mineral had one in acidic conditions and the second in alkaline conditions, with the charge increasing, reaching a maximum and subsequently decreasing between the 2 IEPs. The zeta potential profiles for bornite and chalcocite are similar in magnitude indicating similar extents of electrical double layer compression. Unoxidized sulphide mineral surfaces typically exhibit an IEP between pH 2 and 3, which is similar to the IEP of sulphur (Wills & Finch, 2016). However, there is typically some superficial oxidation on the mineral surface, which shifts the IEP to higher pH values as shown in Figure 6-2 (Wills & Finch, 2016). The higher first IEP values for bornite and chalcocite indicate the presence of oxy-hydroxide species that are present in the system. Multivalent metal ions such as Cu and Fe are hydrolysable, meaning they go through a series of speciation reactions with hydroxide ions shown in Equation 6-14 (Rao, 2004). The presence of these species is detected through zeta potential measurements as the monohydroxy and hydroxide precipitate species are both active on the mineral surface (Wills & Finch, 2016). The second IEPs for both bornite and chalcocite indicate hydrolysation of the metal ions and presence of the monohydroxy species. From the trend observed, it can be extrapolated that at higher pH values, a third IEP could possibly be observed which would correspond to the activity of the hydroxide precipitate. IEP's have also been linked to agglomeration due to the lack or repulsive forces between the minerals, which is typically counterproductive for physio-chemical separation processes.

$$M^{2+} + OH^- \longrightarrow M(OH)^+ + OH^- \longrightarrow M(OH)_2\,(s) + OH^- \longrightarrow M(OH)^-_3 \qquad \text{Equation 6-14}$$

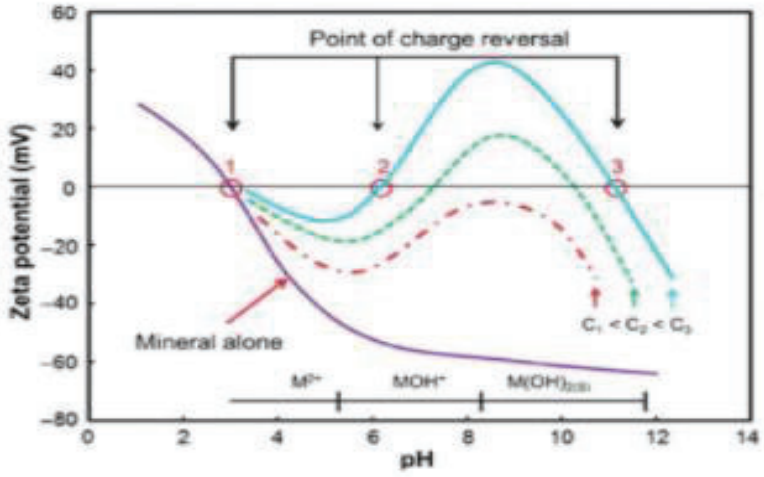

Figure 6-2 Zeta potential as a function of pH and concentration of hydrolysable metal ions taken from (Wills & Finch, 2016)

6.3 Changes in surface charge of bornite and chalcocite in the presence of other minerals and ions

The equi – mass mixed mineral potential was measured in DIW and produced 2 IEPs: pH 3.85 and pH 8.50. This indicates the presence of mono-hydroxy species and possible hetero-coagulation of particles due to a lack of repulsive forces between them at the pH values. The zeta potential of the mixed mineral has a more negative profile compared to that of individual minerals. This implies more electrical double layer compression in the single minerals compared to the mixture as the zeta potential becomes more negative. Bornite and chalcocite have relatively close rest potentials (400 mV and 440 mV respectively), implying minimal galvanic interactions between the two minerals. However, the presence of pyrite and marcasite as impurities in the chalcocite sample which are more noble (rest potential of 600 mV), a more complex galvanic cell is setup that results in bornite, and chalcocite becoming anodes and being oxidized to form various sulphur – oxygen species and ionic metals. Two sites for oxygen reduction exist, the surface of pyrite and marcasite, and the surface of bornite which acts as an intermediary to some extent and experiencing both oxidation and reduction. The reduction sites are both iron containing surfaces, resulting in the possibility of iron – hydroxy species formation which are hydrophilic and alter the surface properties of both minerals.

The zeta potential for bornite, chalcocite and the mineral mixture was tested in 2 water conditions, DIW and SPW1 with an ionic strength of 0.024 mol/L. Bornite had a potential range from -23 mV to 24 mV in DIW and had a shorter range in SPW1 from -16 mV to 2 mV. A similar trend is observed for chalcocite with range of -10 mV to 25 mV and -4 mV and -10 mV for DIW and SPW1 respectively. This could indicate adsorption of the cations present onto an oxidized mineral surface comprised of negatively charged sulphur and metal oxides, resulting in charge neutralization and a reduction in repulsive forces, resulting in a lower zeta potential in ionic water. This is contrary to most literature as an increase in ionic strength is associated with double layer compression which should increase the zeta potential resulting in a profile shifted upwards.

6.4 Adsorption

Collector adsorption was tested for bornite, chalcocite and the mineral mixture in DIW and SPW1 using 2 doses: 0.5 monolayer and 1 monolayer. There was higher collector adsorption across all pH values with minimal residual collector in the system for chalcocite dosed with 0.5 monolayer. Generally, higher collector adsorption was observed in the region of weakly acid to weakly alkaline pH (5 – 9), with less adsorption at pH 3 and 11. The differences in collector adsorption across the pH range are twofold; the specific collector mineral interactions, and the xanthate species form under differing aqueous conditions. Collector mineral interactions are strongly dependent on the pulp potential of the system, which is strongly influenced by the pH among several other variables.

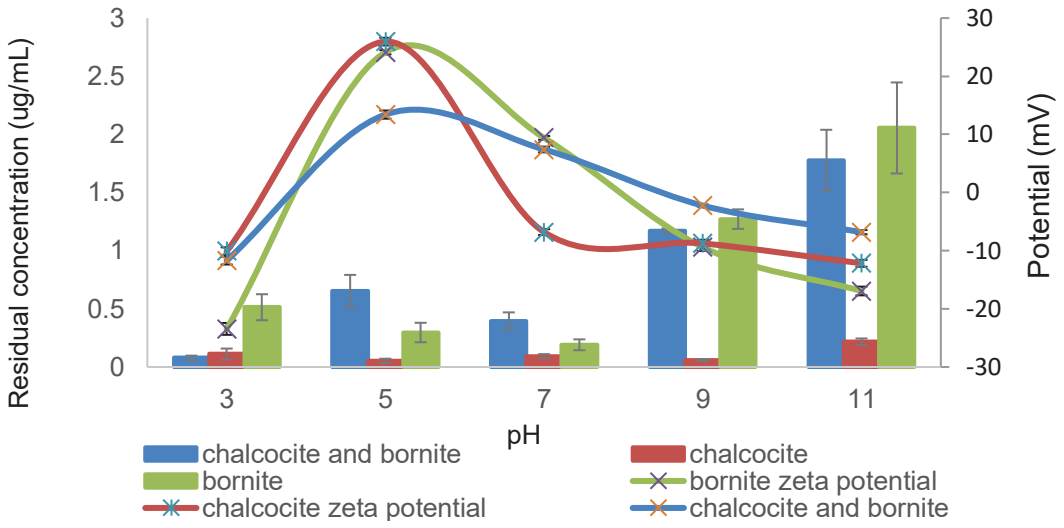

Figure 6-3 Zeta Potential profiles superimposed on the residual SIBX plots for bornite, chalcocite and the mixed mineral in DIW with a collector dosage of 0.5 monolayer

Figure 6-3 shows the residual collector for all the minerals with the respective zeta potential overlayed to relate the adsorption with the potential in DIW. In DIW, residual xanthate for bornite at pH 3 is 0.5 mg/L and continues to decrease until pH 7 which has a residual concentration of 0.2 mg/L. In alkaline conditions, the residual concentration increases to 2mg/L at pH 11. The zeta potential starts off at -23mV at pH 3 and increases to 24mV at pH 5, and subsequently decreases from there with the potential at pH 7 being 7mV and continues to decrease to -17mV at pH 11. For bornite, more positive potentials are corresponding to low residual xanthate. Positive potential environments are more oxidising, and the corresponding low residual xanthates suggest high collector adsorption which implies that there is xanthate oxidation likely to dixanthogen (Equation 6-5) which improves collector adsorption onto the mineral surface. Chalcocite exhibits relatively constant residual collector concentration with pH 3 recording a concentration of 0.1 mg/L and pH 11 the highest of 0.2 mg/L. However, the zeta potential does vary like bornite, with a low of -23 mV at pH 3, a high of 25 mV at pH 5 and then subsequently decreasing to -12 mV at pH 11.

The differences in residual xanthate present between bornite and chalcocite could lie in the presence and lack thereof of iron respectively. For chalcocite, copper xanthate formation would take place from copper oxides and hydroxides as shown in Equation 6-13, resulting in minimal xanthate ion remaining in solution. For bornite, the presence of iron results in the formation of iron hydroxide that is hydrophilic and thus will inhibit

the adsorption of collector onto the mineral surface in alkaline conditions. The mineral mixture residual xanthate profile closely traces that of bornite, which alludes to the presence of iron being the critical factor in determining the behaviour of the mixed mineral system.

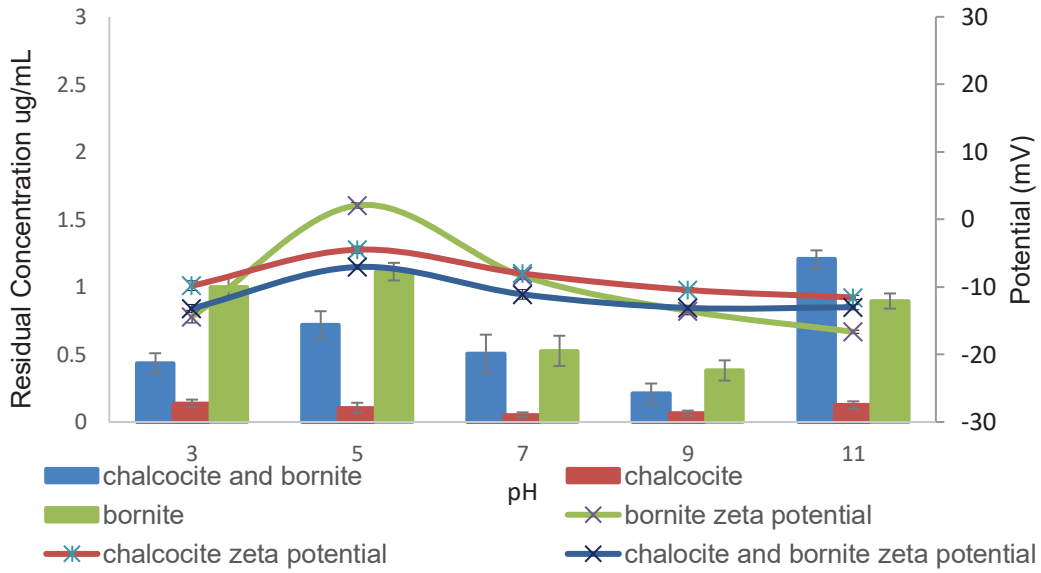

Figure 6-4 Potential profiles superimposed on the residual SIBX plots for bornite, chalcocite and the mixed mineral in SPW1 with a collector dosage of 0.5 monolayer

Figure 6-4 shows the residual collector for all the minerals with the respective zeta potential overlayed to relate the adsorption with the potential in SPW1. For bornite, the residual xanthate concentration varies between 0.4 mg/L at pH 9 and 1.1 mg/L at pH 5. The zeta potential profile follows a similar path to that of DIW, starting off at -14 mV at pH 3, goes through a maximum of 5 mV at pH 5 then decreases to -16 mV at pH 11. However, the extent of change of the surface charge is less in SPW1 compared to that of DIW. For chalcocite, the residual xanthate concentration continues to be minimal at around 0.15 mg/L, with the zeta potential profile also becoming more constant at around -10 mV.

The presence of ions in SPW1 results in higher residual xanthate between pH 3 and 7 compared to DIW for bornite and the mineral mixture. This is likely due to the cations competing with xanthate for adsorption onto the mineral surface, and simultaneously causing charge neutralization and results in a lower zeta potential profile.

6.5 Effect of mixed mineral flotation of bornite and chalcocite

Batch flotation tests using SPW1 under natural conditions were done using a synthetic ore comprised of 96.5% quartz, 2.5% mineral and 1% talc. Flotation of bornite yielded 99% copper recovery which is consistent with bornite flotation studies that have yielded over 90% recovery. Chalcocite had a lower recovery of 89% which can be correlated to the higher ORP in the mill during chalcocite grinding, indicating the possibility of strong surface oxidation modifying the hydrophobicity of the chalcocite surface, resulting in lower mineral recovery. This is consistent with studies from (Goncalves, et al., 2003) that showed that the grinding conditions for chalcocite produced a relatively high ORP which resulted in a 75% recovery of chalcocite after 8 minutes of flotation. The mineral mixture flotation yielded a 99% recovery of copper, similar to that of bornite but with a slightly lower grade of 21% compared to 23% for bornite. Considering the single mineral flotation of chalcocite, the recovery of the mineral mixture is higher than the combined individual mineral flotation recovery, suggesting a synergistic effect that increases recovery of copper from chalcocite in the presence of bornite. Despite bornite and chalcocite being distinguishable by the presence of iron (Fe) in the bornite structure, and lack thereof in chalcocite, separation by flotation continues to be challenging due to similar or minimal differences in electrochemical behaviour – which makes exploiting electrochemical differences to separate the two an arduous task, as flotation is by definition an electrochemically intense process.

7 Conclusion

The objective of this study was to determine how the electrochemical environment influences the interactions of chalcocite and bornite and the subsequent impact on flotation. Key questions were asked to test the hypothesis and this chapter outlines the high-level findings of this investigation.

1. **What is the effect of pH on the collector adsorption and flotation of chalcocite and bornite?**

The pH controls collector adsorption and flotation recovery by dictating what type of species is present in the electrochemical environment through redox reactions. Under acidic conditions, xanthate collector decomposes to carbon disulphide and the respective alkyl alcohol (Rao, 2004). For bornite, acidic conditions limit the formation of oxide products that typically encompass the mineral surface reducing the area available for adsorption. For chalcocite, acidic conditions result in metal dissolution and form metal deficient sulphur that is increasingly hydrophobic (Wills & Finch, 2016). The carbon disulphide (which is hydrophobic) that can form a film around the mineral surface, coupled with the limited hydrophilic oxidation products on the mineral surface for bornite and the more hydrophobic metal deficient sulphur for chalcocite result in high bornite and chalcocite recoveries at low pH respectively.

In alkaline conditions, the xanthate ion is stable and can adsorb onto the mineral surface. For chalcocite, copper xanthate formation takes place through hydrolysis, resulting in high collector adsorption. For bornite, alkaline conditions can result in the formation of iron hydroxide species that cover the mineral surface and reduce the surface area available for collector adsorption, resulting in lower collector adsorption.

2. **What is the effect of pH on the surface charge of chalcocite and bornite?**

The surface charge is greatly influenced by the pH due to its control over the redox reactions taking place on the mineral surface. As the pH increases, the surface charge increases, goes through a maximum and decreases. This is due to the pH changing the surface-active species in the systems. For both chalcocite and bornite, IEPs have indicated that the electrochemically active species in acidic conditions are the oxidized mineral surfaces. As the pH increases, metal ion hydrolysation takes

place resulting in the formation of hydroxy species ($CuOH^+$ and $Cu(OH)_2$) in alkaline conditions (Wills & Finch, 2016). This implies that a further increase in the pH would result in the formation of the solid metal hydroxide precipitate $Cu(OH)_2$ (Rao, 2004).

3. **How does the surface charge of chalcocite and bornite change in the presence of another mineral and ions?**

Due to the presence of the marcasite and pyrite impurities in the bornite sample, no discernible impact of chalcocite and bornite in the same system on their respective surface charges could be established. This is due to the impurities present also being electrochemically active and much more noble than chalcocite and bornite, resulting in a more complex galvanic cell in the system with chalcocite and bornite as the anodic minerals. The effect of ionic species resulted in a dampened (smaller range of variation/change) charge range for both chalcocite and bornite between pH 3 and 11 compared to in deionised water, indicating possible adsorption of cations on the mineral surfaces that cause charge neutralization.

4. **Is there a synergistic effect on recovery by floating chalcocite and bornite together?**

Batch flotation of chalcocite and bornite as a mineral mixture resulted in a higher recovery compared to the average recovery obtained from the single mineral batch flotation, suggesting a synergistic effect when floated together. The increased recovery is likely to result in more chalcocite being recovered, suggesting that the presence of bornite in the system enhances the floatability of chalcocite. However, this emphasizes the difficulty in separating these two minerals by flotation.

The impurities in the chalcocite and bornite samples present a challenge of making it difficult to determine the pure mineral interactions as they also contribute to the galvanic interactions and electrochemical reactions taking place in the system. Despite this complication, the results still provide industrial relevance due similar complex systems being more prevalent in industrial scale operations.

8 Recommendations

From the results and conclusion, the following recommendations are made.

1. **Changing the grinding chemistry to understand its impact on the surface chemistry observed**

The grinding in the mill was all done under natural conditions. The impact of the grinding environment could be further investigated by adjusting parameters such as the DO, pH and Eh, using a combination of different conditions to better understand their impact and inter-dependency.

2. **Fundamental studies to determine species and reactions taking place on the surface**

The observations made during adsorption and zeta potential studies were interpreted from inference. To have a better understanding of what is happening on the surface of the particle, fundamental studies such as XPS and FTIR in aqueous conditions would provide more insight into the exact surface species and reactions taking place. Given the importance of processing ores with chalcocite and bornite, more rigorous studies with comprehensive procedures would provide more conclusive evidence

9 References

Anon., 2020. *My Stone Meaning.* [Online] Available at: https://mystonemeaning.com/peacock-ore-bornite-stone-meaning/

Anthony, J. W., Bideaux, R. A., Bladh, K. W. & Nichols, M. C., 1990 . *Handbook of Mineralogy.* Tucson, Arizona: Mineral Data Publishing.

Barrera, P., 2020. *Investing News: Copper - Types of Copper Deposits in the World.* [Online]
Available at: https://investingnews.com/daily/resource-investing/base-metals-investing/copper-investing/types-copper-deposits-world/#:~:text=Exploration%20companies%20estimate%20grade%20through,volume%20of%20the%20ore%20rock.
[Accessed 13 October 2020].

Beverskog, B. & Puigdomenech, I., 1995. *Revised Pourbaix Diagrams for Copper at 5-150 degrees Celcius,* s.l.: Swedish Nuclear Power Inspectorate.

Bradshaw, D., Harris, P. & O'Connor, C., 2005. *The Effect of Collectors and their Interactions with Depressants on the behaviour of the Froth phase in flotation.* Brisbane, Australia, Presented at Centenary of Fllotation Symposium .

Bruckard, W., Sparrow, G. & Woodcock, J., 2011. A reviw of the Effects of the Grinding Environment on the Flotation of Copper Sulphides. *International Journal of Minerals Processing,* pp. 1-13.

Bulatovic, S. M., 2007. *Handbook of Flotation Reagents-Chemistry, Theory and Practice Volume 1.* s.l.:Elsevier.

Bundy, K. J., 2008. Biomaterials and the chemical environment of the body. In: P. A. Revell, ed. *Joint Replacement Technology.* s.l.:s.n.

Chaplin, M., 2003. *Hydrophobic Hydration.* [Online] Available at: http://www1.lsbu.ac.uk/water/hydrophobic_hydration.html [Accessed 26 May 2020].

Chhabra, R. & Basavaraj, M. G., 2019. *Coulson and Richardson's Chemical Engineering, Volume 2A - Particulate Systems and Particle Technology.* 6th ed. s.l.:Butterworth-Heinemann.

Chmielewski, T. & Kaleta, R., 2011. Galvanic Interactions of Sulphide Minerals in Leaching of Flotation Concentrate from Lubin Concentrator. *Physicochemical Problems of Mineral Processing,* pp. 21-35.

Da Silva, O., 2019. Types of Copper Deposits in the World- An Investor's Perspective. *Investing News Network*, 23 May.

Daintith, J., 2008. *Dictionary of Chemistry.* 6th ed. s.l.:Oxford University Press.

Darling, P., 2011. 14.5.6.2.1 Function of Frothers . In: *SME Mining Engineering Handbook.* s.l.:Society for Mining, Metallurgy and Exploration.

Fee, B. S. & Klimpel, R. R., 1986. *Chemical Reagents in the Minerals Industry.* Littleton: SME Inc. .

Finch, J., 1995. Column Flotation: A Selected review - Part IV: Novel Flotation Devices. *Minerals Engineering,* pp. 587-602.

Fuerstenau, M. C., Chandler, S. & Woods, R., 2007. *Sulphide mineral flotation. In: Fuerstenau, M.C., Jameson, G., R-H, Yoon (Eds), Froth Flotation. A Century of Innovation.* Littleton: Society for Mining, Metallurgy, and Exploration.

Garcia-Zuñiga, H., 1935. La eficiencia de la flotación es una función exponencial. *Boletín Minero, Sociedad Nacional de Minería,* Issue 47, pp. 83-88.

Goncalves, K. L. C., Andrade, V. L. L. & Peres, A. E. C., 2003. The effect of grinding conditions on the flotation of a sulphide copper ore. *Minerals Engineering,* pp. 1213-1216.

Grano, S. R., Akroyd, T. & Mular, M. A., 2007. *A Model Study of Copper Rougher Recovery Optimisation at PT Freeport Indonesia.* s.l., s.n.

Grano, S. R., Prestidge, C. A. & Ralston, J., 1997. Solution interaction of ethyl xanthate and sulphite and its effect on galena flotation and xanthate adsoprtion. *International Journal of Mineral Processing,* Issue 52, pp. 161-186.

Greet, C. J., 2009. The significance of grinding envrionment on the flotation of UG2 ores. *Journal of the Southern African Institute of Mining and Metallurgy,* Volume 108.

Greet, C. J., Bruckard, W. J. & MacKay, D., 2010. Collector – addition point and consumption. *Mineral Processing and Extractive Metallurgy,* pp. 235-241.

Greet, C. J., Kinal, J. & Mitchell, I., 2006. Is Measuring pH Enough?. *Metallurgical Plant Design and Operating Strategies. The Australasian Institute of Mining and Metallurgy*.

Greet, C. J., Small, G. L., Steinier, P. & Grano, S. R., 2004. The Magotteaux Mill®: Invesigating the effect of grinding on pulp chemistry and flotation performance. *Minerals Engineering,* Issue 17, pp. 891-896.

Heyes, G. W. & Trahar, W. J., 1979. Oxidation–reduction effects in the flotation of chalcocite and cuprite. *International Journal od Mineral Processing,* Issue 6, pp. 229-252.

Hintikka, V. V. & Leppinen, J. O., 1995. Potential control in the flotation of sulphide minerals and precious metals. *Minerals Engineering,* 8(10), pp. 1151-1158.

Holmberg, K., 2002. *Handbook of Applied Surface and Colloid Chemistry, Volumes 1-2 - 10.4 Zeta Potential (Electrokinetic Potential).* s.l.:John Wiley & Sons.

Holmes, P. R. & Crundwell, F. K., 1995. Kinetic aspects of galvanic interactions between minerals during dissolution. *Hydrometallurgy,* Issue 39, pp. 353-375.

Huang, G., Grano, S. & Skinner, W., 2006. Galvanic Interactions between grinding media and arsenopyrite and its effect on flotation: Part II. Effect if grinding on flotation. *International journal of Mineral Processing,* Issue 78, pp. 198-213.

Hu, Y., Sun, W. & Wang, D., 2009. *Electrochemistry of Flotation of Sulphide Minerals.* s.l.:Springer.

Israelachvili, J. N. & Ninham, B. W., 1976. Intermolecular forces-the long and short of it. *Journal of Colloid and Interface Science,* 58(1), pp. 14-24.

Johnson, N. W., 1988. Application of Electrochemical Concepts to Four Sulphide Separations. *The Proceedings of the Electrochemistry in Mineral and Metal Processing ,* Volume II, p. 131 to 149.

Kawatra, K. S., 2006. *Advances in Comminution.* s.l.:Society for Mining, Metallurgy and Exploration.

Kawatra, S. K., 2011. Fundamental principles of froth flotation. In: *SME mining engineering handbook 3.* s.l.:s.n.

King, R. P., 2012. Kinetic Approach to Flotation Modeling. In: *Modeling and Simulation of Mineral Processing Systems .* s.l.:Society for Mining, Metallurgy and Exploration.

Klimpel, R., 1984. *Froth Flotation: The Kinetic Approach,* Johannesburg: Mintek 5.

Kohli, R. & Mittal, K. L., 2015. 5.2.4.1 Factors Affecting the Zeta Potential. In: *Developments in Surface Contamination and Cleaning, Volume 8 - Cleaning Techniques .* s.l.:Elsevier.

Kumbar, S. G., Laurencin, C. T. & Deng, M., 2014. Surface Hydrophobicity. In: *Natural and Synthetic Biomedical Polymers.* s.l.:Elsevier.

Kwong, Y. T., Swerhone, G. W. & Lawrence, J. R., 2003. Galvanic Sulphide Oxidation as a Metal-Leaching Mechanism and its Environmental Implications. In: *Geochemistry: Exploration, Environment, Analysis 3.* s.l.:s.n., pp. 337-343.

Liming, L., 2015. Tumbling Mills. In: *Iron Ore - Mineralogy, Processing and Environmental Sustainability .* s.l.:s.n., pp. 251-282.

Manono, M., Corin, K. & Wiese, J., 2019. The Effect of the Ionic Strength of Process Water on the Interaction of Talc and CMC: Implications of Recirculated Water on Floatable Gangue Depression. *Minerals.*

Mineral Processing & Metallurgy, 2009. *Froth Flotation Process.* [Online] Available at: https://www.911metallurgist.com/blog/froth-flotation-process [Accessed 20 March 2019].

MSR Blog, 2020. *MSR Blog.* [Online] Available at: http://www.msrblog.com/science/chemistry/chalcocite.html

Owusu, C., Addai-Mensah, J., Fornasiero, D. & Zanin, M., 2013. Estimating the electrochemical reactivity of pyrite ores-their impact on pulp chemistry and chalcopyrite flotation behaviour. *Advanced Powder Technology,* Issue 24, pp. 801-809.

Parga, J. R., Valenzula, J. L. & Aguayo, S., 2009. Bacís flotation cell for gold- and silver-beard pyrite recovery. *Minerals and Metallurgical Processing,* 26(1), pp. 25-29.

Payant, R., Rosenblum, F., Nesset, J. E. & Finch, J. A., 2012. Galvanic Interaction and Particle Size Effects in Self-Heating of Sulphide Mixtures. In: *Materials Science.* s.l.:s.n., pp. 359-379.

Peng, Y., Grano, S., Fornasiero, D. & Ralston, J., 2003. Control of grinding conditions in the flotation of chalcopyrite and its separation from pyrite. *International Journal of Mineral Processing,* Issue 69, pp. 87-100.

Poole, C. F., 2020. *Solid-Phase Extraction.* Elsevier: s.n.

Pozzo, R., Malicsi, R. & Iwasaki, I., 1990. Pyrite-pyrrhotite-grinding media contact and its effects on flotation. *Minerals and Metallurgical Processing,* 29(1), pp. 16-21.

Rao, S. R., 2004. *Surface Chemistry of Froth Flotation.* 2nd ed. New York: Kluwer Academic Publishers.

Rao, S. R., Moon, K. S. & Leja, J., 1976. *Effect of grinding media on the surface reactions and flotation of heavy metal sulphides.* New York, American Institute of Mining, Metallurgical, and Petroleum Engineers.

Wei, Y. & Sandenbergh, R. F., 2007. Effects of grinding environment on the flotation of Rosh Pinah complex Pb/Zn ore. *Minerals Engineering,* Issue 20, pp. 264-272.

Wiese, J., Harris, P. & Bradshaw D, 2005. The influence of the reagent suite on the flotation of ores from Merensky reef. *Minerals Engineering,* pp. 189-198.

Wills, B. A. & Finch, J. A., 2016. *Wills' Mineral Processing Technology - An Introduction to the Practical Aspects of Ore Treatment and Mineral Recovery.* 8th ed. s.l.:Elsevier.

Wills, B. & Napier-Munn, T., 2006. *WILLS' Mineral Processing Technology: An Introduction to the Practical Aspects of ore treatment and mineral recovery.* 7th ed. s.l.:Butterworth-Heinemann Elsevier.

Woods, R., 2003. Electrochemical potential controlling flotation. *International Journal of Mineral Processing,* Issue 72, pp. 151-162.

Workman, L. & Eloranta, J., 2003. *The Effects of Blasting on Crushing and Grinding Efficiency and Energy Consumption. Proceedings of the Annual Conference on Explosives and Blasting Technique.* s.l., s.n.

Xiangning, B. et al., 2017. Kinetics of flotation. Order of process, rate constant distribution and ultimate recovery. *Physiochemical problems of Mineral processing,* 53(1), pp. 342-365.

Yoa, W. et al., 2019. Effects of grinding media on flotation performance of calcite. *Minerals Engineering,* Issue 132, pp. 92-94.

Young, C. A., Basilio, C. I. & Yoon, R. H., 1990. Thermodynamics of chalcocite-xanthate interactions. *International Journal of Mineral Processing,* Issue 31, pp. 265-279.

Zachwieja, J. B., Walker, G. W. & Richardson, P. E., 1987. Electrochemical Flotation of sulfides: the bornite ethylxanthate system. *Minerals and Metallurgical Processing,* pp. 146-151.

Zanin, M., Lambert, H. & du Plessis, C. A., 2019. Lime use and functionality in sulphide mineral flotation. *Minerals Engineering.*

10 Appendices

10.1 Microflotation

Bornite - SPW1												
Run1	C1	C2	C3	C4	Tails							
Conc. + Paper	0.4185	0.5657	0.7885	0.8603	1.0124			pH	3			
Paper	0.2772	0.2763	0.2759	0.2863	0.2799			Water	SPW1			
Conc.	0.1413	0.2894	0.5126	0.574	0.7325	2.2498						
Run 2												
Conc. + Paper	0.4962	0.487	0.4955	0.6371	1.3677			C1	C2	C3	C4	Tails
Paper	0.276	0.282	0.2768	0.2782	0.2821		Conc.	0.18075	0.42795	0.7936	1.26005	0.90905
Conc.	0.2202	0.205	0.2187	0.3589	1.0856	2.0884	Error	0.03945	0.0422	0.14695	0.10755	0.17655
Run1	C1	C2	C3	C4	Tails							
Conc. + Paper	0.3695	0.4592	0.5736	0.5029	2.0099			pH	5			
Paper	0.2837	0.2824	0.2869	0.2832	0.56			Water	SPW1			
Conc.	0.0858	0.1768	0.2867	0.2197	1.4499	2.2189						
Run 2												
Conc. + Paper	0.3703	0.4054	0.4818	0.5634	2.2869			C1	C2	C3	C4	Tails
Paper	0.2927	0.2893	0.2827	0.2773	0.5482		Conc.	0.0817	0.22815	0.47105	0.72395	1.5943
Conc.	0.0776	0.1161	0.1991	0.2861	1.7387	2.4176	Error	0.0041	0.03035	0.0438	0.0332	0.1444
Run1	C1	C2	C3	C4	Tails							
Conc. + Paper	0.3493	0.4363	0.5177	0.5842	2.1154			pH	7			
Paper	0.25831	0.2628	0.261	0.2589	0.2552			Water	SPW1			
Conc.	0.09099	0.1735	0.2567	0.3253	1.8602	2.70669						
Run 2												
Conc. + Paper	0.4296	0.6407	0.7058	0.5487	1.776			C1	C2	C3	C4	Tails
Paper	0.2829	0.2593	0.2756	0.2592	0.2768		Conc.	0.118845	0.396295	0.739745	1.047145	1.6797
Conc.	0.1467	0.3814	0.4302	0.2895	1.4992	2.747	Error	0.027855	0.10395	0.08675	0.0179	0.1805

Run1	C1	C2	C3	C4	Tails								
Conc. + Paper	0.4127	0.5628	0.674	0.6635	1.7041			pH	9				
Paper	0.2772	0.2763	0.2759	0.2863	0.2799			Water	SPW1				
Conc.	0.1355	0.2865	0.3981	0.3772	1.4242	2.6215							
Run 2													
Conc. + Paper	0.4136	0.5107	0.5352	0.5642	2.0021			C1	C2	C3	C4	Tails	
Paper	0.2745	0.2727	0.2855	0.2839	0.2764		Conc.	0.1373	0.39955	0.72345	1.0522	1.57495	
Conc.	0.1391	0.238	0.2497	0.2803	1.7257	2.6328	Error	0.0018	0.02425	0.0742	0.04845	0.15075	

Run1	C1	C2	C3	C4	Tails								
Conc. + Paper	0.3574	0.6378	0.5751	0.6668	1.5778			pH	11				
Paper	0.2755	0.2812	0.2813	0.2784	0.2814			Water	SPW1				
Conc.	0.0819	0.3566	0.2938	0.3884	1.2964	2.4171							
Run 2													
Conc. + Paper	0.4326	0.531	0.5174	0.5807	2.0055			C1	C2	C3	C4	Tails	
Paper	0.285	0.2868	0.2803	0.2864	0.2798		Conc.	0.11475	0.41515	0.6806	1.02195	1.51105	
Conc.	0.1476	0.2442	0.2371	0.2943	1.7257	2.6489	Error	0.03285	0.0562	0.02835	0.04705	0.21465	

Bornite - DIW													
Run1	C1	C2	C3	C4	Tails								
Conc. + Paper	0.3689	0.4818	0.4472	0.5056	2.0073			pH	3				
Paper	0.2789	0.2819	0.2741	0.2751	0.2777			Water	DIW				
Conc.	0.09	0.1999	0.1731	0.2305	1.7296	2.4231							
Run 2													
Conc. + Paper	0.3514	0.4042	0.4909	0.4766	1.8985			C1	C2	C3	C4	Tails	
Paper	0.2778	0.2803	0.2753	0.2824	0.2755		Conc.	0.0818	0.2437	0.43805	0.6504		1.6763
Conc.	0.0736	0.1239	0.2156	0.1942	1.623	2.2303	Error	0.0082	0.038	0.02125	0.01815		0.0533

Run1	C1	C2	C3	C4	Tails				
Conc. + Paper	0.5856	0.8957	0.9407	0.7778	0.8251		pH	5	
Paper	0.278	0.2848	0.2761	0.2767	0.2756		Water	DIW	
Conc.	0.3076	0.6109	0.6646	0.5011	0.5495	2.6337	Count	2	
Run 2									

Conc. + Paper	0.6034	0.7628	0.9045	0.7206	1.0094			C1	C2	C3	C4	Tails	
Paper	0.2712	0.2784	0.2827	0.2725	0.2725		Conc.	0.3199	0.86755	1.51075	1.98535		0.6432
Conc.	0.3322	0.4844	0.6218	0.4481	0.7369	2.6234	Error	0.0123	0.06325	0.0214	0.0265		0.0937
Run1	C1	C2	C3	C4	Tails								
Conc. + Paper	0.7121	0.7775	0.9457	0.6973	0.6958			pH	7				
Paper	0.2739	0.2799	0.2758	0.2814	0.2718			Water	DIW				
Conc.	0.4382	0.4976	0.6699	0.4159	0.424	2.4456							
Run 2													
Conc. + Paper	0.5079	0.6153	0.7826	0.8055	1.3485			C1	C2	C3	C4	Tails	
Paper	0.2748	0.2756	0.28	0.2748	0.2754		Conc.	0.33565	0.7543	1.34055	1.81385		0.74855
Conc.	0.2331	0.3397	0.5026	0.5307	1.0731	2.6792	Error	0.10255	0.07895	0.08365	0.0574		0.32455
Run1	C1	C2	C3	C4	Tails								
Conc. + Paper	0.6777	0.8662	0.8744	0.789	0.7181			pH	9				
Paper	0.2786	0.2787	0.2763	0.2819	0.2752			Water	DIW				
Conc.	0.3991	0.5875	0.5981	0.5071	0.4429	2.5347							
Run 2													
Conc. + Paper	0.4971	0.6501	0.7287	0.7165	1.4346			C1	C2	C3	C4	Tails	
Paper	0.2846	0.2801	0.2819	0.275	0.2789		Conc.	0.3058	0.78455	1.307	1.7813		0.7993
Conc.	0.2125	0.37	0.4468	0.4415	1.1557	2.6265	Error	0.0933	0.10875	0.07565	0.0328		0.3564
Run1	C1	C2	C3	C4	Tails								
Conc. + Paper	0.6743	0.7746	0.9613	0.6552	0.9874			pH	11				
Paper	0.2755	0.2812	0.2813	0.2784	0.2814			Water	DIW				
Conc.	0.3988	0.4934	0.68	0.3768	0.706	2.655							
Run 2													
Conc. + Paper	0.5003	0.6323	0.7886	0.7653	1.3548			C1	C2	C3	C4	Tails	
Paper	0.2804	0.2753	0.275	0.2755	0.2778		Conc.	0.30935	0.73455	1.33135	1.76465		0.8915
Conc.	0.2199	0.357	0.5136	0.4898	1.077	2.6573	Error	0.08945	0.0682	0.0832	0.0565		0.1855

Chalcocite - SPW1													
Run1	C1	C2	C3	C4	Tails								
Conc. + Paper	0.586	0.7013	0.8953	0.7477	0.9969			pH	3				
Paper	0.2737	0.2845	0.2831	0.284	0.2775			Water	SPW1				
Conc.	0.3123	0.4168	0.6122	0.4637	0.7194	2.5244							
Run 2													
Conc. + Paper	0.6667	0.8521	0.9622	0.8586	0.6855			C1	C2	C3	C4	Tails	
Paper	0.2791	0.2746	0.275	0.2845	0.2784		Conc.	0.34995	0.8471	1.4968	2.0157		0.56325
Conc.	0.3876	0.5775	0.6872	0.5741	0.4071	2.6335	Error	0.03765	0.08035	0.0375	0.0552		0.15615
Run1	C1	C2	C3	C4	Tails								
Conc. + Paper	0.3728	0.4819	0.5291	0.5934	2.1109			pH	5				
Paper	0.2782	0.2787	0.2845	0.2779	0.2808			Water	SPW1				
Conc.	0.0946	0.2032	0.2446	0.3155	1.8301	2.688							
Run 2													
Conc. + Paper	0.3902	0.4805	0.508	0.4931	2.132			C1	C2	C3	C4	Tails	
Paper	0.2843	0.2845	0.2779	0.2776	0.2742		Conc.	0.10025	0.29985	0.5372	0.8027		1.84395
Conc.	0.1059	0.196	0.2301	0.2155	1.8578	2.6053	Error	0.00565	0.0036	0.00725	0.05		0.01385
Run1	C1	C2	C3	C4	Tails								
Conc. + Paper	0.5721	0.9624	0.8624	0.8021	0.9893			pH	7				
Paper	0.2798	0.2788	0.2834	0.2819	0.2735			Water	SPW1				
Conc.	0.2923	0.6836	0.579	0.5202	0.7158	2.7909							
Run 2													
Conc. + Paper	0.6663	0.8035	0.7951	0.7509	1.1602			C1	C2	C3	C4	Tails	
Paper	0.281	0.2804	0.282	0.2813	0.2789		Conc.	0.3388	0.94215	1.4882	1.9831		0.79855
Conc.	0.3853	0.5231	0.5131	0.4696	0.8813	2.7724	Error	0.0465	0.08025	0.03295	0.0253		0.08275
Run1	C1	C2	C3	C4	Tails								
Conc. + Paper	0.6055	0.6125	0.7015	0.6591	1.4263			pH	9				
Paper	0.2835	0.2823	0.2762	0.2802	0.2799			Water	SPW1				
Conc.	0.322	0.3302	0.4253	0.3789	1.1464	2.6028							
Run 2													
Conc. + Paper	0.4782	0.4732	0.5987	0.5273	1.9521			C1	C2	C3	C4	Tails	

Paper	0.2745	0.2727	0.2855	0.2839	0.2764		Conc.	0.26285	0.5282	0.89745	1.2086	1.41105
Conc.	0.2037	0.2005	0.3132	0.2434	1.6757	2.6365	Error	0.05915	0.06485	0.05605	0.06775	0.26465

Run1	C1	C2	C3	C4	Tails							
Conc. + Paper	0.5109	0.5119	0.8024	0.5251	1.6854			pH	11			
Paper	0.2759	0.2751	0.2771	0.2778	0.2774			Water	SPW1			
Conc.	0.235	0.2368	0.5253	0.2473	1.408	2.6524						
Run 2												
Conc. + Paper	0.6742	0.6983	0.9753	0.809	1.1827			C1	C2	C3	C4	Tails
Paper	0.2811	0.2752	0.2772	0.2762	0.5652		Conc.	0.31405	0.644	1.2557	1.64575	1.01275
Conc.	0.3931	0.4231	0.6981	0.5328	0.6175	2.6646	Error	0.07905	0.09315	0.0864	0.14275	0.39525

Chalcocite - DIW												
Run1	C1	C2	C3	C4	Tails							
Conc. + Paper	0.7091	0.903	0.987	0.5946	0.7514			pH	3			
Paper	0.2816	0.2822	0.2775	0.2779	0.2819			Water	DIW			
Conc.	0.4275	0.6208	0.7095	0.3167	0.4695	2.544						
Run 2												
Conc. + Paper	0.8596	0.973	0.6551	0.8506	0.7325			C1	C2	C3	C4	Tails
Paper	0.2818	0.2748	0.2871	0.2788	0.2786		Conc.	0.50265	1.16215	1.7009	2.14515	0.4617
Conc.	0.5778	0.6982	0.368	0.5718	0.4539	2.6697	Error	0.07515	0.0387	0.17075	0.12755	0.0078

Run1	C1	C2	C3	C4	Tails							
Conc. + Paper	0.4118	0.6785	0.7699	0.7183	1.4354			pH	5			
Paper	0.2832	0.2768	0.2852	0.2824	0.2795			Water	DIW			
Conc.	0.1286	0.4017	0.4847	0.4359	1.1559	2.6068						
Run 2												
Conc. + Paper	0.4108	0.5576	0.5581	0.5495	2.115			C1	C2	C3	C4	Tails
Paper	0.28	0.2802	0.2838	0.2876	0.2752		Conc.	0.1297	0.46925	0.84875	1.19765	1.49785
Conc.	0.1308	0.2774	0.2743	0.2619	1.8398	2.7842	Error	0.0011	0.06215	0.1052	0.087	0.34195

Run1	C1	C2	C3	C4	Tails

Conc. + Paper	0.5839	0.7642	0.8742	0.7414	1.1875			pH	7				
Paper	0.2847	0.2825	0.2813	0.2848	0.2792			Water	DIW				
Conc.	0.2992	0.4817	0.5929	0.4566	0.9083	2.7387							
Run 2													
Conc. + Paper	0.4232	0.5687	0.5468	0.5458	2.0851			C1	C2	C3	C4	Tails	
Paper	0.2821	0.2795	0.2822	0.2829	0.2789		Conc.	0.22015	0.6056	1.03435	1.3941		1.35725
Conc.	0.1411	0.2892	0.2646	0.2629	1.8062	2.764	Error	0.07905	0.09625	0.16415	0.09685		0.44895
Run1	C1	C2	C3	C4	Tails								
Conc. + Paper	0.6399	0.8998	0.8971	0.7852	0.7519			pH	9				
Paper	0.2803	0.2856	0.282	0.2847	0.284			Water	DIW				
Conc.	0.3596	0.6142	0.6151	0.5005	0.4679	2.5573							
Run 2													
Conc. + Paper	0.7543	0.9452	0.9527	0.7364	0.8494			C1	C2	C3	C4	Tails	
Paper	0.2826	0.281	0.2857	0.2833	0.2845		Conc.	0.41565	1.05485	1.6959	2.1727		0.5164
Conc.	0.4717	0.6642	0.667	0.4531	0.5649	2.8209	Error	0.05605	0.025	0.02595	0.0237		0.0485
Run1	C1	C2	C3	C4	Tails								
Conc. + Paper	0.6996	0.7417	0.8449	0.7974	0.9664			pH	11				
Paper	0.2815	0.2729	0.2757	0.2813	0.2791			Water	DIW				
Conc.	0.4181	0.4688	0.5692	0.5161	0.6873	2.6595							
Run 2													
Conc. + Paper	0.6304	0.9087	0.8634	0.7308	1.097			C1	C2	C3	C4	Tails	
Paper	0.2758	0.2761	0.2783	0.2797	0.277		Conc.	0.38635	0.93705	1.5142	1.9978		0.75365
Conc.	0.3546	0.6326	0.5851	0.4511	0.82	2.8434	Error	0.03175	0.0819	0.00795	0.0325		0.06635

10.2 Adsorption

Bornite											
1 monolayer		DIW					SPW1				
pH		A1	A2	A	Concentration	error	A1	A2	A	Concentration	error
	3	0.171	0.151	0.161	2.121212121	0.186326	0.064	0.068	0.066	0.869565217	0.037265
	5	0.097	0.095	0.096	1.264822134	0.018633	0.011	0.019	0.015	0.197628458	0.07453
	7	0.025	0.036	0.0305	0.401844532	0.102479	0.003	0.015	0.009	0.118577075	0.111796
	9	0.08	0.088	0.084	1.106719368	0.07453	0.033	0.031	0.032	0.421607378	0.018633
	11	0.113	0.118	0.1155	1.52173913	0.046581	0.129	0.153	0.141	1.85770751	0.223591
0.5 monolayer											
	3	0.033	0.045	0.039	0.513833992	0.111796	0.08	0.072	0.076	1.001317523	0.07453
	5	0.018	0.027	0.0225	0.296442688	0.083847	0.081	0.088	0.0845	1.113306983	0.065214
	7	0.017	0.012	0.0145	0.191040843	0.046581	0.046	0.034	0.04	0.527009223	0.111796
	9	0.101	0.092	0.0965	1.27140975	0.083847	0.025	0.033	0.029	0.382081686	0.07453
	11	0.177	0.135	0.156	2.055335968	0.391284	0.071	0.065	0.068	0.895915679	0.055898
Chalcocite											
1 monolayer		DIW					SPW1				
pH		A1	A2	A	Concentration	error	A1	A2	A	Concentration	error
	3	0.058	0.043	0.0505	0.665349144	0.139744	0.055	0.07	0.0625	0.82345191	0.139744
	5	0.027	0.021	0.024	0.316205534	0.055898	0.02	0.03	0.025	0.329380764	0.093163
	7	0.011	0.019	0.015	0.197628458	0.07453	0.05	0.041	0.0455	0.599472991	0.083847
	9	0.076	0.1	0.088	1.15942029	0.223591	0.015	0.011	0.013	0.171277997	0.037265
	11	0.191	0.176	0.1835	2.417654809	0.139744	0.074	0.081	0.0775	1.021080369	0.065214
0.5 monolayer											
	3	0.006	0.011	0.0085	0.11198946	0.046581	0.012	0.009	0.0105	0.138339921	0.027949
	5	0.003	0.005	0.004	0.052700922	0.018633	0.006	0.01	0.008	0.105401845	0.037265
	7	0.008	0.006	0.007	0.092226614	0.018633	0.003	0.005	0.004	0.052700922	0.018633
	9	0.004	0.005	0.0045	0.059288538	0.009316	0.006	0.004	0.005	0.065876153	0.018633
	11	0.018	0.015	0.0165	0.217391304	0.027949	0.011	0.008	0.0095	0.12516469	0.027949

Chalcocite and Bornite											
1 monolayer		DIW					SPW1				
pH		A1	A2	A	Concentration	error	A1	A2	A	Concentration	error
	3	0.033	0.038	0.0355	0.467720685	0.046581	0.069	0.065	0.067	0.882740448	0.037265
	5	0.084	0.063	0.0735	0.968379447	0.195642	0.055	0.087	0.071	0.93544137	0.298121
	7	0.035	0.029	0.032	0.421607378	0.055898	0.031	0.023	0.027	0.355731225	0.07453
	9	0.059	0.047	0.053	0.69828722	0.111796	0.017	0.022	0.0195	0.256916996	0.046581
	11	0.156	0.174	0.165	2.173913043	0.167693	0.184	0.163	0.1735	2.285902503	0.195642
0.5 monolayer											
	3	0.007	0.005	0.006	0.079051383	0.018633	0.037	0.029	0.033	0.434782609	0.07453
	5	0.042	0.057	0.0495	0.652173913	0.139744	0.06	0.049	0.0545	0.718050066	0.102479
	7	0.026	0.034	0.03	0.395256917	0.07453	0.046	0.031	0.0385	0.507246377	0.139744
	9	0.09	0.088	0.089	1.17259552	0.018633	0.02	0.012	0.016	0.210803689	0.07453
	11	0.121	0.149	0.135	1.778656126	0.260856	0.088	0.095	0.0915	1.205533597	0.065214

10.3 Zeta Potential

	SPW1						DIW				
	Bornite										
pH	**11**	**9**	**7**	**5**	**3**		**11**	**9**	**7**	**5**	**3**
mV	-16.20	-14.40	-7.55	2.21	-15.30		-17.54	-7.99	8.50	24.40	-21.60
	-16.40	-15.10	-8.98	1.26	-15.50		-14.87	-9.84	9.70	23.40	-22.60
	-17.30	-14.90	-10.00	2.69	-15.70		-15.22	-9.49	10.00	24.80	-20.00
	-17.10	-11.90	-7.46	2.34	-15.20		-16.22	-9.07	8.34	23.30	-24.30
	-17.00	-12.60	-9.55	1.95	-14.90		-19.71	-12.20	9.65	24.20	-26.50
	-15.80	-12.40	-6.71	2.01	-9.76		-18.01	-7.82	10.20	24.60	-25.70
Average	**-16.63**	**-13.55**	**-8.38**	**2.08**	**-14.39**	**Average**	**-16.93**	**-9.40**	**9.40**	**24.12**	**-23.45**
Error	0.24	0.57	0.54	0.42	0.93	Error	0.75	0.65	0.32	0.36	1.02

	Chalcocite										
mV	-12.20	-9.30	-6.92	-5.78	-10.10		-14.25	-10.90	-5.32	25.70	-9.10
	-11.30	-10.70	-7.16	-5.70	-9.23		-10.30	-9.75	-5.17	23.60	-9.31
	-12.70	-11.00	-7.85	-3.02	-7.06		-13.45	-9.26	-7.50	25.10	-8.18
	-11.60	-9.45	-7.83	-4.51	-9.19		-12.21	-8.06	-7.90	27.60	-9.98
	-10.70	-11.30	-8.90	-3.36	-11.30		-11.58	-7.71	-7.57	27.10	-11.30
	-10.80	-10.90	-9.41	-4.50	-12.00		-11.25	-6.78	-7.39	26.60	-12.70
Average	**-11.55**	**-10.44**	**-8.01**	**-4.48**	**-9.81**	**Average**	**-12.17**	**-8.74**	**-6.81**	**25.95**	**-10.10**
Error	0.32	0.35	0.40	0.52	0.72	Error	0.60	0.61	0.50	0.65	0.67
	Chalcocite and Bornite										
mV	-13.30	-13.60	-8.96	-6.56	-13.10		-8.79	-2.38	6.50	13.00	-9.18
	-12.10	-12.70	-11.20	-7.03	-14.40		-7.23	-2.28	7.62	14.60	-12.20
	-14.20	-13.10	-9.61	-7.30	-13.10		-6.54	-2.67	5.00	14.70	-11.90
	-12.70	-13.20	-10.40	-6.57	-11.10		-5.89	-2.32	7.42	9.72	-13.10
	-14.40	-13.90	-10.30	-7.05	-12.00		-6.41	-1.70	7.94	11.80	-13.70
	-11.80	-14.10	-13.50	-7.74	-15.30		-6.54	-1.56	8.46	12.70	-10.00
	-12.50	-11.10	-13.70	-7.05	-13.21		-6.29	-2.81	8.86	17.30	-11.90
Average	**-13.00**	**-13.10**	**-11.10**	**-7.04**	**-13.17**	**Average**	**-6.81**	**-2.25**	**7.40**	**13.40**	**-11.71**
Error	0.38	0.38	0.70	0.17	0.58	Error	0.36	0.18	0.49	0.70	0.67

10.4 Batch Flotation

Bornite								
Run 1	**C1**	**C2**	**C3**	**C4**	**FEED**	**TAILS**	**TAILS2**	**TAILS3**
Solids (g)	50.55	15.67	16.44	14.40	26.05	18.81	20.11	1661.61
Water (g)	273.01	512.13	806.44	948.06				
Cu recovery (%)	94.72	98.42	99.21	99.49		ORP	-20	mV
Cu grade (%)	40.83	32.38	26.15	22.34		pH	6	
Fe recovery (%)	26.10	33.09	38.95	43.48		DO	7	ppm
Fe grade (%)	8.60	8.32	7.85	7.46				

Run 2	**C1**	**C2**	**C3**	**C4**	**FEED**	**TAILS**	**TAILS2**	**TAILS3**
Solids (g)	49.83	14.67	17.18	12.99	10.31	18.00	23.29	1689.04
Water (g)	255.41	478.42	841.00	869.55				
Cu recovery (%)	93.89	98.41	99.36	99.61		ORP	0	mV
Cu grade (%)	42.21	34.18	27.25	23.57		pH	6	
Fe recovery (%)	23.09	29.05	35.14	39.31		DO	6	ppm
Fe grade (%)	8.77	8.53	8.14	7.86				

Chalcocite								
Run 1	**C1**	**C2**	**C3**	**C4**	**FEED**	**TAILS**	**TAILS2**	**TAILS3**
Solids (g)	42.37	16.64	18.62	17.90	18.53	22.81	23.10	1723.00
Water (g)	293.09	512.33	725.99	981.26				
Cu recovery (%)	70.72	81.29	89.19	93.37		ORP	60	mV
Cu grade (%)	27.63	22.81	19.02	16.18		pH	5	
Fe recovery (%)	26.69	38.55	51.12	61.75		DO	6	ppm
Fe grade (%)	7.24	7.51	7.57	7.43				

Run 2	C1	C2	C3	C4	FEED	TAILS	TAILS2	TAILS3
Solids (g)	38.30	17.38	17.86	18.71	29.48	21.27	23.93	1798.35
Water (g)	291.14	561.11	780.14	1030.57				
Cu recovery (%)	60.48	74.80	82.35	86.08		ORP	100	mV
Cu grade (%)	25.20	21.44	17.87	14.89		pH	5	
Fe recovery (%)	23.77	34.25	44.22	52.87		DO	8	
Fe grade (%)	6.58	6.52	6.37	6.08				

Chalcocite and Bornite								
Run 1	**C1**	**C2**	**C3**	**C4**	**FEED**	**TAILS**	**TAILS2**	**TAILS3**
Solids (g)	49.08	13.86	17.55	16.45	24.00	15.48	16.62	1689.61
Water (g)	385.07	463.93	786.76	917.84				
Cu recovery (%)	90.48	97.27	98.87	99.49		ORP	25	mV
Cu grade (%)	37.53	31.46	25.01	20.89		pH	6	
Fe recovery (%)	32.33	40.35	48.90	56.23		DO	6	ppm
Fe grade (%)	8.20	7.98	7.56	7.22				

10.5 Monolayer Dosage Calculations

Chalcocite		
Step	Calculation	Result
1	$2\ (g) \times\ 0.9938\ (\frac{m^2}{g})$	$1.9876(m^2)$
2	$1.9876\ (m^2) \div 2.88\ x\ 10^{-19}\ \frac{m^2}{molecule}$	$6.901\ x\ 10^{18}\ (molecules)$

3	$6.901\ x\ 10^{18}\ (molecules) \div 6.022\ x\ 10^{23}\ \frac{molecules}{mole}$	$1.146\ x\ 10^{-5}$ (mol)
4	$1.146\ x\ 10^{-5}(mol) \times\ 172.2\ \frac{g}{mol}$	$1.97\ x\ 10^{-3}(g)$
5	$1.97\ x\ 10^{-3}\ (g) \div 1.0\ x\ 10^{-5}\ \frac{g}{ul}$	$197.3\ (ul)$
Bornite		
Step	Calculation	Result
1	$2\ (g) \times\ 0.7783\ (\frac{m^2}{g})$	$1.5566(m^2)$
2	$1.5566\ (m^2) \div 2.88\ x\ 10^{-19}\ \frac{m^2}{molecule}$	$5.405\ x\ 10^{18}\ (molecules)$
3	$5.405\ x\ 10^{18}\ (molecules) \div 6.022\ x\ 10^{23}\ \frac{molecules}{mole}$	$8.975\ x\ 10^{-6}$ (mol)
4	$8.975\ x\ 10^{-6}(mol) \times\ 172.2\ \frac{g}{mol}$	$1.55\ x\ 10^{-3}(g)$
5	$1.55\ x\ 10^{-3}\ (g) \div 1.0\ x\ 10^{-5}\ \frac{g}{ul}$	$154.5\ (ul)$